Fluorescence Studies of
Photosystem II Fluorescence Quenching During Desiccation

by

Kristin S. Schaven, B.Sc.

A Thesis

submitted to the Department of Biological Sciences

in partial fulfillment of the requirements

for the degree of

Master of Science

December 2013

Brock University

St. Catharines, Ontario

Acknowledgements

I would like to thank Dr. Doug Bruce for giving me an opportunity to work in the lab, and play with some really neat (and expensive!) equipment. All of the help and encouragement is greatly appreciated, and will never be forgotten. All of the members of the Bruce lab and the van der Est lab deserve recognition for help and encouragement, as well as providing a great atmosphere and sense of community in the Cairns gloomy basement. Allen Dirks was a great mentor allowing for conversation of ideas as well as designing and building new equipment (or upgrading old equipment) to allow for interesting experiments. Dr. Vassiliev graciously guided me through learning linux commands and computational fitting procedures as well as providing a fresh take on experimental results. Last but not least, while no longer a member of the lab team, special thanks to Jill Eeuwes for spending TWO summers in the lab, aiding in experiments, culture maintenance (haha!) and just being a friend.

Collaborators from The Marine Biological Institute Dr. Zoe Cardon and team deserve special recognition for providing algae cultures, and great enthusiasm and encouragement. Thank you to the examiners (both internal and external) for taking the time to be a part of this project.

Abstract

Poikilohydric organisms have developed mechanisms to protect their photosynthetic machinery during times of desiccation. In hydrated conditions nonphotochemical quenching (NPQ) mechanisms are able to safely dissipate excess excitation energy as heat, but mechanisms of NPQ associated with desiccation tolerance are still largely unclear. In the lichen *Parmelia sulcata*, photosystem protection has been associated with an energy quenching energetically coupled to PSII and characterized by a fast-fluorescence decay lifetime, and long-wavelength emission. The present study compares the relative ability of green algae and lichens to recover photosynthetic activity after periods of desiccation using steady state fluorescence emission spectroscopy, and picosecond time-resolved fluorescence decay measurements. It was determined that desiccation induced quenching involves an antenna quenching mechanism with similar characteristics appearing in both *P. sulcata* and green algae. Algae isolated from lichens suggest symbiosis in the lichen appears to enhance this naturally occurring phenomenon and provide greater protection during desiccation.

Summary

Vascular plants are unable to survive periods of desiccation, and have developed mechanisms by which they are able to control water loss. This is not the case for poikilohydric organisms that lack mechanisms to prevent desiccation, such as lichens and some green algae that live in soil crusts, and lose internal water in dry conditions. For these organisms, the development of mechanisms used to protect their photosynthetic machinery during times of desiccation is most important. In hydrated conditions, when absorbed light energy exceeds photosynthetic capacity, there are mechanisms (nonphotochemical quenching; NPQ) present in all photosynthetic organisms that are able to effectively compete with photosystems for excitation energy that can then be dissipated safely as heat. Mechanisms of NPQ associated with desiccation tolerance in poikilohydric organisms are still largely unclear. In lichens, photosystem protection has been associated with an energy quenching within the algae symbiont, energetically coupled to PSII and characterized by a fast-fluorescence decay lifetime, and long-wavelength emission. The present study compares the relative ability of green algae and lichens to recover photosynthetic activity after periods of desiccation. This study also used steady state fluorescence emission spectroscopy, and picosecond time-resolved fluorescence decay measurements to determine if fluorescence quenching in the green algae exhibits the same spectral and kinetic features as previously observed in lichens, and thus if there is one main mechanism of desiccation NPQ exhibited by all species. Results suggest that desiccation induced quenching involves an antenna quenching mechanism with similar characteristics appearing in both *Parmelia sulcata* and green algae. Symbiosis in the lichen appears to enhance this naturally occurring phenomenon and provide greater protection during desiccation.

Table of Contents

List of Tables:

List of Figures

Literature Review

Photosynthesis

Oxygenic photosynthesis is the process by which plants, green algae, and cyanobacteria convert solar energy, water, and carbon dioxide into organic compounds and oxygen (1). Photosynthesis is represented by two different reactions, the light and dark reactions, both taking place within the chloroplast (plants and green algae).

$$H_2O + CO_2 \rightarrow O_2 + CH_2O \quad (1)$$

The light reactions of photosynthesis produce ATP and NADPH by the conversion of solar energy. This process takes place within the thylakoid membranes via linear electron transport carried out by four major protein complexes, photosystem II (PSII), cytochrome b_6f ($Cytb_6f$), photosystem I (PSI) and ATP synthase.

Thylakoid membranes of plants are heterogeneous, divided into two continuous regions, stacked grana thylakoids, and unstacked stroma regions. Within the grana thylakoids are PSII and its associated light-harvesting complex (LHCII), while stroma thylakoids contain PSI and ATPases, with the $Cytb_6f$ complex evenly distributed between the two regions. Interestingly, the majority of green algae species lack extensive stacked grana regions, suggesting photosystems are evenly distributed throughout the thylakoid membrane (Gunning & Schwartz, 1999).

Upon absorbing photons, PSII splits water via a light dependent four-step process known as the Kok Cycle. Water splitting results in the release of protons into the stroma, thus contributing to the ΔpH across the thylakoid membrane required for the chemiosmotic production of ATP. After PSII absorbs a photon of light, charge separation results with subsequent redox mediated electron transfer to the final acceptor quinone

within PSII, Q_B. Q_B is protonated after two reduction reactions, leaves PSII and is free to move through the thylakoid membrane to the plastoquinone pool and $Cytb_6f$ complex. $Cytb_6f$ then reduces the electron carrier plastocyanin in a process releasing more protons to the lumenal side of the thylakoid membrane and increasing the electrochemical proton gradient. Reduced plastocyanin then shuttles electrons to reduce photochemically oxidized PSI. After charge separation in PSI occurs, the electron again is moved through a sequence of electron carriers bound to PSI, to ferredoxin, which then transfers the electron to the ferredoxin-$NADP^+$ reductase (Figure 1).

As PSII is responsible for the oxidation of water, and is the most highly prone to damage during times of stressful environmental conditions, it is the primary photosystem of interest in this study, and will be described in the most detail.

Photosystem II

PSII consists of about 20 polypeptide subunits with a combined molecular mass of 350kDa. The X-ray structure of PSII from the cyanobacterium *Thermosynechococcus vulcanus* has been resolved to 1.9Å providing a pigment count of 35 chlorophylls, 11 β-carotene, two pheophytin, two plastoquinone, two iron haems, one non-iron haem, the MN_4Ca cluster, three calcium ions (outside MN_4Ca cluster), three chlorine ions, one bicarbonate ion, with over 20 lipid molecules per monomer (Umena *et al*, 2011). A belt of 11 lipids surrounding the reaction centre was also resolved allowing for a mobile flexibility of PSII subunits which may play a large role in providing a slippery environment for protein insertion and removal during PSII repair from photoinhibition (Loll *et al*., 2005).

Each monomer contains three main structural domains, the transmembrane reaction core, the inner light-harvesting antenna, and extrinsic proteins bound on the

lumenal side of the protein complex. The inner light-harvesting antenna consist of two chlorophyll a antenna proteins CP43 and CP47, which transfer energy from the outer antenna to the reaction centre within the transmembrane reaction core. The core contains the heterodimer D1/D2 that represents the reaction centre, P680.

Light Absorbance of PSII

Absorbance of a photon by chlorophyll results in the excitation of an electron from the ground state, to an excited state (Figure 2). An excited state of chlorophyll is singlet chlorophyll (^{1}Chl) where the excited electron has an anti-parallel spin to the ground state electron. Once in the excited state, the electron falls to the lowest vibrational energy level of the excited state, releasing some energy as heat, called internal conversion (IC). If the electron is not moved through photochemistry, the singlet state allows for the transition back to the ground state, releasing the absorbed energy as fluorescence or heat. Energy may also be transferred to another pigment molecule by resonance energy transfer, if the second pigment has a suitable excited state energy, and is in a favorable position. This molecule may then lose the energy as fluorescence, heat or by energy transfer to a third molecule, and so on. The energy may also be transferred to a quenching molecule to be dissipated as heat (fluorescence quenching), or, the molecule may form a triplet state via intersystem crossing. Triplet chlorophyll (^{3}Chl) has an excited state electron spin parallel to the ground state spin, and therefore transition to the ground state is forbidden, thus the triplet state has a characteristically long lifetime (Figure 2). This long-lived triplet state increases the chances of ^{3}Chl interacting with oxygen to create harmful ROS.

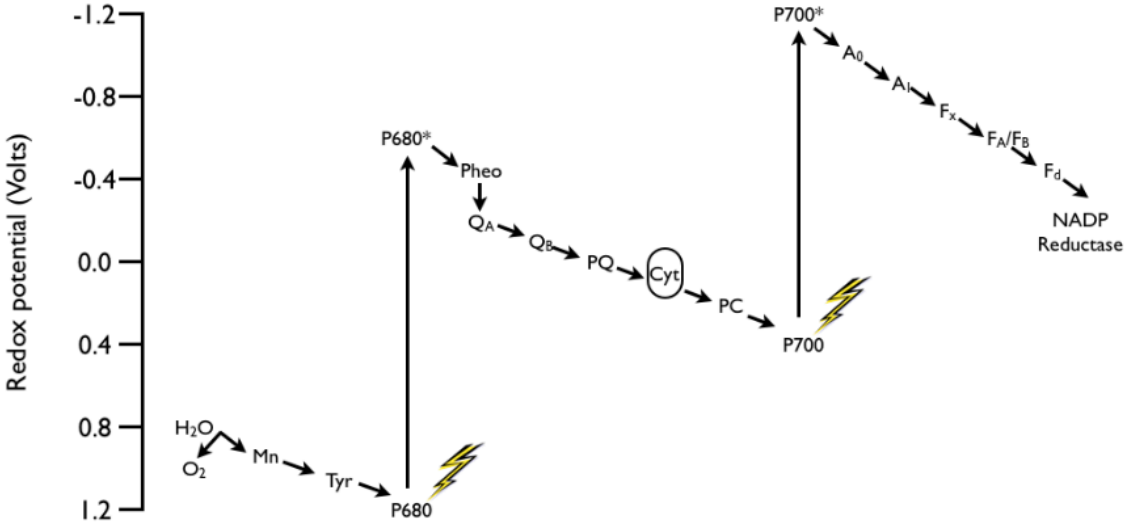

Figure 1: Z-scheme of photochemical electron transfer in photosynthesis indicating electron movement through carriers associated with both PSII (P680) and PSI (P700). Redox potentials of these carriers determine the linear electron flow between the two systems in the thylakoid membrane. The high redox potential of oxidized P680 (P680+) is the driving force for water splitting.

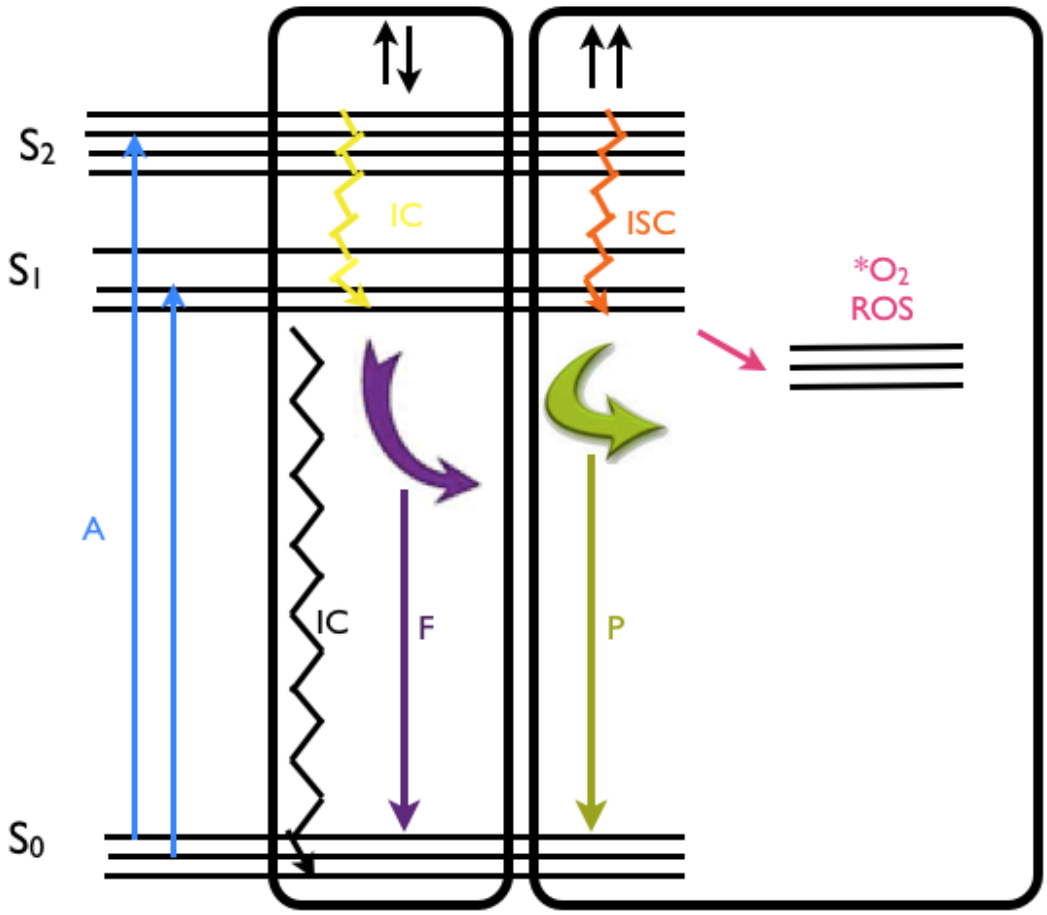

Figure 2: Jablonski diagram of the excitation of chlorophyll molecules and the different fates. Blue A shows the absorption of light energy and the excitation of electrons to higher energy orbital. In the case of singlet chlorophyll (shown within first black box) the excited electron is quickly dropped to the lowest level of S1 by internal conversion (IC). From here, the energy of the electron may be released as fluorescence as it returns back to the ground state, or, loses the energy thermally through non-radiative recombination. If the electron in the excited state becomes triplet chlorophyll through inter-system crossing (ISC), the electron may be potentially passed to an oxygen molecule creating ROS, or may return to the ground state by long-lived phosphorescence.

Energy Transfer and charge separation in PS II

Energy transfer begins in PSII with the excitation of chlorophyll antenna pigments by absorbed light, with subsequent energy transfer from outer antenna, to inner antenna ending at the reaction centre resulting in charge separation. Primary charge separation (simplified in Figure 3) begins with an accessory chlorophyll in the D1 subunit (Chl_{D1}), passing its electron to Pheophytin (Phe_{D1}). This is followed by the reduction of Chl_{D1} by one chlorophyll of reaction centre P680 on the D1 subunit (P_{D1}). This results in the formation of the radical pair (P_{D1}^{+} $Pheo_{D1}^{-}$). P_{D1}^{+} is reduced by tyrosine Z (Y_Z) that then is reduced by the oxygen-evolving complex (Holzwarth *et al*, 2006; Prokhorenko & Holzwarth, 2000). This stepwise radical pair formation is the basis of charge separation in PSII (2).

Chl_{D1}^{*} $Pheo_{D1}$ --> $Chl_{D1}^{+}Pheo_{D1}^{-}$ --> $P_{D1}^{+}Pheo_{D1}^{-}$ (2)

Photosystem II can exist in two different photochemical states that influence the measured fluorescence yield. The "open" state is when the primary quinone electron acceptor, Q_A, is oxidized and is able to accept a photochemically generated electron from $Pheo_{D1}^{-}$. Q_A can subsequently reduce Q_B, which then is free to diffuse through the membrane to the plastoquinone pool. The signature of an open PSII is a minimal fluorescence yield, termed F_O. The "closed" photochemical state is associated with exposure to high light and the saturation of photochemistry. Under these conditions, Q_A^{-} remains reduced and is unable to accept electrons. In this case, the energy of the radical pair cannot be "trapped" or stabilized by electron transfer to Q_A. This state is termed F_M and is characterized by the maximal fluorescence yield of PSII. The difference between these values (F_M –F_O) is the variable fluorescence, F_V, which is commonly used to

monitor effects of environmental stresses on PSII, and fluorescence quenching parameters. Using these measures, the overall "health" of PSII can be determined by a relative quantum efficiency calculated as F_V/F_M. This measurement roughly represents what percent of the absorbed photons are being utilized for photochemistry. The typical value for healthy plant leaves being about 0.8, no matter what the species (See reviews, Maxwell & Johnson, 1999; Krause & Weis, 1991). Terrestrial green algae have shown a value of below 0.6, (Luttge & Budel, 2010) and up to 0.7 only after long periods of dark adaption (Gray *et al*, 2007).

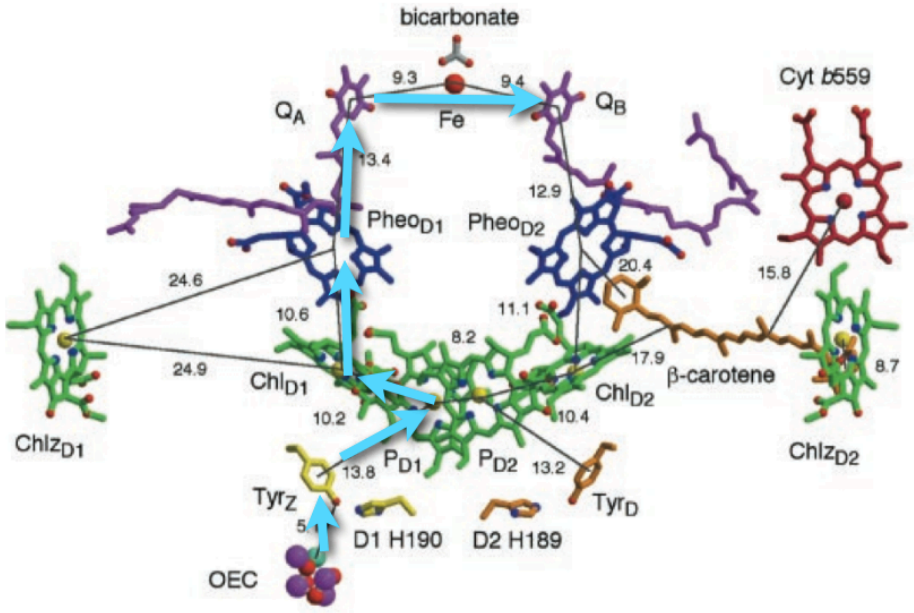

Figure 3: Electron transfer pathway through photosystem II indicated by blue arrows. While both D1 and D2 proteins contain the same pigment electron carriers, electrons are passed from the oxygen-evolving complex (OEC) mainly through carriers located within the D1 subunit. (Ferreira *et al*, 2004)

PSII Damage and Protection

High light and lack of water to act as an electron donor to PSII can cause extreme damage to the reaction centre leaving it inactive. Within one PSII dimer, there are a total of 2 795 water molecules at a given time (Umena *et al*, 2011). The main site of damage to PSII is to the D1 protein, and repair requires large amounts of protein synthesis. The D1 protein must first be removed from the complex and targeted for degradation. A new protein must be synthesized *de novo* and inserted into the membrane. In higher plants, this process also involves the moving of the PSII protein complex from the grana thylakoid region to the stroma, where repairs take place (For a review see Aro *et al*, 2004).

Fluorescence Quenching

Fluorescence quenching is a term used to describe any processes that reduces fluorescence yield below its maximum value. Photochemical quenching is most efficient (90% of absorbed photons) and involves electron transport through photochemistry. In high light environments, energy is quenched from the antenna complexes to reduce damage by dissipating excess energy as heat, preventing the formation of harmful reactive oxygen species (ROS). This process is termed non-photochemical quenching (NPQ) and is characterized by a decrease in photochemistry and fluorescence yield of PSII. There are two branches of NPQ involved in photoprotection, photoinhibition (qI) and energy quenching (qE). Photoinhibition is the photoinactivation of PSII when the rate of damage exceeds that of repair (Baena-Gonzalez *et al*, 1999) and has the slowest relaxation time (hours). Energy quenching on the other hand is influenced by changes in ΔpH, is rapidly induced and reversed (within seconds), and involves the recruitment

and/or rearrangement of pigment protein molecules to aid in energy dissipation via the xanthophyll cycle. NPQ can be determined through the equation $(F_M/F_M')/F_M'$.

The xanthophyll cycle involves three carotenoid proteins, violaxanthin in an inactive form, which is rapidly converted to zeaxanthin via the intermediate antheraxanthin (Figure 4). Zeaxanthin is able to bind to the outer PSII antenna complex and is thought to compete with the antenna for excitation energy (Jahns & Holzwarth, 2012). The PsbS subunit in higher plants is necessary in this process (Li *et al*, 2000) and becomes protonated under high acidity conditions and causes allosteric conformational change of LHCII to allow for zeaxathin binding (Horton *et al*, 2005). Green algae NPQ involves a different LHC like protein, LHCSR (Mou *et al*, 2012; Gagne & Guertin, 1992) but is hypothesized to work in a similar fashion.

Lichen Desiccation Survival

In periods of desiccation, lichens are still potentially exposed to high light within their environments. With the lack of intercellular water, repair mechanisms, protein synthesis, and other biochemical pathways are turned off and the organism is in a state of stasis. In order to protect the photosynthetic machinery, these organisms must either accumulate protective proteins (ie xanthophyll carotenoids) before they become desiccated, or, possess a different mechanism of protection to enable rapid growth when water becomes available. Unlike higher plants, lichens lack mechanisms to stop water loss, and are therefore exposed to repeated cycles of moderate to severe desiccation and rehydration. Times of desiccation in the lichen *Parmelia sulcata*, are characterized by a thallus grey in appearance (compared to green pigmented when hydrated), curled, and brittle to the touch. *P. sulcata* contains a *Trebouxia sp*. green algae photobiont, which loses internal cellular water resulting in a shriveling of the cells and chloroplasts,

accompanied by the shut down of photosynthesis activity, and quenched fluorescence yield (Veerman *et al*, 2007; Heber *et al*, 2010). To ensure growth can occur quickly when water becomes available, a protective mechanism to circumvent lengthy and costly repairs would be a strong advantage.

Table 1: Fluorescence measurement equations using parameters noted in Figure 7. For reviews see Maxwell & Johnson, 2000; Schreiber, 2004. Parameters denoted with ' indicate the measurement was taken while illuminated.

Fluorescent Parameter	Abbreviation	Formula	Definition
Basal Fluorescence	F_O		Open Centre, Q_A^+
Maximal Fluorescence	F_M		Closed Centre, Q_A^-
Variable Fluorescence	F_V	F_M-F_O	
Fluorescence Transient	F_T		Steady-State Yield, Illuminated
PSII Efficiency	Quantum Efficiency	F_V/F_M	% Absorbed Photons Dark Adapted
PSII Efficiency	ΦPSII	$(F_M'-F_T)/F_M'$	% Absorbed Photons Illuminated
Maximum PSII Efficiency	F_V/F_{Mmax}	ΦPSII/qP	% Absorbed Photons Illuminated, All Centres Open
Nonphotochemical Quenching Broad term including:	NPQ	$(F_M/F_M')/F_M'$	Lower Fluorescence Below maxima
•Photochemical Quenching	qP	$(F_M'-F_T)/(F_M'-F_O')$	Proportion of Open Centres
• Energy Quenching	qE		Fast Relaxation
• Photoinhibitory Quenching	qI		Slow Relaxation

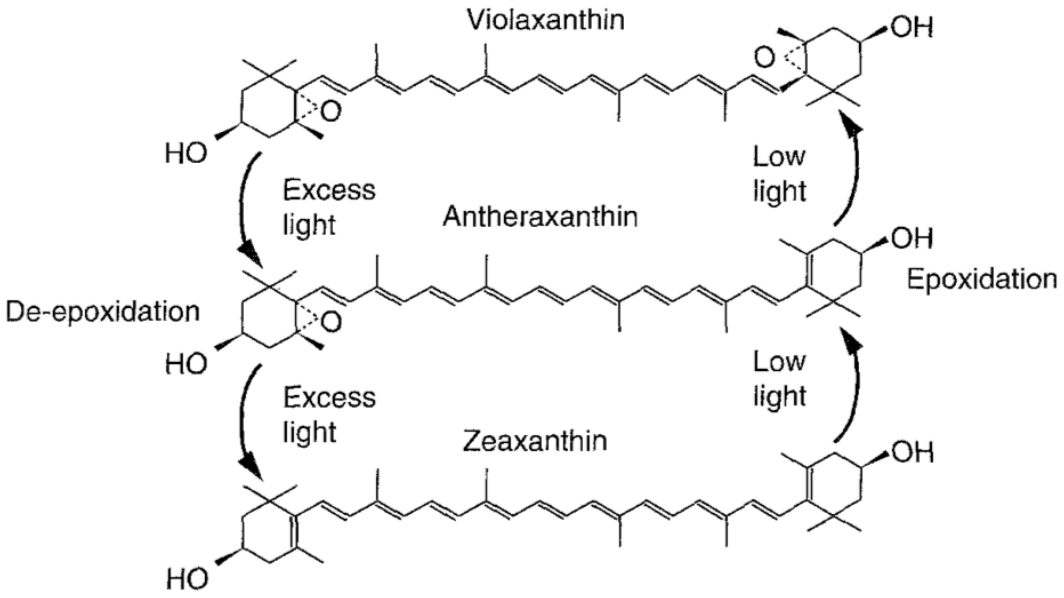

Figure 4: Xanthophyll cycle from violaxanthin to zeaxanthin during high light exposure. Violaxanthin de-epoxidase is the enzyme catalyzing de-epoxidation reactions from violaxanthin through the intermediate antheraxanthin to zeaxanthin. Zeaxanthin is then able to bind with LHCII to effectively compete with PSII RC for excitation energy. This energy is then dissipated as heat. When high light levels decrease, epoxidation reactions are then catalyzed to turn zeaxanthin back into violoxanthin. Image From Demmig-Adams & Adams, 1996

Protection by Lower Light Absorbance

To protect the photosynthetic machinery from excess light, the lichen thallus undergoes morphological changes to reduce the amount of light reaching the algae cells. This is accomplished by desiccation induced curling of the lichen upper cortex in all types of lichens (Bartak *et al*, 2006, Lumbsch & Kothe, 1988). A similar type of behaviour has been shown in desiccation tolerant plants (Alpert & Oliver, 2002). Bartak *et al*. (2006) showed thallus curling significantly decreased photodamage to cells versus uncurled. Loss of surface pigmentation has been shown to increase light scattering during desiccation, which also aids in decreasing the amount of light available for absorption by the photobiont (Heber *et al*, 2006). While these mechanisms are helpful they only play a partial role in photoprotection (20%) during desiccation (Heber *et al*, 2011; Veerman *et al*, 2007). When analyzing fluorescence emission of lichen in a hydrated and desiccated state, the fluorescence kinetics has been shown to differ, suggesting additional photoprotective mechanisms within the photobiont (Veerman *et al*, 2007).

Protection by Fluorescence Quenching

Parmelia lichens desiccated in the dark show a slow decline in fluorescence values, F_O, F_V, and F_V/F_M until approximately 30% relative water content, where there is a sharp reduction (Calatayud *et al*, 1997). In this desiccation state, F_O remains significantly lower than in the hydrated state, with no induction of F_M with saturating light pulses (Veerman *et al*, 2007, Calatayud *et al*, 1997). Drastic lowering of F_O and F_M fluorescence parameters suggests a strong photoprotective mechanism of the PSII-LHCII, and the reaction centre. The drastic decrease in F_O fluorescence level indicates a quenching mechanism present that is able to thermally deactivate excess energy faster than can be trapped by the reaction centre, owing to the lack of F_V in the desiccated state

(Heber & Luttge, 2011). Low temperature (77K) steady-state measurements show a fluorescence yield 10x lower in the desiccated lichen compared to the hydrated. The remaining emission is dominated by the PSI fluorescence peak and there is no indication of PSII fluorescence at 685 and 695nm or of a 760nm shoulder of unknown origin, all normally observed in hydrated lichens, thus suggesting a highly effective quenching mechanism coupled to PSII (Veerman *et al*, 2007; Komura *et al*, 2008; Heber & Shuvalov, 2005). Upon rehydration of desiccated lichens, F_O increases instantly, with F_V increasing within a few seconds indicating a very fast reversibility of desiccation-induced fluorescence quenching (Veerman *et al*, 2007; Calatayud *et al*; 1997, Heber *et al*, 2009).

In attempts to determine the identity of the quencher, the xanthophyll carotenoids have been studied in a number of lichens. In, *Parmelia sp*., and *Lobaria pulmonaria*, the xanthophyll cycle has been reported to play a role in desiccation induced NPQ (Heber *et al*, 2009; Calatayud *et al*, 1997). This however remains controversial, as this result varies depending on experimental methods and species used (Fernandez-Marin & Becerril, 2010; Heber *et al*, 2010). In addition, time-resolved fluorescence spectroscopy has shown the presence of quenching mechanisms displaying faster kinetics than shown by xanthophyll quenching, and thus focus has been shifted towards the identification of desiccation induced photoprotective mechanisms that are independent of the xanthophyll cycle (Veerman *et al*, 2007).

Using time-resolved and steady state fluorescence measurements, Veerman *et al* (2007) were able to observe a novel chlorophyll pigment species with long-wavelength emission present in both hydrated and desiccated lichen thallus of *Parmelia sulcata.* Fluorescence decay kinetics and decay associated spectra (DAS) showed a shortening of

excited lifetime of this species upon desiccation, indicative of a quencher capable of fast energy dissipation. The DAS of this quenching component showed two distinct peaks (680 and 740nm) at 77K. The presence of this quencher showing DAS with an identical shape to PSII emission suggests a strong energetic coupling to PSII antenna (Figure 5). This result was confirmed by Miyake *et al*, (2011) who by using higher resolution time-resolved measurements at 5K were able to hypothesize the location of this "quenching" component to be within the peripheral PSII antenna. Rapid isolation of the photobiont from the lichen thallus and the resulting time-resolved fluorescence measurements showed consistent lifetime components and DAS spectra in the hydrated *Trebouxia sp.* algae to those present in intact lichen thalli, showing these lifetimes were indeed originating from the algal component (Miyake *et al*, 2011).

Quencher Identity

These quenching species are hypothesized to be representative of a chlorophyll-chlorophyll charge transfer (CT) state formed by the aggregation of chlorophyll molecules within close proximity in LHCII. Charge transfer states show a shift in wavelength of the emission to the red by the overlap of excited states and the passing of charge between a donor and acceptor chlorophyll (Heber *et al*, 2006; Heber & Shuvalov, 2005; Veerman *et al*, 2007, Miloslavina *et al*, 2008). This correlates with the presence of the unique spectral characteristic of a fluorescence shoulder present at ~760nm in lichen fluorescence emission spectra, which becomes quenched in desiccated lichens (Veerman *et al*, 2007, Heber & Shuvalov, 2005). The formation of oligomers of LHCII under NPQ conditions in the higher plant *Arabidopsis thalliana,* resulted in a broad spectral shape and far-red fluorescence enhancement much like that seen in lichens (Johnson & Ruban,

2009; Miloslavina *et al*, 2008), suggesting perhaps a similar mechanism of protein conformational changes.

Microscopy and electron paramagnetic resonance (EPR) spectroscopy measurements of desiccated plant leaves (of resurrection plants) and lichen green algae have shown there is a drastic difference in chloroplast structure and thylakoid membrane organization in desiccated compared to hydrated samples. Desiccation causes a compaction of algae layers with decreased space between the algae and the lichen cortex. Photobionts experience a collapsing of their cell walls during desiccation, becoming star-shaped instead of oval, with a drastic decrease in cellular volume (Brown *et al*, 1987; Scheidegger *et al*, 1995). Algae cells have reduced cytoplasm and chloroplasts with densely packed thylakoids (de los Rios *et al*, 1999). Interestingly, photosynthetic ability was still found in cells that were semi-collapsed providing some insight into the fast rehydration nature of lichens. The use of the protein cross-linker glutaraldehyde by Heber *et al*, (2011) on a lichen showed the inhibition of desiccation induced fluorescence quenching, and heating desiccated lichens to 80°C, reversed the desiccation-induced loss of fluorescence (Heber & Shuvalov, 2005; Heber, Azarkovich & Shuvalov, 2007), suggesting photosystem conformational changes are indeed required for survival and in bringing together proteins and pigment molecules for thermal energy dissipation.

Green Algae Desiccation Survival

The most common green algae photobionts are *Trebouxia sps*. (75%; Green *et al*, 2002) which are rarely seen living outside symbiosis, which raises the question, is green algae desiccation survival a trait that requires symbiosis? Previous studies documenting the desiccation tolerance of green algal symbionts isolated from their lichen partner have shown anti-oxidative and photoprotective mechanisms to be orders of magnitude lower in

isolated algae vs. in symbiosis, stemming from the lack of protective free-radical scavengers and UV- protective proteins provided by a fungal partner (Kranner *et al*, 2005; Ramakrishnan & Subramain, 1966). Isolated algae were also shown to not fully inactivate photosynthetic machinery, resulting in a lower level of fluorescence quenching, and a higher sensitivity to light in the desiccated state (Kosugi *et al*, 2009) but still able to still survive periods of desiccation with F_v and F_o quenching, much like in the intact lichen (Wieners *et al*, 2012). Addition of lichen extracts to the isolated algae showed improved desiccation tolerance, leading to the hypothesis that the strong PSII quenching observed in desiccated lichens is a result of concurrent mechanisms provided by both the algae and fungus in the form of unique secondary metabolites (Kosugi *et al*, 2009; Kosugi *et al*, 2013).

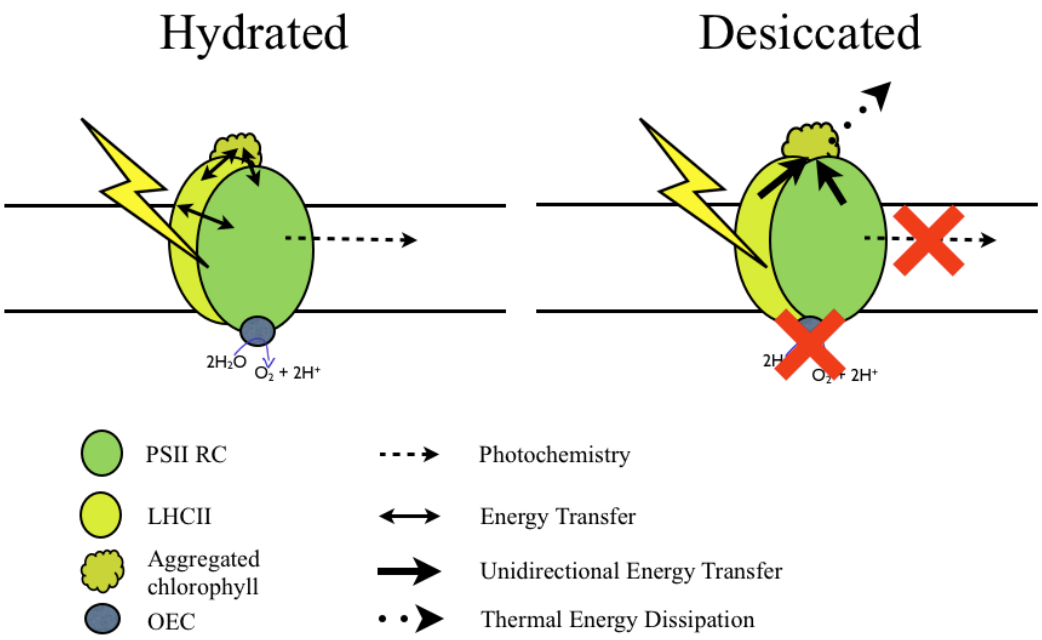

Figure 5: Simplified schematic of desiccation induced fluorescence quenching associated with lichen LHCII. In the hydrated state, water is oxidized by the oxygen-evolving complex (OEC) and electrons are used for photochemistry. Energy transfer in this state is in equilibrium between LHCII and its associated aggregated chlorophylls, and the reaction centre (PSII RC) as determined by the fluorescence signatures of each species present at low temperature (Veerman *et al*, 2007). Upon desiccation, when water oxidation and photochemistry is blocked, desiccation induced nonphotochemical quenching is induced by an increase in chlorophyll aggregation in LHCII, forming a highly effective quencher. Excitation energy is successfully funneled to the quencher from other areas of the LHCII and RC, as denoted by the thick arrows. Energy is safely dissipated as heat as seen by the quenching of F_O and F_M, and no fluorescence detected from PSII and its associated long-wavelength peak in fluorescence emission spectra.

The drastic morphological and physiological changes that occur in photobionts during symbiosis, such as an increase in cell and chloroplast size, inability of cells to reproduce, and overall genetic reprogramming in response to symbiosis (Green & Smith, 1974; DePriest, 2004; Joneson *et al*, 2011), leads to the question of whether lichens are a suitable comparison/model for free-living green algae. Free-living green algae are most thought of being associated with aquatic environments, however some green algae have adapted to terrestrial environments and live in a wide range of habitats and niches. Green algae are found in arctic (Davey, 1989) and desert soil crusts (Gray *et al*, 2007), tree bark (Luttge & Budel, 2010) and man-made surfaces (Karsen *et al*, 2007). Without the help of a symbiotic partner, these algae must adapt to periods of drought, as well as fluctuating weather patterns, and increased probability of exposure to high light in both the hydrated and desiccated state, on their own. The ability to regain moisture from humid air to support photosynthesis has allowed green algae to live in terrestrial areas that may not have frequent rainfalls, or a permanent source of water (i.e. tidal zone of lakes/oceans). Both filamentous (Holzinger *et al*, 2011; Holzinger *et al*, 2010) and unicellular terrestrial green algae (Luttge & Budel, 2010; Gray *et al*, 2007) have been characterized in terms of their desiccation survival demonstrating that symbiosis is not the only way to survive in these environments.

Studies of terrestrial green algae in algal mats on tree bark and within desert crust ecosystems have provided preliminary information that their desiccation-induced fluorescence quenching is quite similar to that of lichens (Gray *et al*, 2007, Luttge & Budel, 2010). Desiccation of green algae on tree bark show these algae can withstand periods of desiccation up to 80 days before seeing adverse effects (Luttge & Budel,

2010). Despite being exposed to sunlight in the desiccated state, the cells remain pigmented, and maintain a consistent chlorophyll concentration. Similar quenching kinetics to lichens were observed with an increase of quenching of F_O, and a decline of F_V/F_M during desiccation, leading to inactivation of PSII which was rapidly reversible within 60 seconds of rehydration (Luttge & Budel, 2010), with F_V/F_M reaching almost that of pre-desiccation within an hour of rehydration in the dark (Gray *et al*, 2007).

Desert Crusts

Desert crusts are rapidly becoming an area of interest regarding desiccation survival due to the large diversity of organisms that make up these crusts, including lichens, cyanobacteria, diatoms, and green algae. A recent survey by the members of the Biotic Crust Project (http://pediastrum.eeb.uconn.edu/) has shown a large amount of diversity of green algae within desert crusts representing three major algal classes, Chlorophyceae, Trebouxiophyceae and Charophyceae (Lewis & Flechtner, 2002), which typically contain fresh water species of green algae. Desert crusts are 1mm-5mm in depth, with green algae inhabiting the first 50-100μm (Hu *et al*, 2003; Figure 6). Green algae have been found living in soils containing gypsum, limestone and sandstone, varying levels of pH (including highly acidic), high salinity, and cold temperatures demonstrating their ability to survive in the most extreme of environments (for review see Lewis, 2007). A sample soil crust from Baja California, Mexico, was shown to contain 37 taxa in 19 genera of green algae, including those most commonly found in lichen symbiosis (Flechtner *et al*, 1998). Desert algae collected and studied for desiccation tolerance (Gray *et al*, 2007) have shown the ability of desert algae to regain photosynthetic ability after desiccation under both dark and light illumination trials, out of the crust ecosystem. Using a controlled relative humidity air stream, desert algae were

shown to survive desiccation for up to 4 weeks (furthest time point in the study) in darkness, but when exposed to light not all species recovered suggesting some photosensitivity when removed from their protective niche. These algae, like those on tree bark, and in lichen thallus, showed a high desiccation-induced quenching of both F_O and F_V, which was reversible to high levels of F_V/F_M. This study showed maximal F_V/F_M recovery after 1 hour, a slower time scale than observed in lichens, however rehydration using 100% RH air stream is a much slower process than addition of aqueous water (Gray *et al*, 2007; Scheidegger *et al*, 1995). Given the evolutionary lineage from aquatic to terrestrial environment, aquatic taxa were also examined for desiccation survival (Lewis & Lewis, 2005; Gray *et al*, 2007). Aquatic algae recovered very little after desiccation for only 24 hours, after which if illumination was applied, recovery was increased by *de novo* protein synthesis.

Current Study

The study by Gray *et al* (2007) provides a framework for investigating the evolution of green algae from aquatic to terrestrial habitats- both desert and in symbiosis. This transition has been shown using 18S rDNA to have occurred 14 separate times (Lewis & Lewis, 2005), allowing the opportunity to determine if the ability to survive desiccation is the same for all green algae species in desert crusts. Considering the evolutionary lineage of green algae from aquatic to terrestrial environments allows us to determine how selective pressures have sculpted protection from desiccation. As lichens remain the best-studied desiccation-protected organism, we are able to compare desert algae desiccation strategies to those of lichens. Did symbiosis involve the induction of a novel desiccation survival strategy, or the enhancement of a preexisting one in the future photobiont? In this thesis, these questions have been addressed using both time-resolved

and steady state fluorescence spectroscopy of six different green algae species, lichen (*P. sulcata*) and associated symbiont (*Trebouxia sp.*), *Chlorella sp.* (desert and aquatic relative), and *Scenedesmus sp.* (desert and aquatic relative).

Hypotheses

It is hypothesized that lichen symbiosis enhances a desiccation quenching mechanism present within symbiotic algae. *Trebouxia sp*. isolated from lichens and desert dwelling green algae will exhibit desiccation tolerance, the distinct 760nm spectral shoulder and time-resolved fluorescence spectroscopy will reveal similar quenching signatures for desiccation induced quenching. Aquatic green algae are hypothesized to be unable to survive periods of desiccation and not show the fluorescence quenching characteristics.

As *Chlorella sp.* BC4VF9 is more closely related to the *Trebouxia sp.* found within *P. sulcata*, it is hypothesized that it will show the highest desiccation tolerance of the two desert species tested. It is hypothesized that desiccation tolerance observed by either desert dwelling algae will be less than that recorded for *P. sulcata*, as shown in previous literature, they lack the extra protection provided by a fungal symbiont.

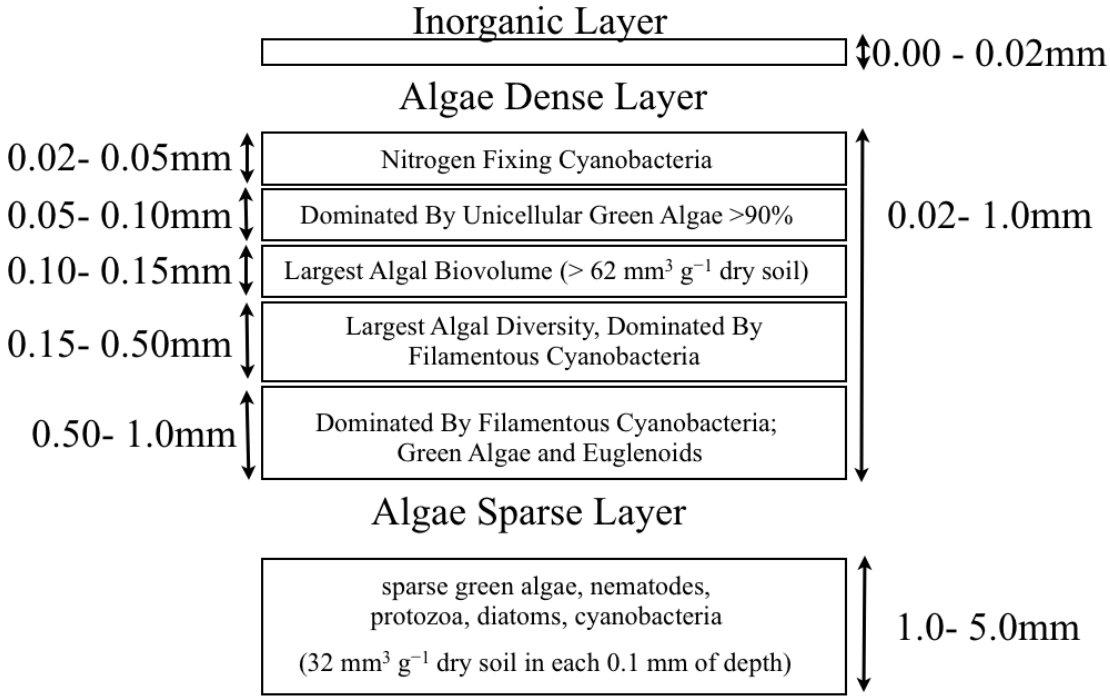

Figure 6: Stratification of desert crust ecosystems. Primarily dominated by filamentous cyanobacteria, desert crust ecosystems not only make up the largest percentage of desert primary production, excretions from organisms within hold together soil and prevent soil surface erosion. Nitrogen fixing cyanobacteria also provide usable nitrogen for the small amount of plants that live in deserts. Specific values in this figure reported from study by Hue *et al*, 2003, from 5 different desert crust sites located in Shapotov, China.

Experimental Approach

A combined fluorescence spectroscopic approach (steady-state, time-resolved and pulse amplitude modulated (PAM) fluorometry) was applied to compare the relatedness of desiccation induced fluorescence quenching (dNPQ) in free-living green algae species, to algae living in a symbiotic relationship within the lichen *P. sulcata*. Room temperature PAM spectroscopy was utilized to determine the real-time physiological response of green algae and lichen to desiccation and highlight stress in the hydrated state. These measurements allow for the determination of various fluorescence parameters that are used to measure photosystem II efficiency during environmental stress and the subsequent recovery. Two specific quenching mechanisms of the general NPQ assignment, energy quenching (qE; the xanthophyll cycle) and photoinhibitory quenching (qI; photoinhibition, photodamage and subsequent repair) were characterized for each species. Appropriate inhibitors were then used to block each of theses responses in hydrated samples to determine their role and relative contribution to dNPQ.

Steady-state fluorescence measurements involve the constant illumination of a sample with a light source and collection of fluorescence emission spectra. These spectra show the wavelength and relative emission intensity of chromophores associated with the two photosystems within the intact algae cells or lichen. Steady-state measurements were used to determine of the presence of spectral characteristics hypothesized to be markers for desiccation tolerance in free-living green algae. These characteristics are the appearance of a 760nm fluorescence shoulder at 77K, and the preferential dNPQ of this shoulder, as well as photosystem II specific wavelengths (685-695nm) as first noted by Veerman *et al*. (2007).

Time-resolved fluorescence measurements are taken with a pulsed laser source to characterize fluorescence emission in more depth, by determining fluorescence lifetimes. Time-resolved measurements were taken to determine if the origin of this observed steady-state dNPQ was derived from the same long-wavelength fast lifetime quencher identified in *P. sulcata* and hypothesized to be located within the PSII antenna LHCII (Veerman *et al*, 2007; Miyake *et al*, 2011).

Both steady-state and time-resolved fluorescence measurements were taken at 77K to allow for visualization of both photosystems and their primary light reactions as low temperature inhibits any other photosynthetic process such as electron transport (Krause & Weis, 1984). At 77K energy transfer is predominately energetically downhill, opposed to room temperature where physiological temperatures permit some uphill energy transfer. Therefore, at 77K, energy tends to be trapped on the longest wavelength pigments, thus creating the various PSI and PSII associated peaks. Ultimately, spectral analysis at 77K allows for isolation of components that would be difficult or impossible to spectrally and kinetically resolve at room temperature. In previous literature regarding desiccation induced quenching in lichens, low temperature studies have been utilized to find specific spectral quenching characteristics, and to help aid in the location of these quenching sites within PSII (Veerman *et al*, 2007; Miyake *et al*, 2011).

Methodology

Algal Growth

Algal species were obtained from Dr. Zoe Cardon at the Marine Biological Institute (Woodshole MA) (Table 2). Algae were grown on their respective media on agar slants, with single colonies transferred to liquid media when required. Both slants and liquid cultures were grown on bench top at a temperature of 25^{o}C, under a 400W Metal Halide high intensity discharge growth light (Sunmaster) at an intensity of ~35 µE (15 hours light and 9 hours dark) and bubbled continuously with ambient air (as per instructions by Dr. Cardon *et al*.) Algae species were grown in liquid culture or allowed to colonize on 2mm diameter glass beads (SIRAN #4711, Jaeger Biotech Engineering, Costa Mesa, California) to be used for spectroscopic analysis (Figure 7A). Each algal species was grown in a different growth media depending on the nutritional requirements. Free-living green algae cultures and isolated algae were all started from a single colony grown on an agar slant, these results are indicative of algae cells with low genetic variation between each other.

Lichen Collection

P. sulcata lichen thalli were collected off tree bark on Brock University campus between a range of 4ft-6ft on the Northern facing side of the trunk. Lichens were collected when hydrated for ease of thalli removal, and transferred back to the laboratory. Lichens were then stored desiccated in the dark. Lichens were rehydrated under the PAM fluorometer prior to experimental use to determine the relative PSII activity of the lichen and that it was indeed in a hydrated state before subsequent experiments regarding desiccation and rehydration.

Isolation of *Trebouxia sp.*

Lichens were washed in distilled water continuously for 5 minutes to remove any bacterial/algal components that may be colonized on the thallus. Using tweezers and a dissecting microscope, top layers of thallus were scraped off in an attempt to expose just the photobiont layer. The lichen was then picked up with tweezers, flipped upside down and rubbed on an agar plate of algae growth medium Bold's Basal Media (BBM) without micronutrients (Bold, 1949), and placed with the algae flasks. Under these conditions the algae component will outgrow the fungal component and single colony collection is possible (Ahmadjian, 1967). Once there was growth on the plate (green colonies, pink colonies, and fungal masses) green cultures were picked and transferred to a new BBM plate and allowed to grow (under the same light conditions). Once there were green individual colonies, one was selected and transferred to a smaller flask of 5mL of BBM. Once green, a drop of culture with a scraping from the bottom of the flask and a drop from just the liquid above were placed on a microscope slide and examined for contaminants. Culture was transferred to a larger flask and allowed to grow for testing. A simple desiccation/rehydration test monitoring F_V/F_M on the PAM fluorimeter and 77K fluorescence emission spectra were used to confirm algae symbiont.

Desiccation Recovery Tests

Algae were taken from respective growth beakers and beads were placed in a self-made rehydration chamber. This chamber is made of a small petri dish (Diameter 7.62cm, 1 petri dish makes two- using lid and bottom) with a piece of cheesecloth, and a small square of plexiglas with a hole the size of the PAM fiber optic (diameter 3.81cm) in the middle to hold algae beads in place (Figure 7B). Plexiglas was attached to the cheesecloth using hot glue so they did not separate and release the beads. Chambers with beads were

placed in the dark to desiccate by equilibrating with the relative humidity of the air (45% RH) at room temperature (~22ºC). Samples were held desiccated for at least 24 hours or longer. Desiccation was checked using the PAM fluorimeter (Figure 7C) to have a F_V/F_M of 0.1 or less. Rehydration was preformed by adding 0.5mL of growth media (distilled water for lichen thalli) to the chamber by allowing the water to wick up the cheesecloth so the beads were not physically disturbed.

Pulse Amplitude Modulated (PAM) Fluorimetry

Rehydration and subsequent return of F_O, F_V and F_V/F_M fluorescence was monitored using a PAM fluorimeter (Figure 8). The sample was subject to a saturating light pulse (SLP) of 1450μE to determine FM (Gray *et al*, 2006; Gray *et al*, 2007). SLPs originated from a purpose built light box using a high luminous efficacy neutral light white LED (LZI-00NW00, LED Engin, California). The first SLP was applied while the sample was desiccated, and then liquid was added so as the next SLP was to a hydrated sample. Rehydration curves were saved via a laboratory built analog to digital converter controlled by purpose-designed software emulating a chart recorder. The software recorded a variety of fluorescent parameters after each SLP. Calculation of yield and quenching measurements were determined from these parameters using the equations described in table 2. Typically a rehydration test is 10 minutes in length (unless otherwise stated) with SLP every 60 seconds. Every SLP was 300ms in duration, followed by a 1 second illumination of far-red light to stimulate PSI and oxidize the plastoquinone pool before the next measurement. Unless otherwise stated F_O measurements were obtained with a blue measuring beam of light intensity 0.06μE at 1.6kHz (Gray *et al*, 2007).

Table 2: Algae and lichen species used in this study, with corresponding habitat and catalog information, listed by desiccation rehydration ranking. *Trebouxia sp.* denoted with symbiotic habitat (S) represents *P. sulcata*, but named for the associated green algae species, where *Trebouxia* isolate is algae after being cultured from symbiosis (C). As these species were collected on Brock University campus and subsequently isolated in lab, there is no corresponding catalog number. As exact locations of all algae species utilized are mostly unknown, habitats are generalized to either desert (D) or aquatic (A) habitats.

Catalog Number	**Family**	**Genus**	**Species**	**Habitat**
N/A	Trebouxiophyceae	*Trebouxia*		S
N/A	Trebouxiophyceae	*Trebouxia*	Isolate	C
SEV3VF49	Chlorophyceae	*Scenedesmus*	*rotundus*	D
BC4VF9	Trebouxiophyceae	*Chlorella*		D
UTEX318	Trebouxiophyceae	*Chlorella*		A
CCAP276/31	Chlorophyceae	*Scenedesmus*	*costatus*	A

S = Symbiotic
C = Cultured from symbiosis
D = Isolated from desert crust
A = Aquatic fresh water habitat

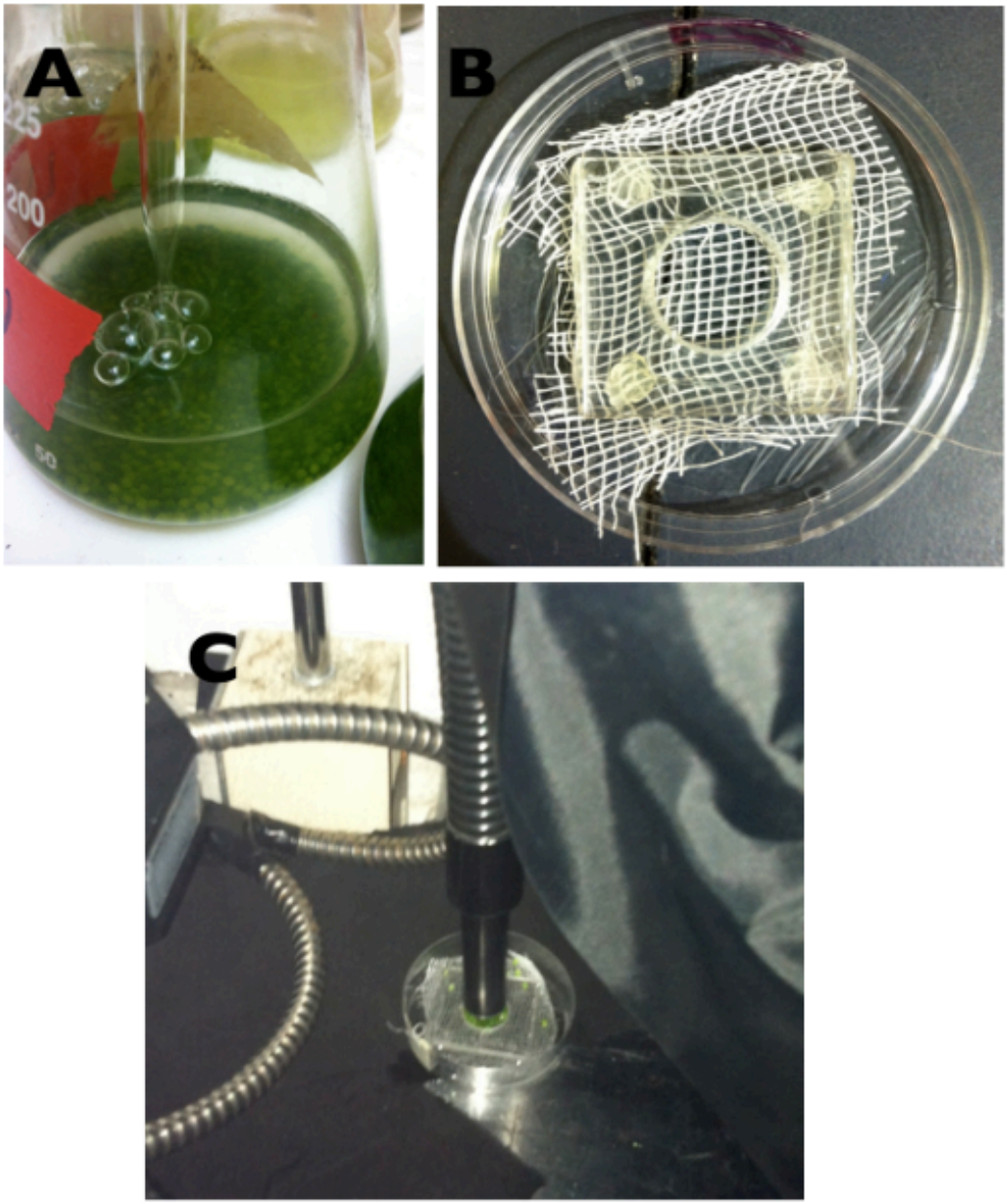

Figure 7: Examples of experimental set-ups used in this study. (A) The algal colonies were grown in the appropriate liquid medium and bubbled with ambient air supplied by an aquarium pump. Sterilized glass beads were added to the bottom of algae growth flasks and algae were allowed to colonize on the beads. (B) Sample holder made to hold beads for PAM fluorimetry. Plexi glass was cut into squares and (C) circles drilled into the middle the size of the PAM fiber optic. Desiccation occurred in these sample holders, and rehydration by adding water to the exposed cheesecloth and allowing it to wick up and rehydrate the algae beads.

Rehydration Light Recovery

Samples were rehydrated as described above starting with control light intensity (0.06μE) and then with subsequent increases in light intensity. The objective was to determine the effect of light on the photosynthetic apparatus and ability of algae/lichen samples to recover from desiccation. Some of the lower light intensities were applied by switching the PAM fluorometer from 1.6kHz, to 100kHz repetition rate, which resulted in an increase in light intensity during F_O recording, thus the 4 and 9μE measurements were collected under the blue measuring light of the PAM. A lab made actinic light using a neutral white light source was used to obtain the higher light intensities.

Photoinhibition

For green algae a high light treatment of 2200μE was applied for 1 hour to induce photoinhibition, as it has been shown to cause damage, degradation and subsequent repair cycles to D1 every 20 mins compared to once every 7 hours in low light intensities (Kim *et al*, 1993). In lichen thalli the light intensity was 4200μE for 1 hour, to ensure the algae in the lichen were exposed and damaged. Both lichens and algae were given 15-minute period of darkness after high light exposure to provide relaxation of NPQ mechanisms. D1 turnover is a light dependent process and therefore 25μE of light were applied to the sample during the 1 hour recovery period (Singh *et al*, 1996; Lidholm *et al*, 1987). Control samples were exposed to high light treatment and recovery light without the application of antibiotics. In addition, antibiotic controls, in darkness, were used to determine any non-specific damaging effects on photosynthesis not related to photoinhibition. In these, F_V/F_M measurements were taken under 25μE illumination for 30 minutes.

de novo Protein Synthesis Inhibition Tests

Photoinhibition: Chloramphenicol & Cycloheximide

The broad-spectrum antibiotics chloramphenicol and cycloheximide treatments are routinely used in photosynthetic studies to determine the necessity of *de novo* protein synthesis (Gibbs, 1979; Ohad *et al*, 1984; Lai *et al*, 2009 and more) specifically in testing the role in desiccation recovery (Proctor & Smirnoff, 2000; Proctor *et al*, 2007). Chloramphenicol is used to inhibit chloroplast protein synthesis by inhibiting protein elongation by blocking translation on the 70S chloroplast ribosomal subunit by peptidyltransferase (Sigma-Aldrich, 2011). Application of chloramphenicol to eukaryotic fungi and yeasts shows no effect, suggesting nuclear encoded protein synthesis to be untouched (Brock, 1961). Cycloheximide is used to inhibit protein synthesis in the cytosol of eukaryotic organisms (Ford & Leach, 1948). Cycloheximide inhibits the binding of the translocase enzyme aminoacyl-tRNA to the ribosomes, and prevents the translocation of messenger RNA on the cytosolic 80S ribosome. The initiation of peptide synthesis is inhibited as well as the elongation of the peptide by the addition of amino acids from aminoacyl- tRNA. Organelle functions remain unaffected (Obrig *et al*, 1971). In photoinhibition studies, cycloheximide has been shown to inhibit D1 protein degradation, while chloramphenicol inhibits the translation of *de novo* D1 synthesis (Trebst & Soll- Bracht, 1996)

Determination of an effective antibiotic concentration for the best effect on *de novo* protein synthesis was achieved by monitoring the recovery from photoinhibition. Chloramphenicol was started at 500µg/ml in tests on lichen thallus and *Chlorella sp.* BC4VF9 and then the concentration increased based on literature values for bryophytes. Chloramphenicol treatments were 2mg/ml for 3 hours (Hader *et al*, 2002), while

cycloheximide was 1.9mg/ml for 2 hours. Concentrations of both inhibitors used in this study were higher than what has been reported in the literature for green algae to account for a greater concentration of algae on the glass beads, and to assure the antibiotic reached the algae cells within the lichen. Recovery was monitored under the PAM to determine the amount of damage endured by the sample, and at what concentration of antibiotics did recovery cease.

Appropriate concentrations of chloramphenicol (Figure 9A) and cycloheximide (Figure 9B) to inhibit *de novo* protein synthesis in lichens and algae have been determined by monitoring photoinhibition under highlight treatment (Lidholm *et al*, 1987). Photoinhibiton of PSII occurs when the rate of damage exceeds the rate of repair. The D1 subunit of the reaction centre must be synthesized *de novo* on chloroplast ribosomes, a process that requires the aid of a nuclear encoded regulatory protein complex (Baena- Gonzalez & Aro, 2002). Newly synthesized D1 is inserted and reassembled into thylakoid membrane and PSII (review Kato *et al*, 2012).

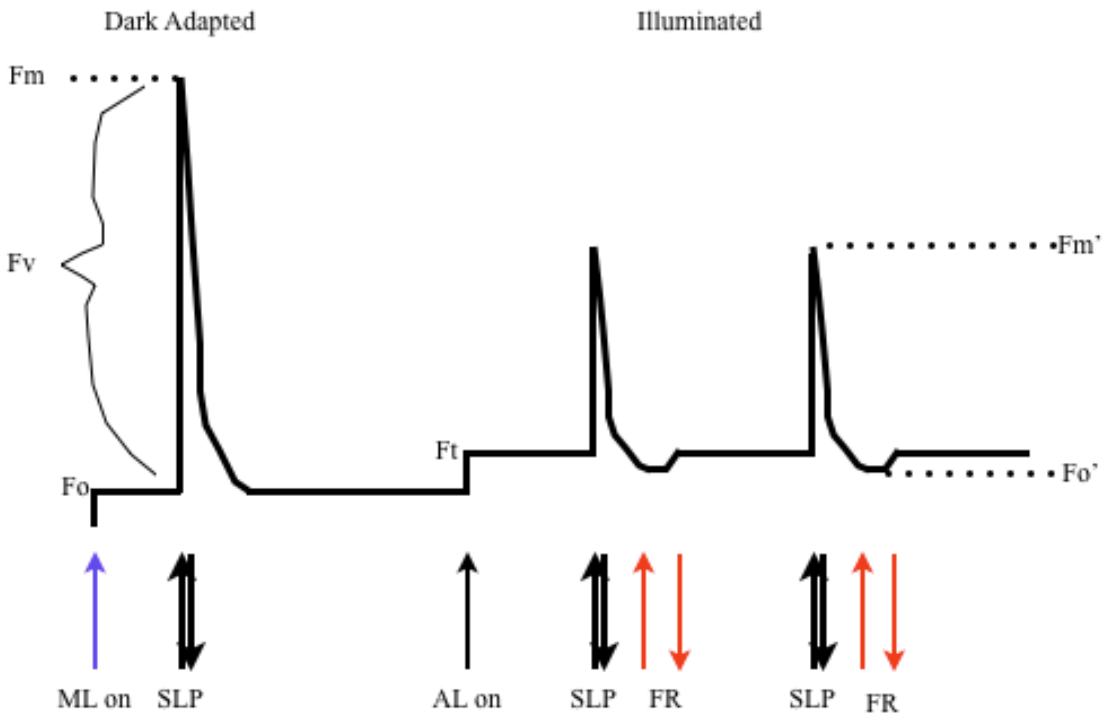

Figure 8: Schematic of PAM trace for both dark adapted and illuminated samples. ML- measuring light; SLP- saturating light pulse; AL- actinic light; FR- far-red light. Fluorescence parameters used in equations in table 1 labeled. F_M- maximal fluorescence yield; F_O- minimal fluorescence yield; F_V- difference in yield of maximum and minimum; F_T- fluorescence transient; F_M'- maximum light intensity under actinic light; F_O'- minimum fluorescence collected with short far-red pulse. For reviews see Maxwell & Johnson, 2000; Schreiber, 2004.

de novo Protein Synthesis Inhibition Tests- Rehydration

Dried lichen thalli and algae beads were floated in water containing 2mg/ml chloramphenicol for 3 hours (n=3), 1.9mg/ml cycloheximide for 2 hours (n=3) and controls (n=3) floated in water containing no antibiotic for 3 hours. Lichens were then placed in desiccation chambers and left to desiccate for 24 hours. Recovery of F_V/F_M after subsequent rehydration was measured as described previously. The total duration of these experiments (not including the 3 hour pre-treatment with antibiotic) was 36-48 hours, where 24-36 of those hours had the samples in a desiccated state. This brings up the question of the stability of chloramphenicol over the course of the experiment. Lai *et al*, (2009) in a study of protein synthesis inhibition with chloramphenicol in *Chlorella pyrenoidosa* found that after treatment of cells for 96 hours, 76.5-93.2% of the chloramphenicol remained in culture.

Non-photochemical Quenching (NPQ): Dithiothreitol (DTT)

Dithiothreitol (Figure 9C) is a well-established mechanism to block the xanthophyll cycle by inhibiting violaxanthin de- epoxidase (VDE) (Yamamoto & Kamite, 1972). DTT works by reducing disulfide bonds in proteins (Scigelova *et al*, 2001). The appropriate concentrations of DTT to inhibit the xanthophyll cycle for lichens and algae were determined by monitoring non-photochemical quenching during light stress. Literature values of 3mM DTT for 5 minutes were sufficient to block zeaxanthin formation. NPQ was monitored via PAM fluorometer using equation in table 1 before, during and after a 15-minute exposure to 500µE of light, followed by a 10-minute recovery of illumination of 0.06µE light. NPQ was determined using this protocol as a function of DTT concentration.

Rehydration: Dithiothreitol (DTT)

Dried lichen thalli were floated in water containing 3mM DTT for 1 hour (n=3), while controls (n=3) were floated in water containing no DTT for 1 hour. Algae beads were placed in growth medium containing 3mM DTT for 5 minutes, with controls in growth media not containing antibiotic for 5 minutes. Samples were then placed in desiccation chambers and left desiccated for 24 hours. Recovery of F_V/F_M after rehydration was then measured as described previously.

Statistical Analysis

A two- tailed students T-test (StatPlus add-in for Microscoft Excel) was used between 2 sample categories to determine the difference between means. A paired test was used to compare time-points within species, while an unpaired test was used to compare two different species. Alpha value was 0.05.

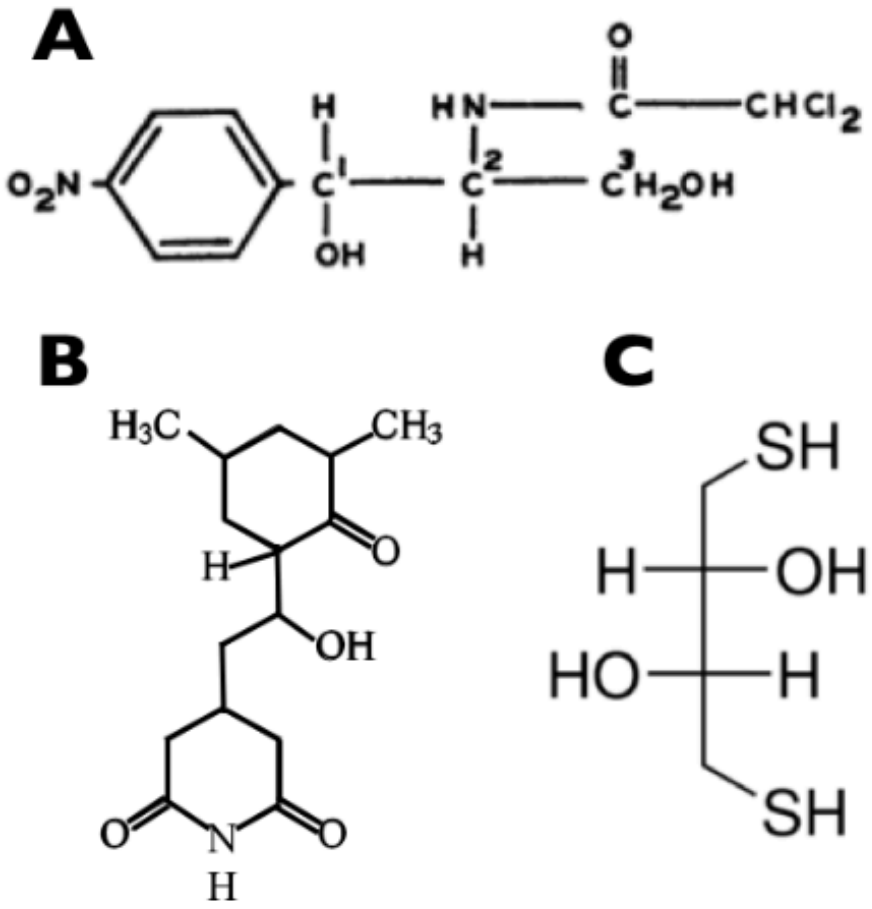

Figure 9: Inhibitor molecules used in study, (A) the structure of Chloramphenicol, image from Brock, 1961. (B) Structure of cycloheximide and (C) structure of dithiothreitol. B and C structures from Sigma- Aldrich.

Steady-State Fluorescence Spectroscopy

Fluorescence Emission Spectra

Fluorescence emission spectra were measured from the algal liquid cultures. 20µL of dark-adapted culture was placed on a specially designed front-faced holder (Figure 10B) and immersed in the dark in liquid nitrogen (77K) in a glass dewar (Figure 10A). Lichen fluorescence emission spectra were taken in the same way with a piece of the thallus inserted into the well of the sample holder. The excitation light source and detector fiber optic were held at a 90^{o} angle to each other, with the sample surface at 45^{o} to each (Figure 10C). Desiccated and hydrated fluorescence emission spectra were taken from the same sample to be sure the comparison was accurate and with the same chlorophyll concentration. The desiccated sample was desiccated on the sample holder, held for 24 hours at 22ºC, and then immersed in liquid nitrogen in the dark. The excitation wavelength used was 440nm, and the resulting emission from the sample was imaged with a Triax-320 spectrograph and nitrogen cooled CCD array (Jobin Yvon) and stored in the computer graphical software Origin as a spectral plot of fluorescence intensity (counts) vs. wavelength (nm) over the visual spectrum. Slit width on the detector monochromator was 0.7mm, equivalent to a spectral resolution of 1nm. 25 individual spectra were averaged, each spectrum was taken over a 500ms time span.

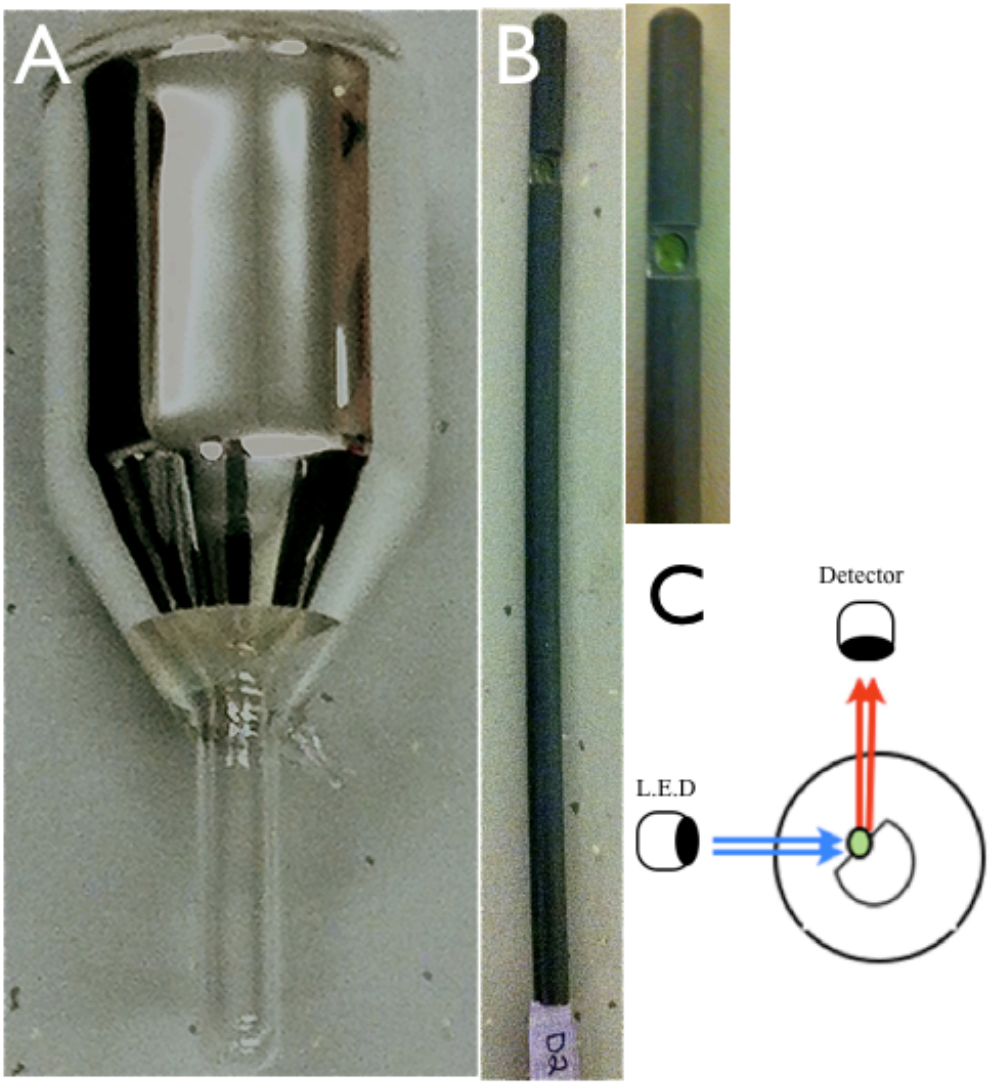

Figure 10: Set up of instruments used to collect fluorescence emission spectra. (A) Liquid nitrogen dewar to hold special designed sample holder. (B) 20μL of liquid culture put in sample holder and (C) held at 45° angle between light source L.E.D. and fibre optic detector.

Time-Resolved Fluorescence Spectroscopy

Fluorescence decay kinetics were monitored from a desiccated or hydrated sample over a wavelength range of 680-760nm (77K samples) as described previously (Veerman *et al*, 2007) using equipment in Figure 11A. The excitation source was a picosecond pulsed diode laser with an emission wavelength of 404nm (PicoQuant, PDL 800-B) and a 54ps pulse width. Fluorescence collected through a monochromator and fluorescent photons detected with a microchannel plate photomultiplier tube, Hammamatsu 3908U. A single photon timing apparatus (PC Card- Becker and Hickle, SPC730) was used to determine the kinetics of chlorophyll decays at each wavelength. The instrument response function had a full width at one-half maxima (FWHM) of 65ps.

Desiccated and hydrated picosecond decay kinetics at 77K were obtained by placing algae covered glass beads in a heat-sealed Pasteur pipette scaled to the size of a liquid nitrogen dewar (Figure 11B). The dewar and sample were filled with liquid nitrogen and placed at a 90^{o} angle between the excitation beam and detector. Samples were frozen in liquid nitrogen in the dark prior to data collection.

Picosecond Fluorescence Decay Kinetics

Fluorescence decays from photosynthetic organisms are well represented as products of multi-exponent decays represented as the sum of individual single exponential decays (van Stokkum *et al*, 2004) represent by equation (3).

$$\mathbf{I(t) = \sum_{i=1}^{n} \alpha_i exp(-t/\tau_i)} \quad \mathbf{(3)}$$

Where n is the number of decay times, α is the amplitude, and τ represents the decay time. Decay curves are collected from a sample with a constant excitation wavelength, over multiple emission wavelengths. Decay curves are de-convoluted from the measured instrument response function (IRF) by equation (4).

F * IRF = H (4)

Where H is the decay curve, and F represents the fluorescence decay. The IRF represents the shortest lifetime profile measured on the equipment, taking into account detector delays and laser pulse width (Lakowicz, 2006). De-convoluted decays may then be subjected to computational global analysis using non-linear least squares where various lifetimes and amplitudes are applied to the collected data set to determine the best statistical fit. Determined amplitudes and lifetimes may then be modeled in a parallel scheme of modeling where the fluorescent system is represented by compartmental models in which every compartment decays to the ground state resulting in decay associated spectra (DAS) plotting amplitude vs. wavelength (van Stokkum *et al*, 2004; Vasil'ev *et al*, 1998; Vasil'ev & Bruce, 1998). Physical parameters were set by fitting against a steady-state fluorescence emission spectra taken under the measurement conditions.

Weighted residuals are used to determine how well the fit matched the experimental data. The fit quality is expressed as deviations between the two values, weighted by the standard deviation of each measurement, and compared using chi-squared statistics. Random deviations in the residuals with a chi-squared value close to 1 indicates a good fit where the deviations in the data are due to random error, and thus the fit is as good as can be within the tested parameters. Systematic deviations in the

residuals with a higher chi-squared value indicates that the fit is not sufficient to explain the data, and there may be more lifetime components present then the ones tested for. Residuals are calculated for fluorescence decays at each wavelength tested with the average chi-squared value set for the whole spectra.

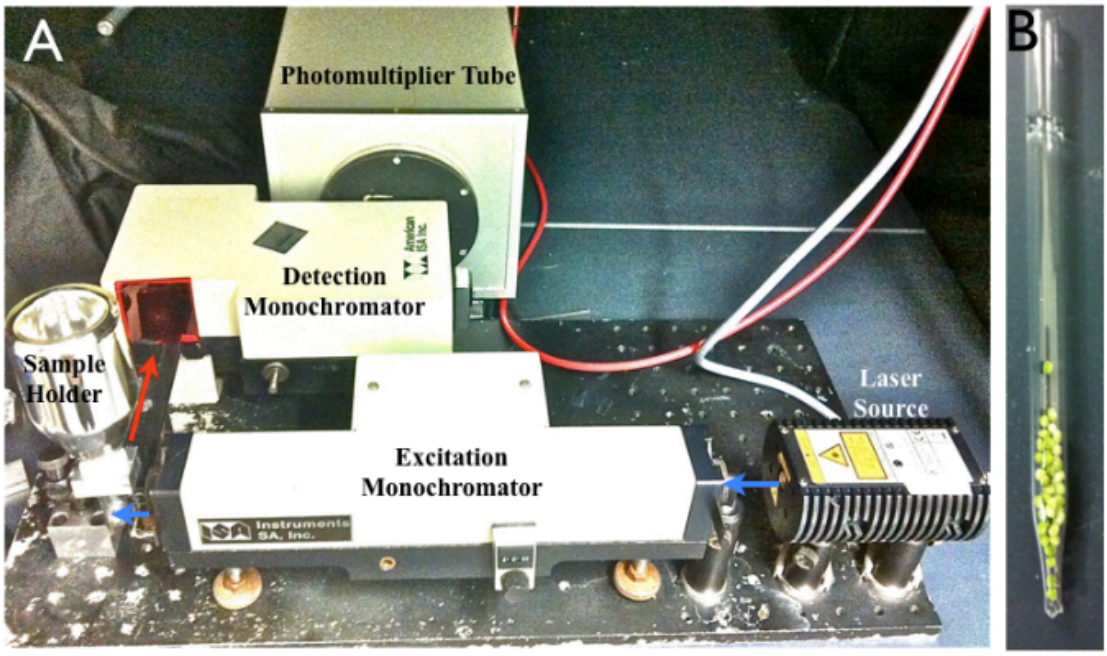

Figure 11: Set up for collection of picosecond decay kinetics. (A) Laser source emits 404nm picosecond pulse through an excitation monochromator illuminating the frozen sample (blue arrows). Fluorescence is detected in detection monochromator set to a specific wavelength (red arrows). Fluorescence photons are amplified in a photomultiplier tube before displayed on computer screen. (B) Algal beads or lichen thallus held in heat sealed Pasteur pipette.

Results
SECTION ONE- PHYSIOLOGY

Morphology of hydration and desiccation

The thallus of hydrated *P. sulcata* is coloured green (Figure 12A), which turns a dull grey when desiccated, becoming very brittle to the touch (Figure 12B). Upon rehydration, the thallus uncurls as it absorbs water, becoming sponge-like and regaining its green colouration. Hydrated algae of all species are a green colour (intensity depending on culture concentration; Figure 12C), and retain their colour during desiccation (Figure 12D). When monitoring the transition from desiccated to hydrated and rehydrated using the PAM fluorometer, we see that in each case, the application and uptake of liquid media is concurrent with the recovery of colour (lichen thallus), and photosynthetic ability (all samples).

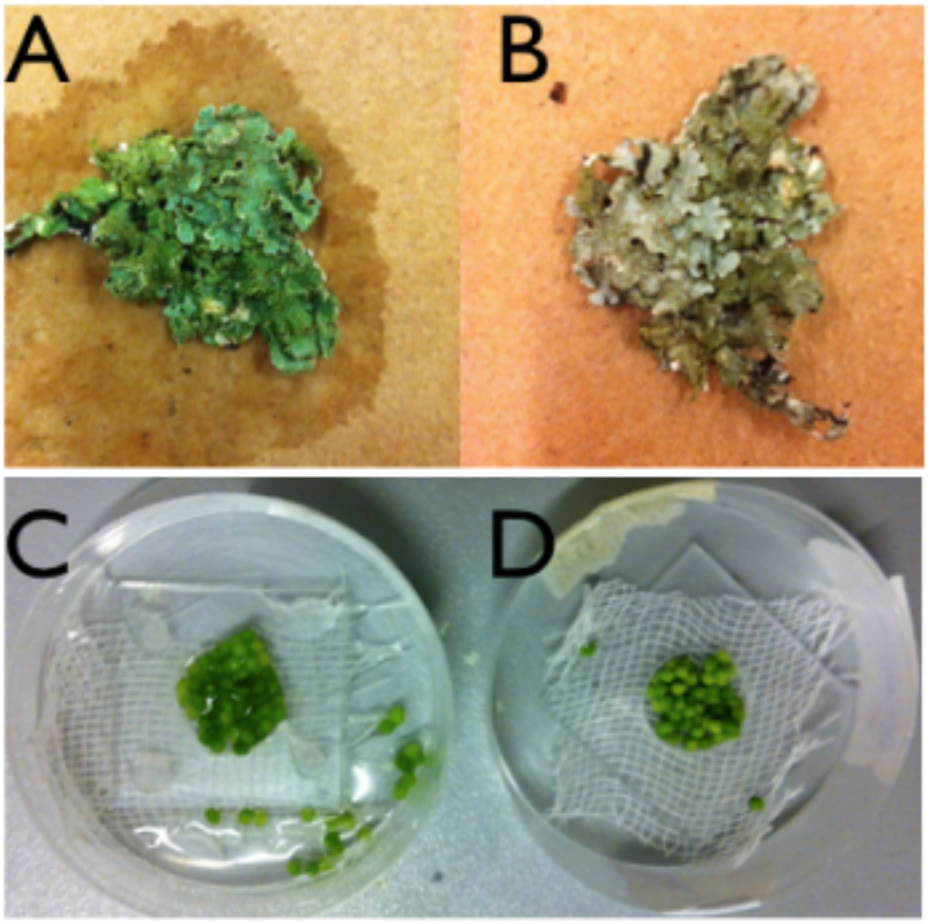

Figure 12: Pigment changes in *P.sulcata* in the (A) hydrated and (B) desiccated state. Hydrated lichen is soft to the touch and vibrant green in appearance. Desiccated lichen thallus is brittle to the touch and dusty grey in appearance. Upon rehydration, green colour appears with the onset of water wicking through the lichen thallus, in correlation with the reappearance of F_V. Isolated green algae (*Trebouxia sp.* pictured) displays green colour in both the (C) hydrated and (D) desiccated state pictured here desiccation of 7 days.

PAM Desiccation/Rehydration Traces

Desiccation is characterized by a decrease in F_O fluorescence, F_V fluorescence and PSII quantum efficiency (F_V/F_M). When desiccated, samples show no F_V when probed with a high saturating light pulse. Corresponding F_V/F_M value is 0.1 or less indicating the lack of photosynthetic ability (Gray *et al*, 2007). This fluorescence quenching response to desiccation, specifically the quenching of F_O, is unique to desiccation tolerant organisms (Heber *et al*, 2006). For example, spinach desiccated in the same manner shows a quenching of F_V fluorescence, with no F_O quenching (Kopecky *et al*, 2005).

During the desiccating process, F_V/F_M and F_V become noticeably quenched indicating the lowering of energy utilization by the saturation of electron transport, as seen previously by Gray *et al.* (2007) and Veerman *et al.* (2007). A noticeable trend in the data is the loss of both of these measurements simultaneously before complete desiccation is reached (Figure 13). Gray *et al*., in their 2007 study correlated this drastic decrease occurring at the time where there was the bulk of water loss from the algae beads. Interestingly, before that specific event, F_V/F_M remains relatively stable (Figure 13- Left). The variation however, can be seen by the change in F_V over time. Before the bulk water loss, there is a spike in F_V, which correlates to a spike also seen in the F_O desiccation trace (Figure 13- Right). This trend is absent in the traces obtained from the desiccation of the lichen thallus. Regardless, both lichen thallus and green algae end with a F_V/F_M of 0.1 or below and an F_V of near zero, indicating the loss of photosynthetic ability.

After desiccation to room relative humidity, saturating light pulses were unable to induce F_V and a F_V/F_M of over 0.1, indicative of the absence of charge separation in this state.

F_O quenching was notable for *P. sulcata* and desert dwelling *Chlorella sp.* BC4VF9. Aquatic algae *Chlorella sp*. UTEX318 did not show F_O quenching, reminiscent of desiccation tests on spinach (Figure 13C).

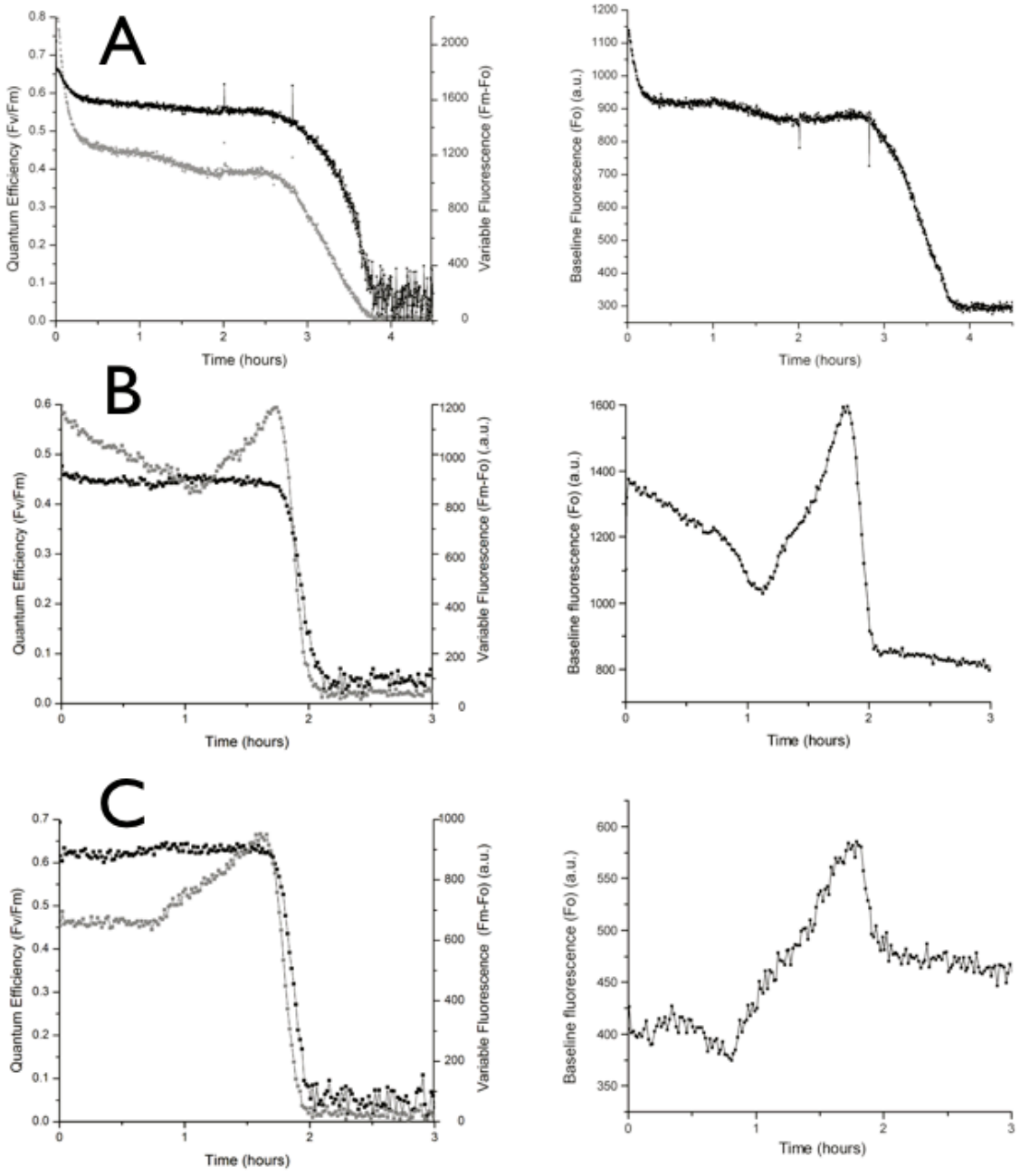

Figure 13: Modulated fluorescence parameters F_O, F_V and F_V/F_M of (A) *P. sulcata,* (B) *Chlorella sp.* BC4VF9 (C) *Chlorella sp.* UTEX318 after being removed from hydrated conditions (liquid culture for algae and moist filter paper for *P.sulcata*) and allowed to equilibrate in air RH. Desiccation process was measured continuously with the PAM fluorometer at 1.6Hz under a measuring light of 0.06μE. Saturating light pulses of 1450μE were taken every 60s to record F_M. (Left) Black squares represent the loss of F_V/F_M over desiccation time to below 0.1, while grey squares show the corresponding loss of F_V during desiccation. Once desiccated, SLPs were unable to induce F_V. Right panel is desiccation plot showing the changes in F_O fluorescence. Spike in F_O fluorescence at approximately 1 hour corresponds with spike in F_V also shown during desiccation.

Upon rehydration, most notable is the release of quenching of F_O, followed closely by the reversal of F_V quenching (Figure 14). Rehydration of *P. sulcata* shows a reversal of F_O fluorescence quenching instantly after the application of liquid water, and continues to rise slowly for the duration of rehydration. F_V fluorescence is regained quickly afterwards, appearing at the first SLP after 1 min of water application. Each subsequent SLP for 10 minutes shows the gradual reversal of F_V quenching with a rise in F_V/F_M, indicating the restoration of PSII charge separation. This reversal occurred in a step-wise fashion until a maxima reached at 10 minutes (Figure 14A). Reversal of F_O and F_V quenching and recovery of F_V/F_M was faster in green algae, both reversals reaching a steady level after 1 minute of water application (Figure 14). *S. costatus* displayed a reversal of F_O quenching, with subsequent release of quenching of F_V for 2-3 SLPs, which disappeared with subsequent measuring time indicating complete loss of PSII activity in this organism (Figure 14D).

In order to rank the ability to regain PSII activity of all species tested, F_V/F_M values were compared upon rehydration after various desiccation lengths. Hydrated, dark-adapted F_V/F_M values ranged from 0.599±0.013 for *S. rotundus* up to 0.665±0.110 for *P. sulcata.* After held desiccated in the dark for 24 hours, 7, 30 and 60 days (RH <40%), samples were rehydrated with their respective growth solutions. *P. sulcata* showed an impressive ability to regain high levels of photosynthetic ability up to 7 days desiccated. A decline was seen at 30 days, and at 60 days desiccated, *P. sulcata* was still able to regain photosynthetic ability, although to a much lower extent (Figure 15). Measurements for isolated *Trebouxia sp.* could not be made past the 24 hour desiccation length for the successful isolate, as the culture was lost before subsequent experiments

could be conducted. The resulting high level of recovered photosynthetic ability even after 3 months of isolated clearly demonstrates this ability is not simply an artifact of symbiosis and fungal protection.

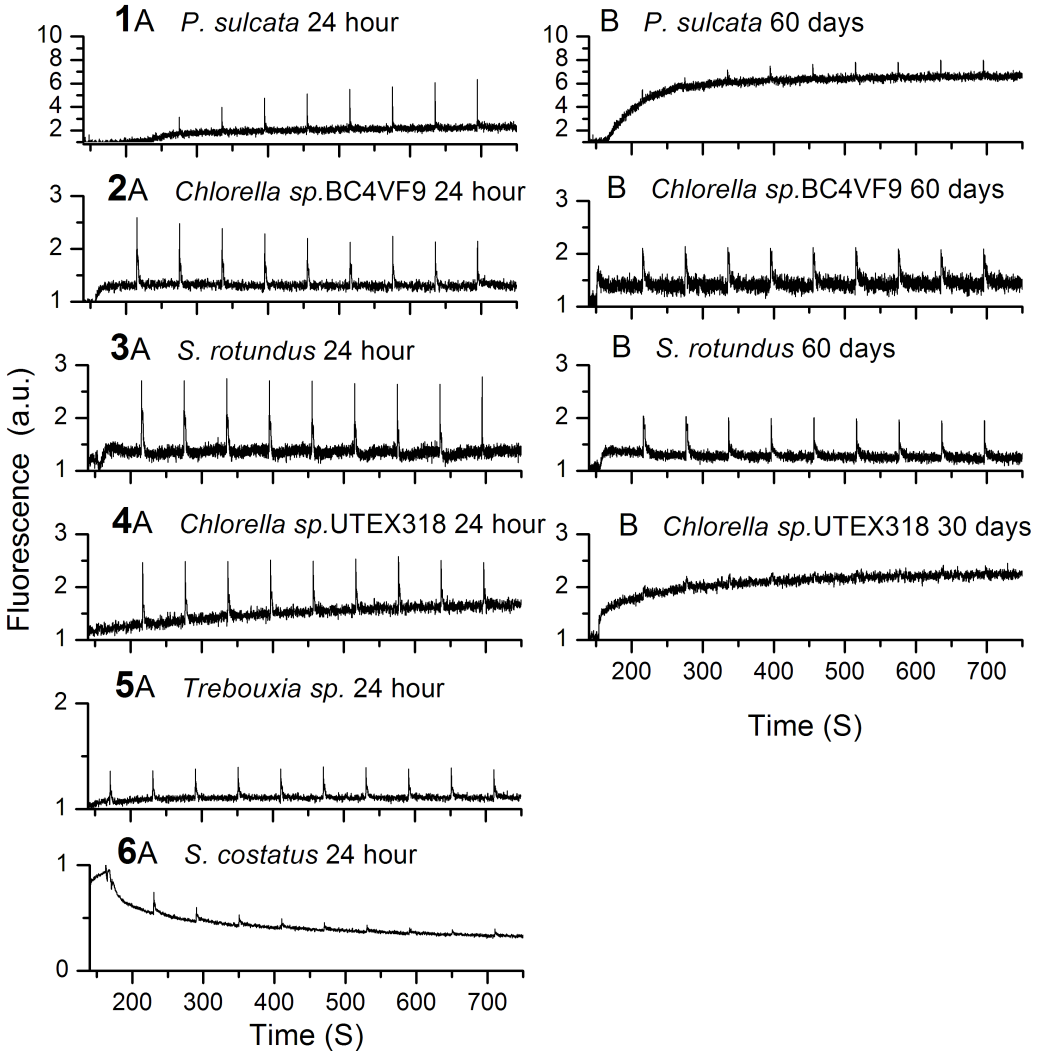

Figure 14: PAM rehydration traces for (1) *P. sulcata* hydrated after 24 hours, and B after 60 days (2) *Chlorella sp.* BC4VF9 hydrated after 24 hours, and B after 60 days (3) *S. rotundus* hydrated after 24 hours, and B after 60 days (4) *Chlorella sp.* UTEX318 hydrated after 24 hours, and B after 30 days (5) *Trebouxia sp.* A after 24 hours and (6) *S. costatus* after 24 hours. Rehydration traces after application of water at time 0 after being held desiccated for 24 hours. Desiccated F_O values are normalized to 1.0a.u. for uniformity of scales between rehydration time points, but does not allow for accurate comparison between sample species. After the application of water, F_O fluorescence rises instantly in all cases except for *S. costatus*, where F_O decreases. After 1 min of water application, 1450μE SLP was able to induce F_V. Algae samples (B-E) show a steady plateau of F_V after 1 min, where *P. sulcata* (1) shows an increase in F_V over time. PAM rehydration traces at 30-60 days (1-4B) shows a decrease in F_V quenching compared to 24 hours desiccation (1-6A).

Desert algae *Chlorella sp.* BC4VF9 and *S. rotundus* were also able to regain high levels of photosynthetic ability with a decline seen at 30 days (Figure 15). *S. rotundus* was shown to have significantly higher recovery at 60 days than *P. sulcata* ($P<0.05$), and *Chlorella sp.* BC4VF9 ($P<0.01$).

It was hypothesized that aquatic dwelling algae would be unable to regain much, if any photosynthetic ability after desiccation. This was indeed the case for aquatic species *S. costatus*. Aquatic *Chlorella sp.* UTEX318 however, showed a surprising ability to regain a high level of photosynthetic ability after 24 hours of desiccation, *Chlorella sp.* UTEX318 had rehydration values mimicking that of desert algae, the difference in desiccation survival ability was clearly seen after 7 days, where recovery F_V/F_M was much lower than the desert representatives (Figure 15).

.

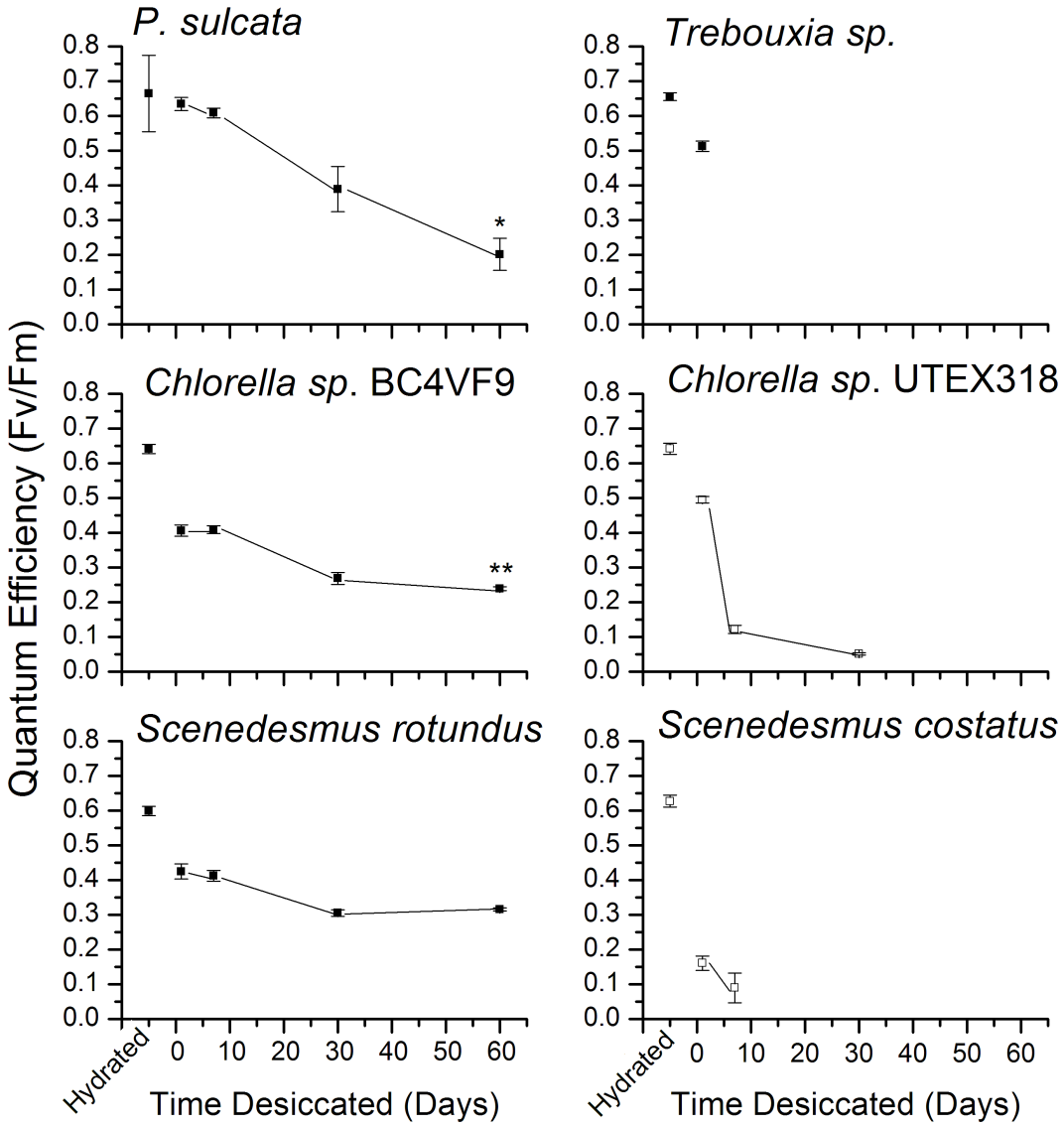

Figure 15: Effect of the duration of desiccation on the F_V/F_M recovery of lichen and algae species when desiccated and rehydrated in the dark compared to hydrated pre-desiccation values. Time course for samples was from 24 hours to 60 days for *P. sulcata*, *S. rotundus* and *Chlorella sp*. BC4VF9. Shorter time scales of aquatic algae (*S. costatus* and *Chlorella sp*. UTEX318) reflect the inability of these algae to regain photosynthetic ability after a certain time point. Lack of data for *Trebouxia sp.* represents the loss of culture during the study. In each measurement the rehydrated F_V/F_M after 10mins is compared to pre-desiccated. Average of three trials and corresponding standard deviation shown. Numerical data presented in Appendix I.

* Recovery F_V/F_M at 60 days less than seen in *S. rotundus* ($P<0.05$)

** Recovery F_V/F_M at 60 days less than seen in *S. rotundus* ($P<0.01$)

Desiccation recovery during light exposure

Recovery after desiccation for 24hr was reasonably high for most of the species tested. The algae were kept in the dark while desiccated, and subsequent rehydration recovery was monitored under very low light conditions, the measuring light from the PAM fluorometer (0.06μE). This very low light level was not sufficient to drive photosynthesis, and therefore not indicative of the alga's ability to recover while illuminated. Interestingly, the application of low actinic light during rehydration was determined to have a negative effect on recovery after dark desiccation in free algae species. This was not the case for dark desiccated *P. sulcata,* in which the application of much higher light intensities was required before the same effect was observed (Figure 16-18).

To determine if reduced recovery with the application of light was due to photodamage or NPQ, measurements of PSII efficiency (ΦPSII), photochemical quenching (qP) and maximum PSII efficiency (F_V/F_{Mmax}) was determined for each recovery SLP using formulas in table 1. ΦPSII is the measurement of the amount of light used by PSII for photochemistry over increasing light intensity. A decrease in this value is caused by various fluorescence-quenching mechanisms. qP gives an indication of the proportion of open PSII reaction centres, values vary between 0 and 1, with a decrease of this value caused by closure of the RCs. These two measurements together allow for the determination of F_V/F_{Mmax} representing the maximum photosynthetic efficiency of PSII if all reaction centres were open.

P. sulcata requires higher light intensities before a decline is shown in the parameters tested. At 120μE and subsequent intensities there is a decrease in ΦPSII, indicating at these light intensities non-photochemical quenching of fluorescence is

necessary. This decrease coincides with decreases of qP, suggesting the closure of RCs into non-radiative dissipation centres is utilized (Figure 16&17). Conversely, F_V/F_{Mmax} at these higher light intensities remain higher and stable compared to ΦPSII, indicating the use of NPQ mechanisms and a low level of RC photodamage (Figure 18).

Fluorescence parameters follow the same trend for both *Chlorella sp*. and *S. rotundus*. Without fungal protection, these algae face adverse reactions to light at much lower intensities. Both species however show a decrease in ΦPSII and qP but a higher relative value of F_V/F_{Mmax}, indicating PSII RCs are still protected during exposure to increasing light intensities.

Contrasting results come from the rehydration of *Chlorella sp.* UTEX318 and *S. costatus,* which both show a decline in both ΦPSII and F_V/F_{Mmax} measurements with increasing light intensity, thus indicating this decrease is not caused by fluorescence quenching, but from damage to the reaction centres. This is further supported by qP value which remain high at 1.2 indicating the reaction centres remain open. A qP of over 1 suggests a higher degree of damage was incurred during desiccation, causing a rise in the F_O' parameter (Gray *et al*, 2007).

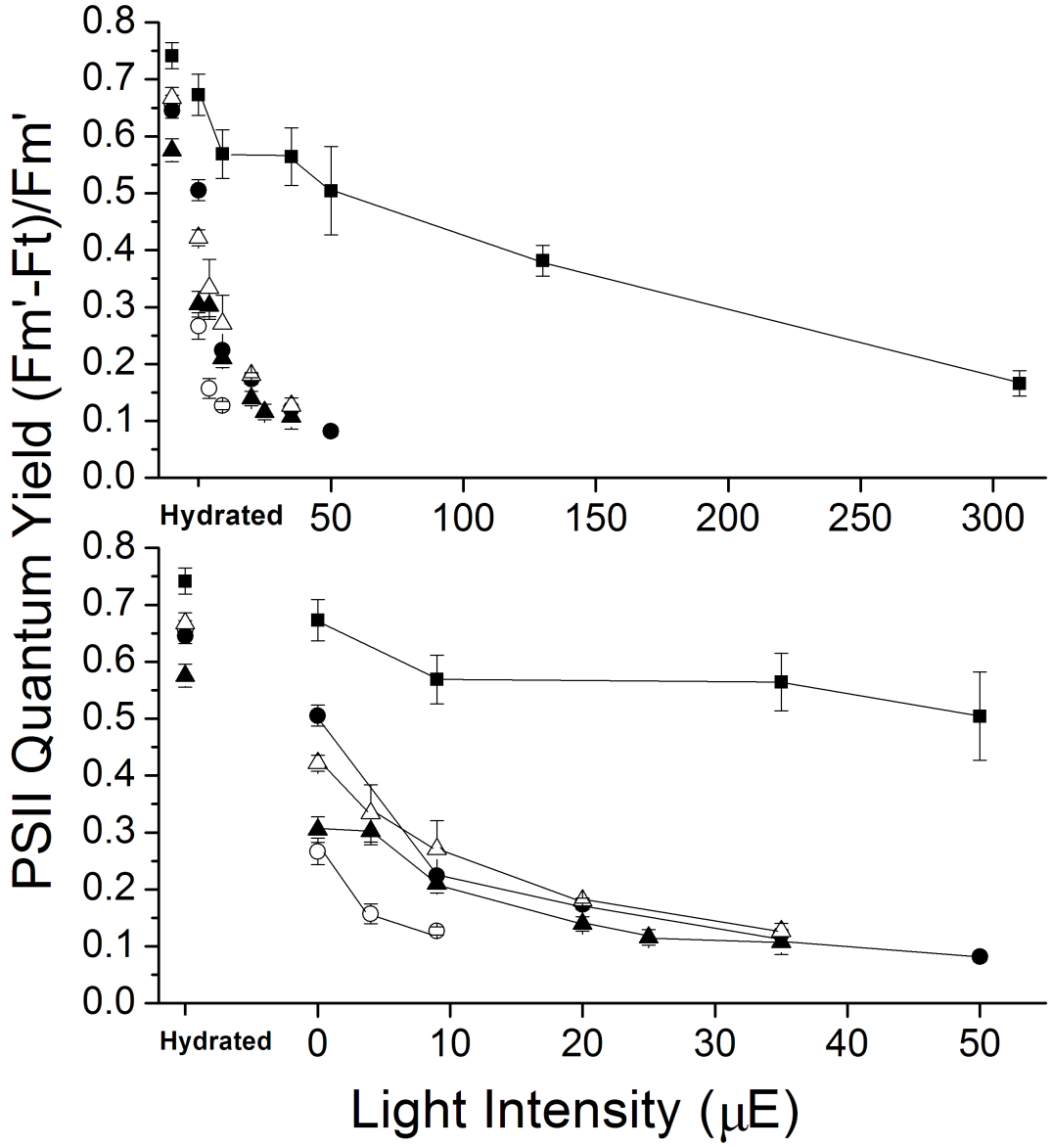

Figure 16: Desiccation recovery of photosynthetic yield (ΦPSII) of algae (-▲-*Chlorella sp.* BC4VF9, -△-*Chlorella sp.* UTEX318, -●-*S. rotundus*, -○-*S. costatus*) and -■- *P. sulcata* under different low light intensities. Samples were desiccated in the dark and held for 24 hours. Time zero represents control sample rehydration (low light intensity 0.06μE). Lower panel shows light intensity from 0-40μE on a smaller scale for comparison of free-living algae species that were unable to handle light intensities *P. sulcata* was exposed to. In all cases, the higher the light intensity samples were exposed to during rehydration, the lower the recovery of ΦPSII. Although *S. costatus* does not recover even under control light, application of low light decreased the few measurements of F_V before complete shut down of photosynthesis. Samples were run in triplicate with averages and standard deviations shown. Numerical data presented in Appendix II.

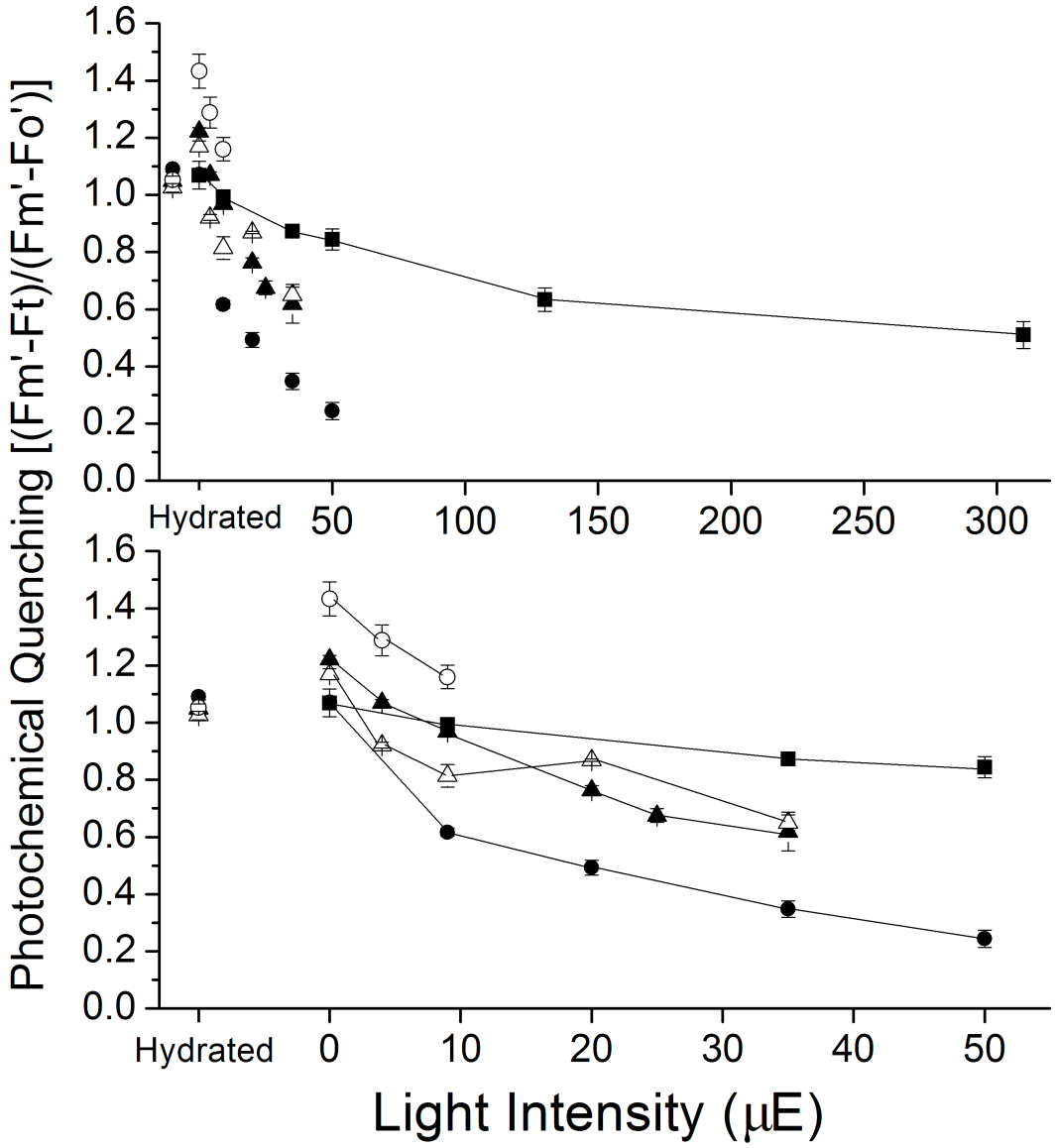

Figure 17: Desiccation recovery of photochemical quenching (qP) of algae (-▲- *Chlorella sp.* BC4VF9, -△- *Chlorella sp.* UTEX318, -●- *S. rotundus*, -○- *S. costatus)* and -■- *P. sulcata* under different low light intensities. Samples were desiccated in the dark and held for 24 hours. Time zero represents control sample (low light intensity 0.06μE). Inset shows light intensity from 0-40μE on a smaller scale for comparison of free-living algae species that were unable to handle light intensities *P. sulcata* was exposed to. In the majority of cases, the higher the light intensity samples were exposed to during rehydration, the smaller proportion of PSII RCs are open. Numerical data presented in Appendix III.

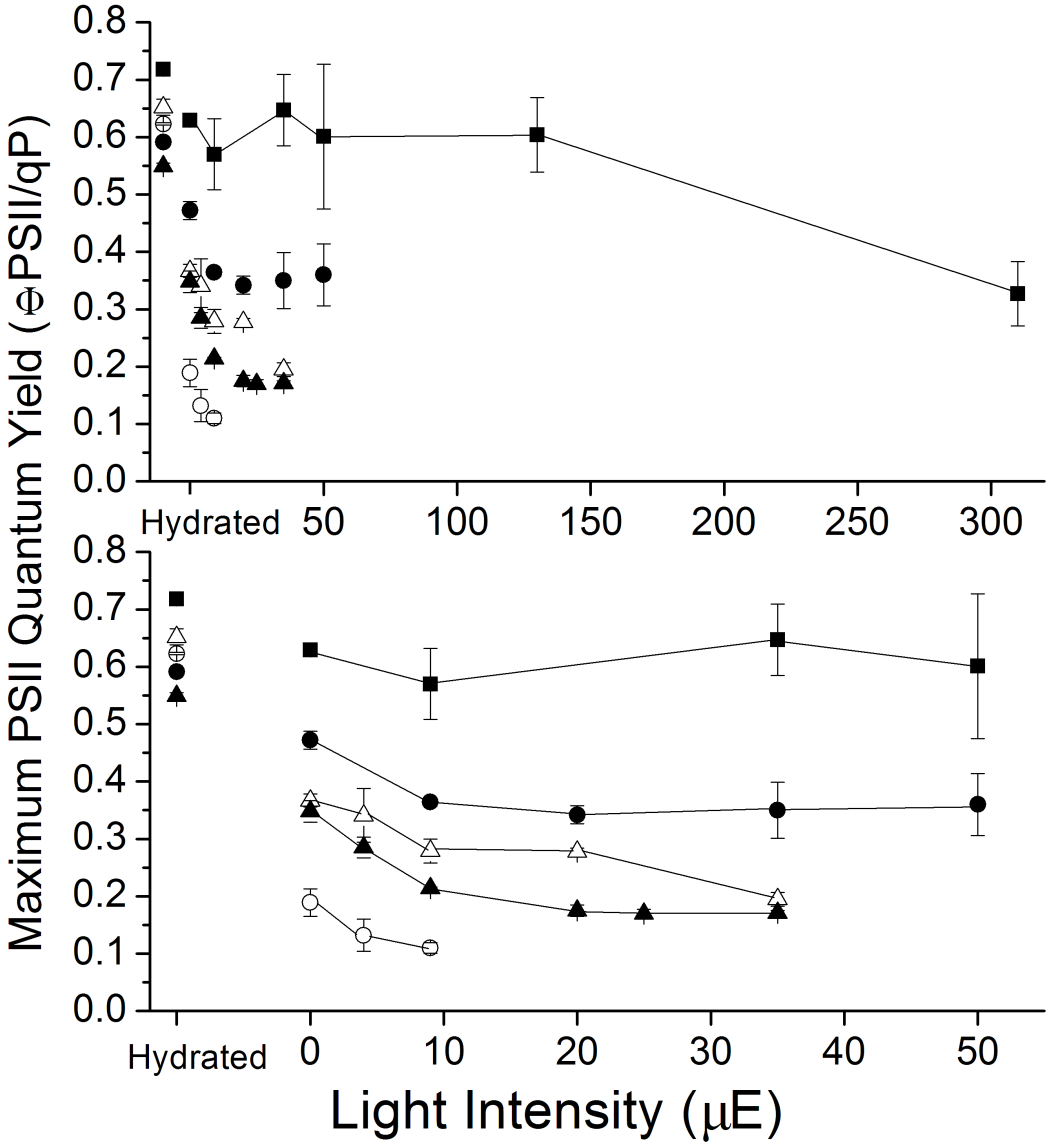

Figure 18: Desiccation recovery of quantum efficiency (ΦPSII/qP) of algae (-▲- *Chlorella sp.* BC4VF9, -△- *Chlorella sp.* UTEX318, -●- *S. rotundus*, -○- *S. costatus*) and -■- *P. sulcata* under different low light intensities. Samples were desiccated in the dark and held for 24 hours. Time zero represents control sample (low light intensity 0.06μE). Lower panel shows light intensity from 0-40μE on a smaller scale for comparison of free-living algae species that were unable to handle light intensities *P. sulcata* was exposed to. In the majority of cases, the higher the light intensity samples were exposed to during rehydration, the lower the recovery of F_V/F_M. Exceptions to this are *P. sulcata* and *S. rotundus*, which even at the highest light intensities measured at, F_V/F_M remained in the photosynthetic active range. Numerical data presented in Appendix IV.

Hydrated Photoprotection- Non-photochemical Quenching

Since some green algae are able to recover photosynthetic ability quickly after prolonged desiccation, there must be a photoprotective quenching mechanism present to limit desiccation-induced damage. Hypothesized mechanisms of this quencher are based on the observed photoprotective responses in plants exposed to high light stress. In order to determine any relatedness of photoprotection in the hydrated and desiccated state, it was necessary to conduct high light experiments on the studied organisms in their hydrated form. Kinetics of each organism's response to highlight treatment in terms of NPQ was monitored in the hydrated state (Figure 19).

After the application of high light, *P. sulcata* displayed a slow build up of NPQ response over the 15 min light treatment. Once recovery in the dark began, the first SLP showed an even higher NPQ response before starting to relax. During 10 min dark recovery there was a slow relaxation of NPQ (Figure 19A). This response is in contrast to the isolated *Trebouxia sp*., in which there was a higher amount of detectable NPQ response within one minute after the application of the light treatment, with a faster, biphasic induction of NPQ response during the light treatment (Figure 19B). Unlike *P. sulcata*, the first SLP in the recovery phase indicated the fast relaxation of NPQ. As expected, both *Chlorella sps.* showed NPQ induction and relaxation kinetics more similar to *Trebouxia sp*. than *P. sulcata* (Figure 19C,D). Unanticipated was the completely different NPQ induction kinetics displayed by *Scenedesmus sps*. NPQ rose drastically within one minute of light exposure with a slow induction of NPQ over 15 minutes (Figure 19E,F).

General NPQ signal can be caused by the induction of the xanthophyll cycle, which can specifically be inhibited by treatment with dithiothreitol (DTT). Treatment of

P. sulcata, Trebouxia sp. and both *Chlorella sp*. with 3mM DTT significantly reduced the maximum NPQ signal indicating all species the xanthophyll cycle under high light stress, despite the kinetic differences seen in *Scenedesmus sps*. As seen in Figure 20 (A-D), F_O and F_V quenching can be shown visually over the course of the experiment via a PAM trace. PAM traces show the typical fluorescence quenching associated with NPQ responses (Figure 20). Both *Scenedesmus sps*. show control and treated NPQ PAM traces with similar F_O and F_V quenching.

Although DTT treatment significantly decreased NPQ signal, the F_V/F_M measurements over the course of the treatment remain similar to non-treated controls, suggesting more than the xanthophyll cycle is responsible for NPQ quenching in hydrated conditions (Appendix VI).

Algae in the hydrated state appear to be much more tolerant of highlight intensities than in their desiccated state. Desiccated algae previously were shown to be highly photosensitive during rehydration, with low light intensities causing either photoinhibition or the need for fluorescence quenching mechanisms (Figures 16-18).

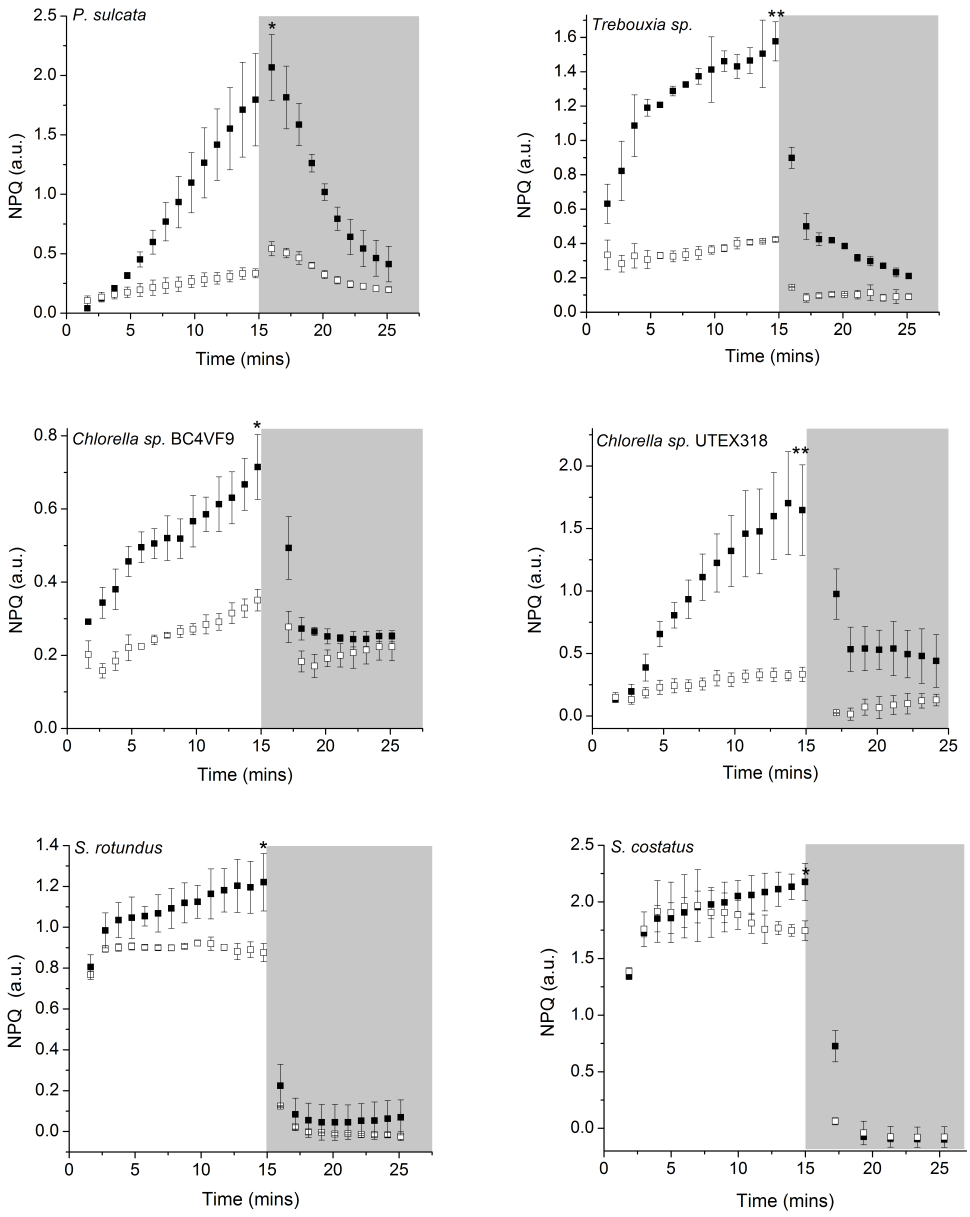

Figure 19: NPQ induction curves upon exposure to 500μE high light treatment (black squares) for 15mins, and subsequent 10min recovery time. White squares represent the addition of 3mM DTT. Differences between *P. sulcata* and isolated *Trebouxia sp* show *P. sulcata* has a slower build up of NPQ signal, while *Trebouxia sp.* matches curves generated by both *Chlorella sp.* BC4VF9 and *Chlorella sp.* UTEX318. *Scenedesmus sps.* show different induction/relaxation kinetics, that unlike in the other species used, DTT is not sufficient to inhibit. Samples were run in triplicate with averages and standard deviations shown. Numerical data presented in Appendix V.

* NPQ values of DTT treated are significantly difference than control ($P<0.05$)

* * NPQ values of DTT treated are significantly difference than control ($P<0.01$)

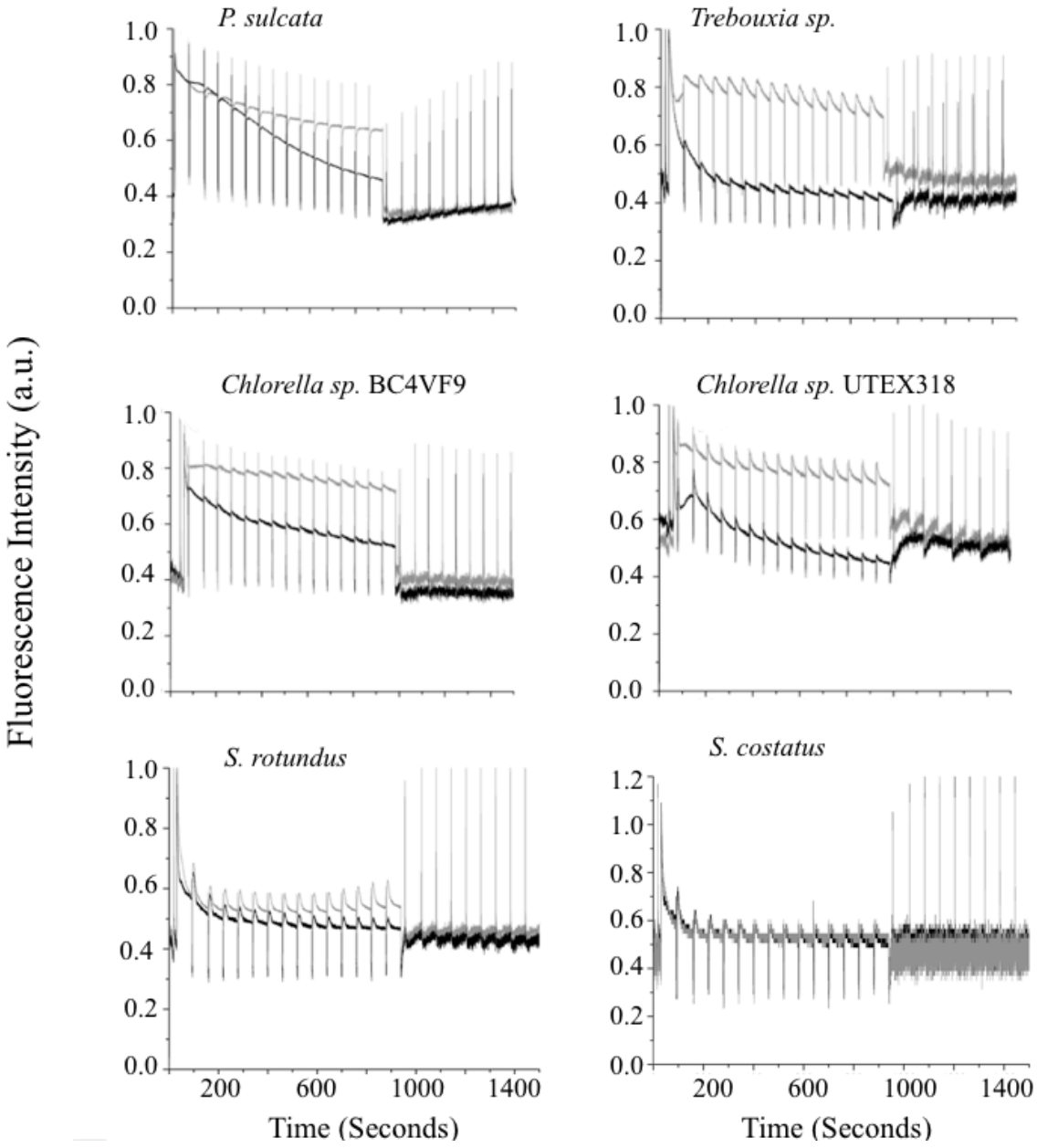

Figure 20: PAM fluorescence traces showing effect of DTT treatment on hydrated *P. sulcata* and algae. NPQ was induced during 15-minute exposure to 500μE of light, and allowed to relax during a 10-minute recovery of illumination of 0.06μE light. Fluorescence parameters were measured every minute with a 1450μE SLP followed by a 1 second exposure to far red light. Both F_o and F_v quenching occurring during NPQ (Black traces) were inhibited by the addition of DTT (grey trace) in all species except *Scenedesmus*. In both control and DTT treated samples, F_o and F_v quenching induced by highlight returned to normal levels during NPQ relaxation. Numerical data presented in Appendix V and VI.

Photoinhibition

Species were evaluated on their ability to survive photoinhibititory high light treatments in their hydrated form by monitoring photoprotection and the PSII repair cycle. Free-living and isolated green algae were exposed to 2200μE of light, while *P. sulcata* was exposed to 4200μE to penetrate through the protective layer of the fungus. All species showed the accumulation of damage caused by excess PSII excitation after 1 hour, and significant subsequent recovery (Figure 21). *Scenedesmus sps*. show less significant recovery values than the others ($P<0.01$).

To determine the overall role of chloroplast and cytosol *de novo* protein synthesis in repairing photodamage, the antibiotics chloramphenicol and cycloheximide were used. Controls to determine the effect of the treatments on samples showed a variation in the reaction of the algae to the presence of the treatments (Table 3). Both *Scenedesmus sps*. showed negative responses to the antibiotic treatments even in the dark. The most notable response is the loss of PSII activity in of *S. costatus* when treated with cycloheximide. When monitoring PSII repair over 1 hour at 25μE in the presence of antibiotics (Figure 22), *P. sulcata* shows a complete inhibition of F_V/F_M recovery, with significantly higher levels of damage after high light treatment compared to control ($P<0.005$), with no subsequent recovery of photosynthetic ability in the treated samples (Figure 22A). Green algae treated with chloramphenicol, except *Chlorella sps*., show a higher accumulation of photodamage vs. controls (*Trebouxia sp*., $P<0.05$, *Scenedesmus sps.* $P<0.005$). All algae species however show significantly lower recovery compared to control (*Chlorella sps.* $P<0.05$; *Trebouxia sp.* & *Scenedesmus sps.* $P<0.005$). Cycloheximide treatment caused significantly more damage in all algae vs. control except *Chlorella sp.* UTEX318 and *S. rotundus* (*Trebouxia sp* $P<0.05$; *Chlorella sp.* BC4VF9 $P<0.005$; *S. costatus* $P<0.005$),

whereas all algae except *Chlorella sp.* BC4VF9 ($P<0.005$) and *S. costatus* ($P<0.005$) were able to recover to the same extend as controls.

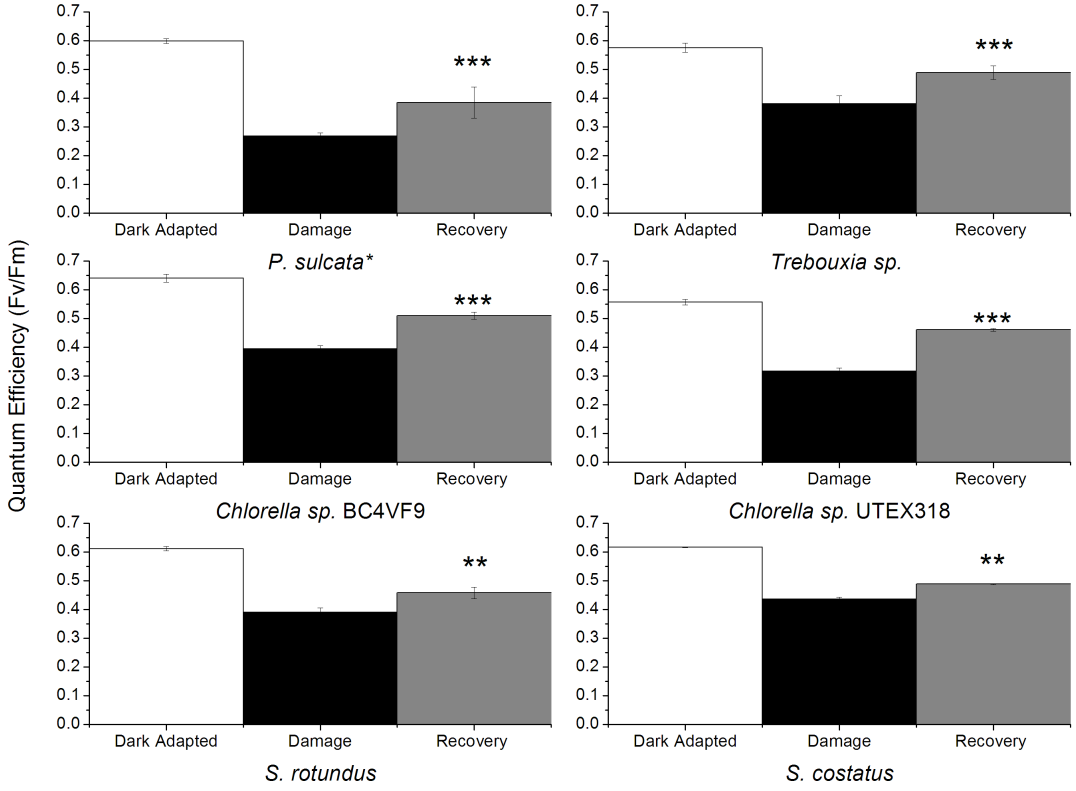

Figure 21: Comparison of photosynthetic ability (F_V/F_M) during photoinhibitory exposure of 2200µE. *4200µE for *P. sulcata* to penetrate fungal thallus. Dark-adapted pre-damage levels (white bars) compared to F_V/F_M measured after 1-hour highlight treatment and 15 subsequent minutes of dark adaption (black bars), and F_V/F_M after samples were allowed to recover under low light conditions (25µE) for 1 hour. Numerical data presented in Appendix VII.

** Recovery F_V/F_M significantly different than F_V/F_M after photodamage ($P<0.01$)

*** Recovery F_V/F_M significantly different than F_V/F_M after photodamage ($P<0.005$)

Table 3: F_V/F_M values of samples after being treated with chloramphenicol, cycloheximide or no treatment to determine the effect on photosynthetic ability. Values were obtained using a PAM fluorometer under control light conditions of 25μE.

Species	**Dark Adapted Control (F_V/F_M ±SD)**	**Dark Adapted Chloramphenicol (F_V/F_M ±SD)**	**Dark Adapted Cycloheximide (F_V/F_M ±SD)**
P. sulcata	0.599±0.008	0.537±0.011**	0.534±0.005*
Trebouxia sp.	0.576±0.002	0.564±0.001	0.531±0.014**
Chlorella sp. BC4VF9	0.641±0.014	0.641±0.004	0.545±0.014**
Chlorella sp. UTEX318	0.557±0.010	0.595±0.003*	0.587±0.004*
S. rotundus	0.611±0.008	0.390±0.005**	0.594±0.015
S. costatus	0.617±0.001	0.548±0.001**	0.098±0.029**

*significant difference from control $P<0.05$ (Paired students T-Test)
**significant difference from control $P<0.005$ (Paired students T-Test)

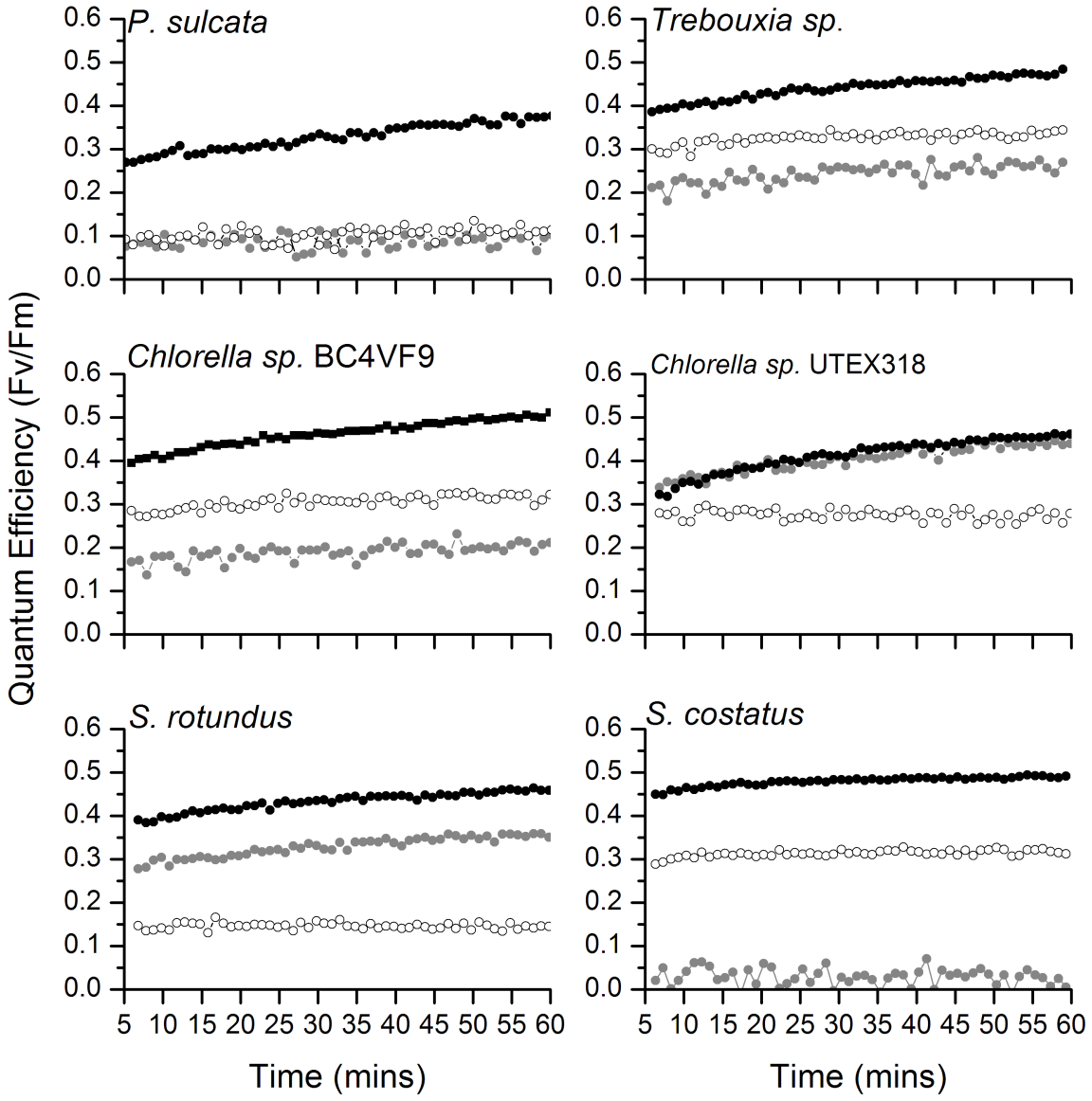

Figure 22: F_V/F_M plots of *P. sulcata* and algae over 1 hour recovery at 25μE after photoinhibition. Samples were treated with chloramphenicol (white) for 3 hours, cycloheximide (grey) for 2 hours, or no treatment (black) in the dark. Photoinhibition in the presence of antibiotics was determined over a 1 hour exposure to 2200μE (algae) or 4200μE (*P. sulcata*). SLPs of 1450μE in 1-minute intervals recorded fluorescence parameters. Plots are averages of three trials. Numerical data presented in Appendix VII.

Rehydration: NPQ and *de novo* Protein Synthesis Inhibitors

Involvement of xanthophyll carotenoids and protein synthesis in desiccation survival of some lichens has been debated in the literature, and therefore has been tested in this study (Figure 23). Samples were desiccated in the presence of DTT, cycloheximide, or chloramphenicol and rehydrated after a period of 24 hours. The ability of each species to recover was negatively affected by cycloheximide. *P.sulcata* showed a large significant decrease in recovery with the treatment of cycloheximide ($P<0.005$). This however may prove to be a result of the inhibitor affecting the lichen fungi, as *Trebouxia sp*. shows a smaller significant decrease to cycloheximide ($P<0.05$) further supported by *Chlorella sps*. showing a similar reaction to *Trebouxia sp.* than *P. sulcata*.

Chlorella sp. UTEX318 was the only algae tested to show a significant decrease in recovery when treated with chloramphenicol ($P<0.005$). DTT negatively affected both *Chlorella sp.* UTEX318 ($P<0.05$) and *S. rotundus* ($P<0.005$).

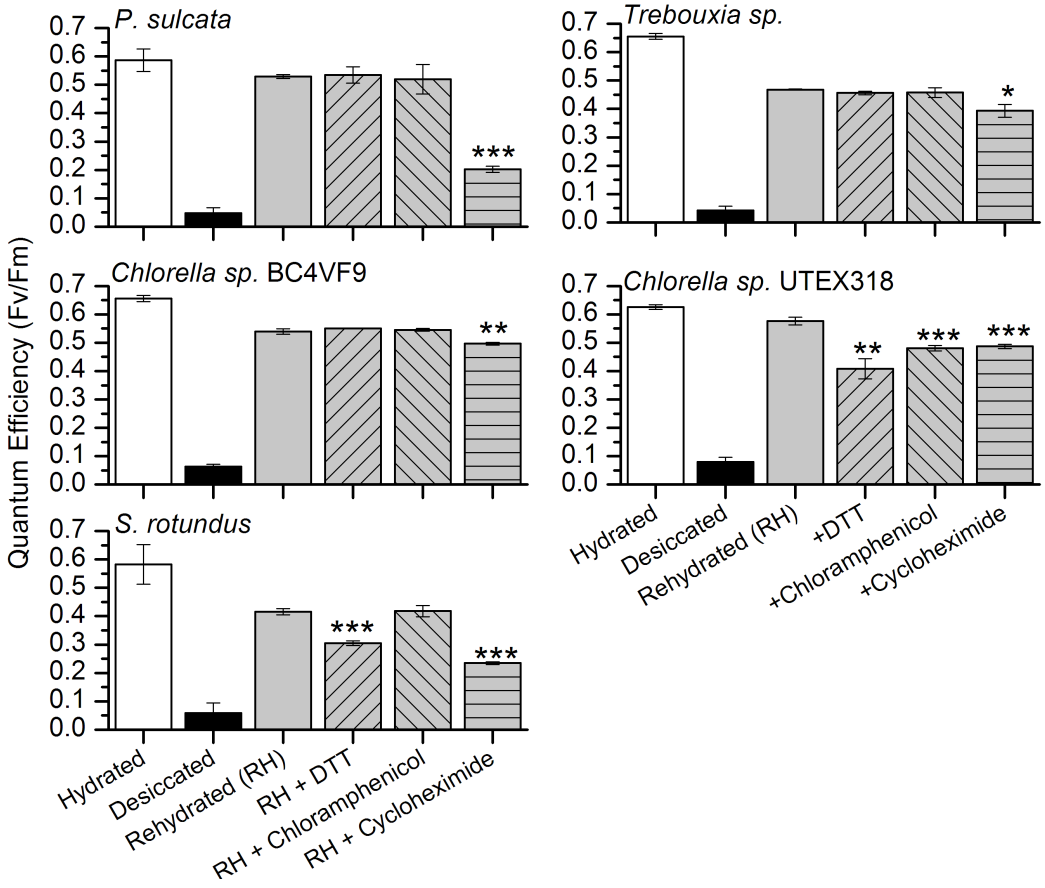

Figure 23: Desiccation recovery of inhibitor treated samples desiccated in the dark for 24 hours with no treatment (grey bar), DTT treatment (left hatched), chloramphenicol treatment (right hatched), or cycloheximide treatment (horizontal hatch). Samples were incubated with their respective treatments (see methodology) before being desiccated in the dark. Samples were held desiccated for 24 hours and rehydrated under the PAM fluorometer measuring light (0.06μE). SLPs of 1450μE every minute were used to determine recovery F_V/F_Ms for 10 mins of rehydration. Final F_V/F_M was compared to pre-desiccation levels (white bar), and other treatments. Black bar indicates samples were successfully desiccated before rehydration, as shown by a F_V/F_M of 0.1 or below. Samples were run in triplicate with averages and standard deviations shown. Numerical data presented in Appendix VIII.

* Recovery F_V/F_M or treatment is less than control ($P<0.05$)

** Recovery F_V/F_M or treatment is less than control ($P<0.01$)

*** Recovery F_V/F_M or treatment is less than control ($P<0.005$)

SECTION TWO- SPECTROSCOPY

Fluorescence Emission Spectra 77K: Hydrated

Fluorescence emission spectra taken at 77K show features typical to photosynthetic organisms containing two peaks (685nm and 695nm) representing PSII, and one major peak representing PSI (720-725nm) (Figure 24). Lichens show an additional fluorescence feature, a shoulder present at 760nm (Andrizhiyevskaya *et al*, 2005; Figure 24C) Despite differences in the spectra between *P.sulcata* and cultured *Trebouxia sp.*, the most important feature is the retention of 760nm shoulder.

A major difference between desert and aquatic species is a shift in PSI emission wavelength to longer wavelengths, 5nm for *Chlorella sps*., and 3nm in *Scenedesmus sps*.

Chlorella sp. BC4VF9 has an extra spectral shoulder at 760nm only previously seen in desiccation tolerant lichens. This feature is absent in *Chlorella sp.* UTEX318 (Figure 24A).

Scenedesmus sps. both show differences in spectra between *Chlorella sp.*, specifically the presence of an extra spectral feature at 705nm (seen most clearly in blue *S. costatus* spectra) in addition to PSII peaks, and both species are lacking the 760nm spectral shoulder (Figure 24B). Upon examination of the absorption spectra of all species tested, there are no main differences in pigment composition that could account for these differences (Appendix IX).

Desiccated

Lichen thallus shows the most pronounced fluorescence quenching in the desiccated state, 10x lower than in the hydrated state (Figure 25A). When the desiccated spectrum is normalized to PSI fluorescence emission in the hydrated spectra, it is obvious the change in fluorescence quenching is associated with changes occurring at the

photosynthetic level as seen by the disappearance of PSII associated peaks. If fluorescence quenching were simply explained by a decrease in the absorbed light reaching the photosystems, desiccated fluorescence emission spectra would be the same as hydrated, but at lower fluorescence intensity. Instead, it is clear the fluorescence is drastically reduced in both 685 and 695nm regions in *P. sulcata*. The PSI peak is also shifted upon desiccation to 720nm (PSI shift wavelengths shown in Appendix X). Noticeable in previous publications (Veerman *et al*, 2007) is the desiccation-induced fluorescence quenching of the 760nm shoulder. This is unclear in this study as the PSI peak becomes broader in the desiccated state and thus difficult to see, it can be seen more clearly in fluorescence emission spectra of *Chlorella sp.* BC4VF9 (Figure 25B).

In desiccation tolerant species *Chlorella sp.* BC4VF9 and *S. rotundus* (Figure 25B,C) quenching of fluorescence is approximately 2x upon desiccation. This is higher quenching than seen in both short-term desiccation tolerant UTEX318 (Figure 26A) and desiccation intolerant *S. costatus* (Figure 26B), both with approximately 1.2x fluorescence quenching. In all algae, fluorescence is quenched the most in PSII regions, specifically at 695nm. In *Chlorella sp.* BC4VF9, fluorescence emission is also quenched in the 760nm region. Lack of quenching in this region is observed in all other algae.

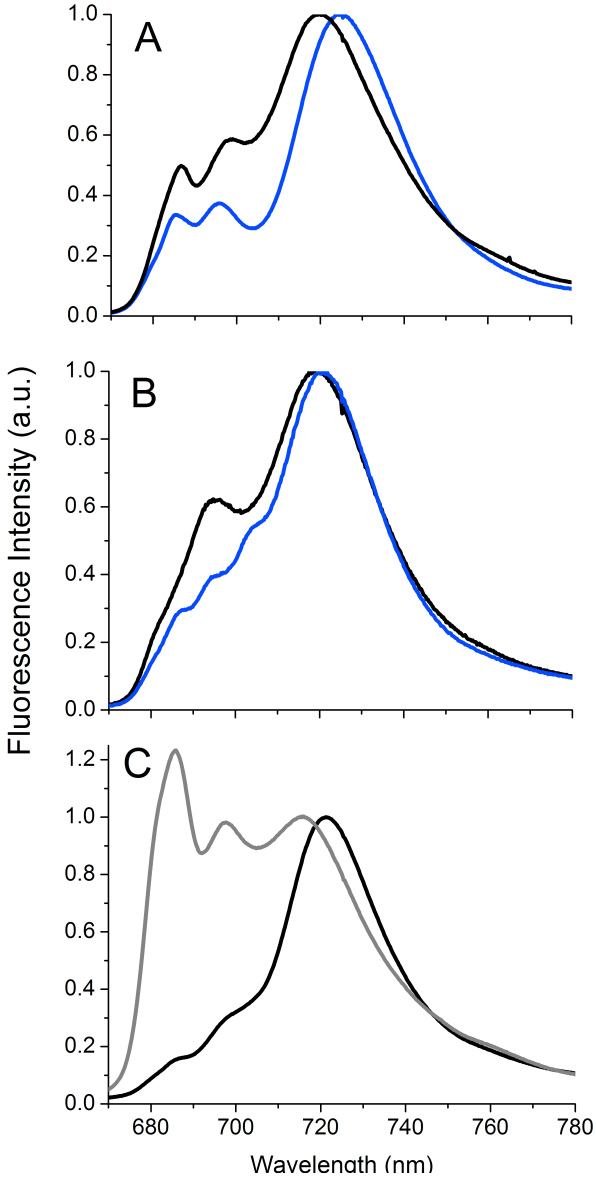

Figure 24: Fluorescence emission spectra taken at 77K of (A) *Chlorella sp.*, and (B) *Scenedesmus sp.* Black traces represent desert dwelling algae, *Chlorella sp.* BC4VF9 and *S. rotundus*, while blue represent aquatic algae, *Chlorella sp.* UTEX318 and *S. costatus*. (C) Fluorescence emission spectra of lichen (solid line) and isolate (dashed). (A) Traces are typical to photosynthetic organisms containing two peaks representing PSII, and one major PSI peak. *Chlorella sp.* BC4VF9 has an extra spectral shoulder at 760nm only previously before seen in desiccation tolerant lichens. (B) *Scenedesmus sps.* both show the presence of an extra spectral feature at 705nm and both species are lacking 760nm spectral shoulder. (C) While there are distinct changes in the spectra between symbiosis and cultured *Trebouxia sp.*, the 760nm shoulder is retained.

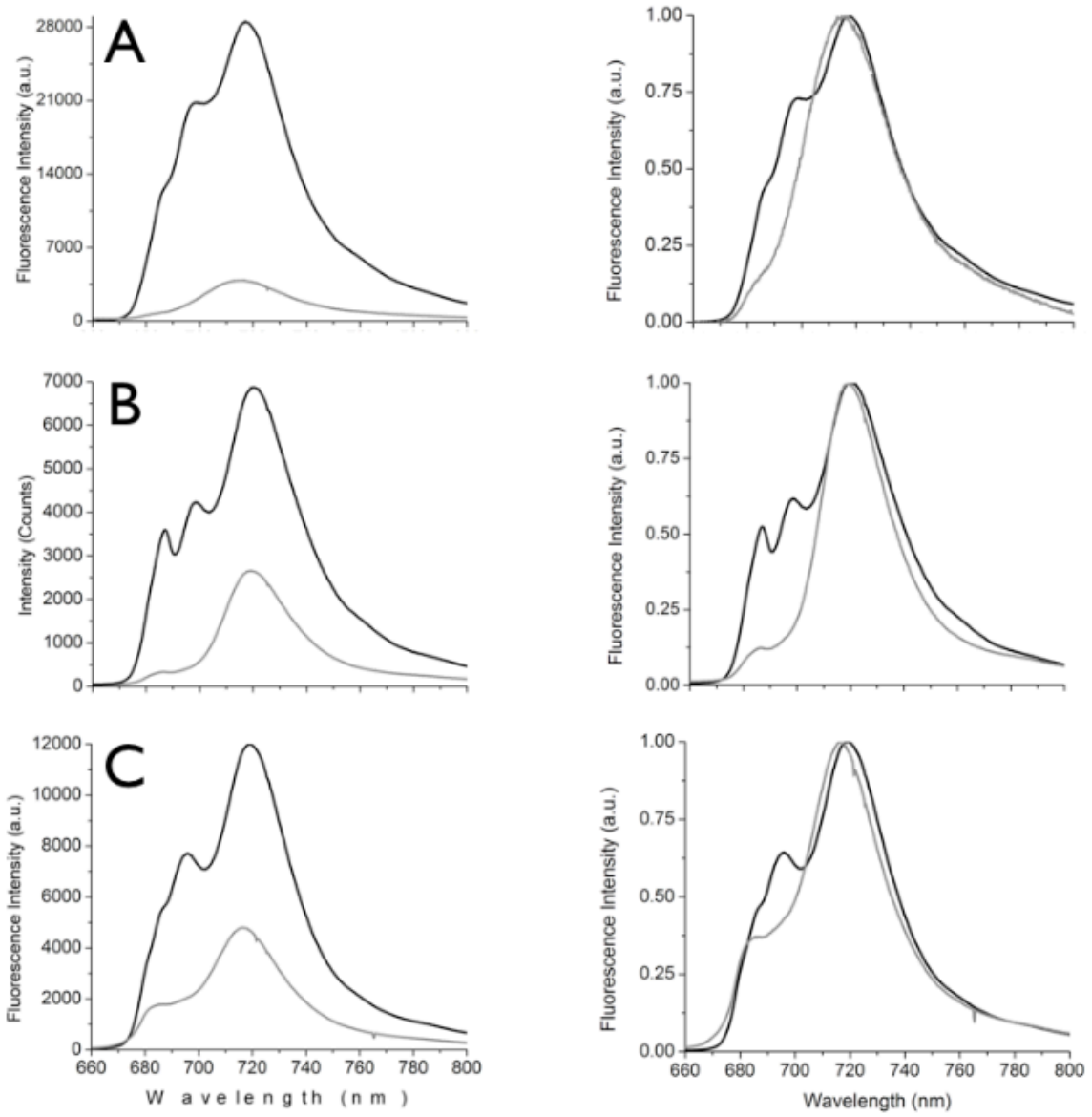

Figure 25: Fluorescence emission spectra at 77K of hydrated (black spectra) and desiccated (gray spectra) of desiccation tolerant species (A) *P. sulcata,* (B) *Chlorella sp.* BC4VF9 and (C) *S. rotundus*. Left side is raw spectra, while right are normalized spectra to PSI peak emission. In normalized spectra shift in PSI emission upon desiccation is approximately 4nm. In *P. sulcata,* quenching of fluorescence is approximately 10x upon desiccation. Desiccation tolerant terrestrial species show quenching of fluorescence of approximately 2x upon desiccation. Quenching is the highest in PSII region, specifically 695nm, and at the long wavelength 760nm region. Desiccated PSI wavelength shift and fluorescence yield ratio presented in Appendix X

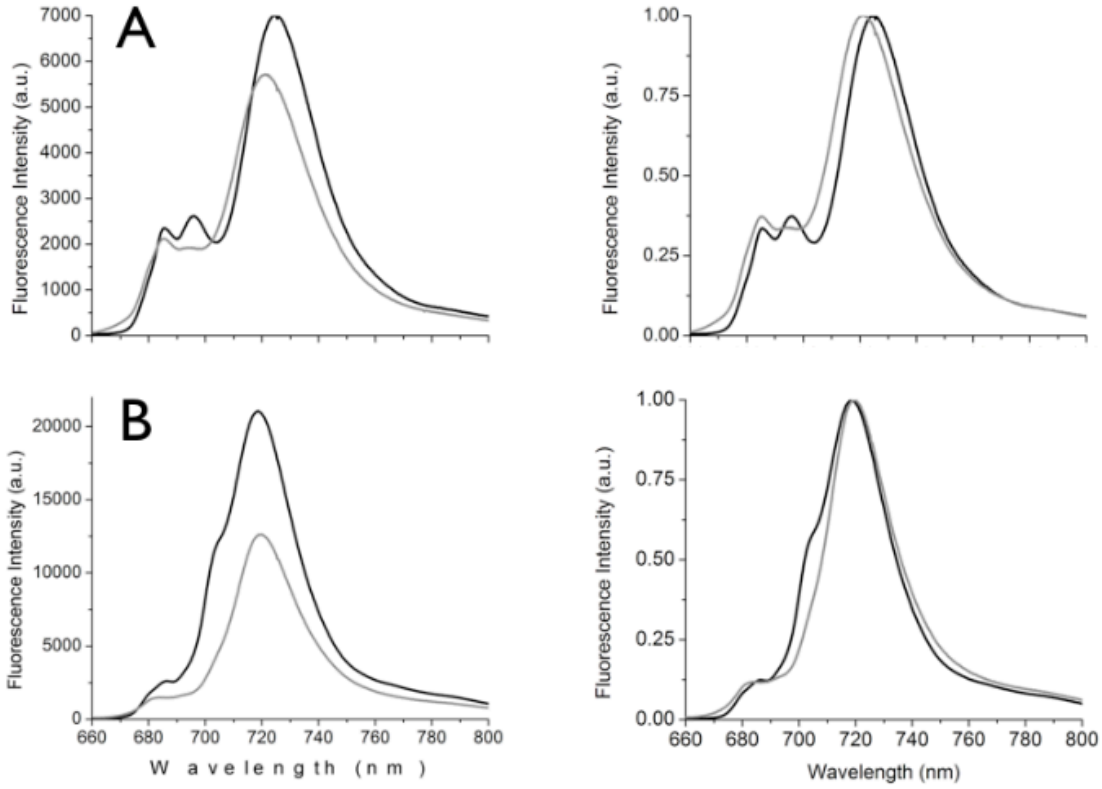

Figure 26: Fluorescence emission spectra at 77K of hydrated (black spectra) and desiccated (gray spectra) of desiccation intolerant species (A) *Chlorella sp.* UTEX318 and (B) *S. costatus*. Left side is raw spectra, while the right is normalized to the PSI peak. Quenching then seen in both short-term desiccation tolerant UTEX318 and desiccation intolerant *S. costatus* is approximately 1.2x hydrated emission. Desiccated PSI wavelength shift and fluorescence yield ratio presented in Appendix X.

Picosecond Decay Kinetics: Decay Curves

Fluorescence decays are the sum of all exponential lifetime decays within a fluorescence system. When displayed in logarithmic format a linear decay represents a single exponential decay component that would arise from a single type or population of decaying fluorophores. Two or more distinct populations of fluorophores generate multiple exponentials and thus a curvature of the decay of these logarithmic plots, representing the different lifetimes. Photosynthetic systems have multiple fluorophores interacting with each other in many different ways and thus are characterized by complex decays (Figure 27).

In fluorescence kinetics, a quenching species is recognized by a decrease in fluorescence lifetime of a fluorescence component. Decay traces at a collection wavelength of 685nm of *Chlorella sp.* BC4VF9, and *S. rotundus* despite the other variations in spectrographic measurements, both have faster decays when desiccated indicative of components with shorter lifetimes (Figure 27). This result suggests that during desiccation a quenching species develops, supporting the fluorescence quenching observations previously seen using the PAM fluorometer (Figure 13) and fluorescence emission spectra for these species (Figure 26). This result mirrors the behaviour of *P. sulcata*, and suggests a quencher is present within all these species in the desiccated state (Figure 27A,B,D). *Chlorella sp.* UTEX318 shows no drastic decrease in kinetics compared to desert and lichen sample (Figure 27C), while *S. costatus* does show an initial fast decay (Figure 27E).

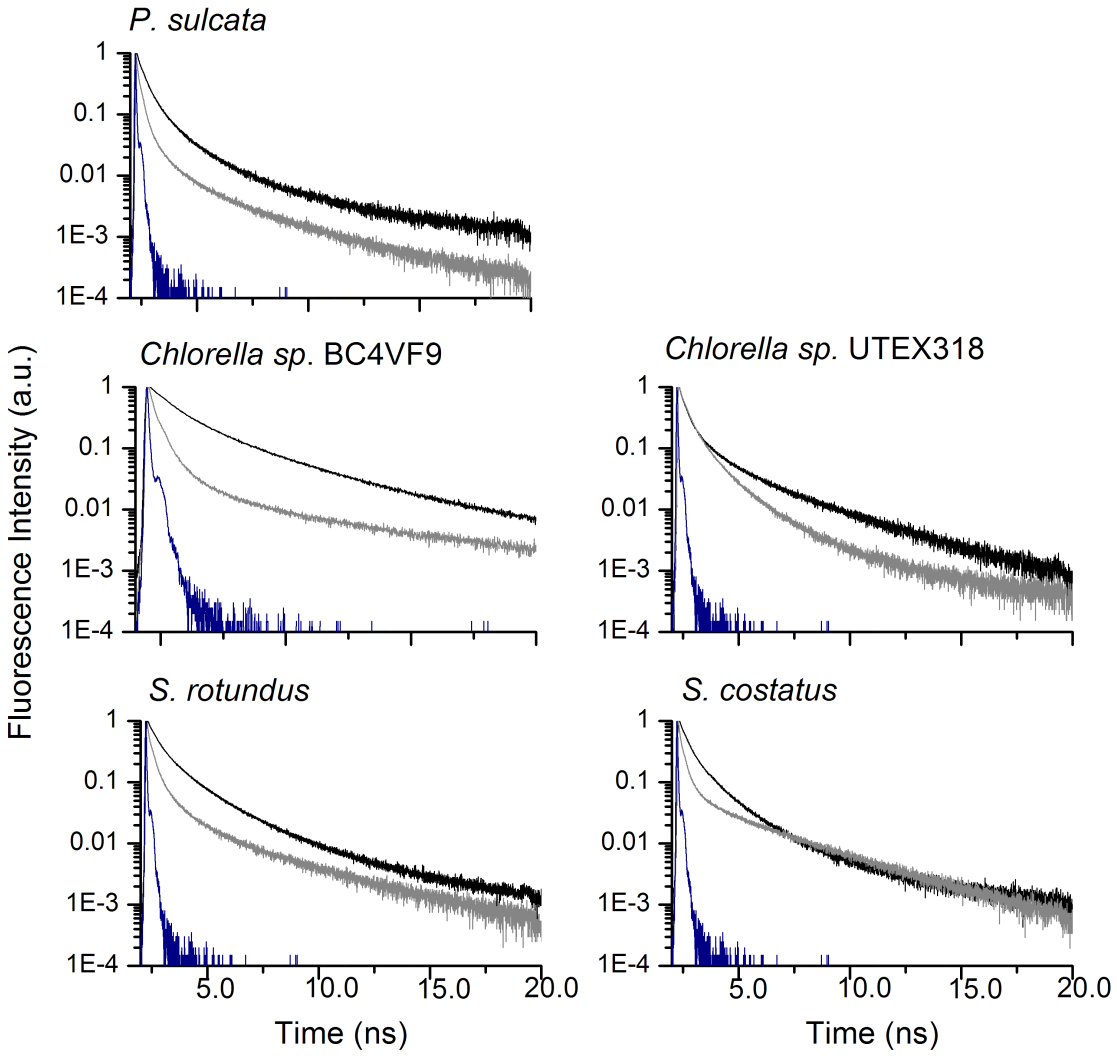

Figure 27: Fluorescence decay curves at 685nm in hydrated (black decay) and desiccated (gray decay) state, compared to the instrument response function (blue). Desiccation tolerant species show similar desiccated decays dominated by a fast-lifetime component. At this wavelength, desiccation intolerant *S. costatus* also shows a faster lifetime component then in the hydrated state. When examined across all wavelengths, *S. costatus* desiccated induced quenching is much different than others (Figure 28). Numerical data presented in Appendix XI.

Overall changes in average lifetime at each wavelength can be determined from these raw decay files in the full width at half maximum (FWHM) measurement. FWHM is the width of individual wavelength decay values (see Figure 27) providing a visualization of the change in average lifetime (of all components) at each wavelength in both hydrated and desiccated state. When collected across the full range of tested wavelengths (Figure 28), FWHM value is decreased upon desiccation in all desiccation tolerant species over the whole range of wavelengths. *Chlorella sp.* UTEX318 shows faster lifetimes at 700nm and in the far red, but not at PSII associated wavelengths, suggesting no formation of a fast lifetime quencher in this region. While *S. costatus* shows a decrease in lifetime in the PSII associated wavelengths, the increase in fluorescence lifetime at 700nm and beyond suggests these PSII associated fast lifetime formation is different than what is formed in desiccation tolerant species.

Smaller FWHM values are seen in the far-red wavelengths (760nm) upon desiccation in all algae, only increasing in *S. costatus*. This fluorescence decrease is the highest in *P. sulcata* and *Chlorella sp.* BC4VF9, as expected, as these species show a clear 760nm spectral shoulder in steady-state fluorescence emission spectra that disappears upon desiccation. Fluorescence yield is also decreased in *S. rotundus* and *Chlorella sp.* UTEX318 despite the lack of this 760nm feature in steady-state fluorescence emission spectra (Figures 25&26).

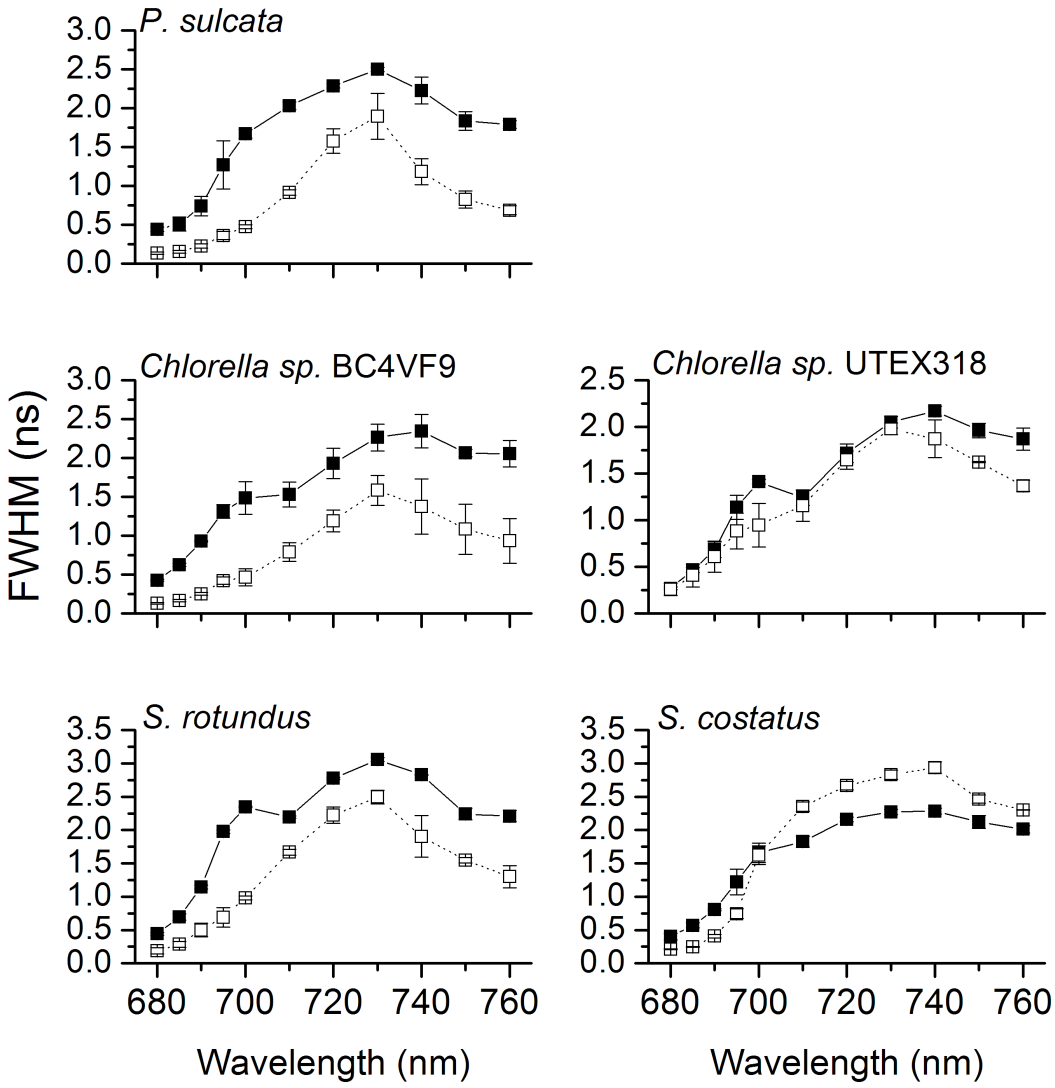

Figure 28: Full width half maximum across all wavelengths calculated from hydrated (black squares) and desiccated (white squares) DAS. In all cases there is an observable quenching in short wavelength areas to varying degrees. In desiccation tolerant organisms this quenching is also extended into long wavelengths, regardless of fluorescence emission at 760nm. *S. costatus* initially shows decreased FWHM only at shorter wavelengths, and is the only species to have an increased FWHM at longer wavelengths. Numerical data presented in Appendix XI.

Global Analysis: Residuals

Decay curves over a wavelength range of 680-760nm were collected. Using a computer-fitting program, these decay curves were used to create Decay Associated Spectra (DAS) via a global fitting approach (Holzwarth, 1996; van Stokkum *et al*, 2004) to describe fluorescence components within the sample. All algae species were fit with a sum of 6 decay components for both desiccated and hydrated decays all yielding a chi-squared statistic of less than 1.1. *P. sulcata* was fit with 5 components for both desiccated and hydrated, hydrated decays had a chi-squared statistic less than 1.1, where desiccated decays had a chi squared of 1.13 (Figure 29; green algae residuals in appendixes XIII and XIV).

77K Decay Associated Spectra (DAS)

Low temperature DAS allow for the rapid identification of a quenching signature as well as overall changes in kinetics of photosystems in the hydrated and desiccated state. By collecting DAS at low temperatures, downhill energy transfer is highly favoured, simplifying energy transfer possibilities and enhancing the visibility of the lowest energy accepting emitters.

Using *P. sulcata* as a model (Figure 29), assignments will be made to components in the hydrated and desiccated DAS. Pigments can receive excitation energy via direct excitation from the light source, or energy transfer from other pigments. The fitting program generates DAS that are normalized to the largest peak amplitude, therefore to determine the effect of desiccation on derived components, the fluorescence maxima ratio was calculated from 77K fluorescence emission spectra taken in each state. For *P. sulcata*, the fluorescence maximum was decreased by an average of 10x in the desiccated state. *Chlorella sp.* BC4VF9 was 2.6x, and *S. rotundus* was 2.8x. *Chlorella sp.* UTEX318

was decreased by 1.4x, while *S. costatus* was 1.5x. Amplitudes of each of the desiccated DAS components were divided by the above numbers to give an accurate representation of desiccated amplitudes (green algae DAS in appendixes XV and XVI).

Positive amplitudes in DAS are representative of fluorescence emission decay from pigment complexes, while negative amplitudes arise from fluorescence rise components that are indicative of energy transfer from one set of pigment pools (or individual pigment) to another. Amplitudes of energy transfer components can be used to determine which sets of pigment pools are receiving the transferred energy. Peak wavelength and lifetime are used to determine origin of fluorescence, shorter wavelengths, 680-700nm, are mostly representative of PSII associated pigments, where 700nm+ mostly represent associations with PSI. Lifetime components with multiple peaks, in both the short wavelengths and the long, suggest a mixing of components with similar lifetimes and do not always suggest energetic coupling between the two species, simply that they share a fluorescence lifetime.

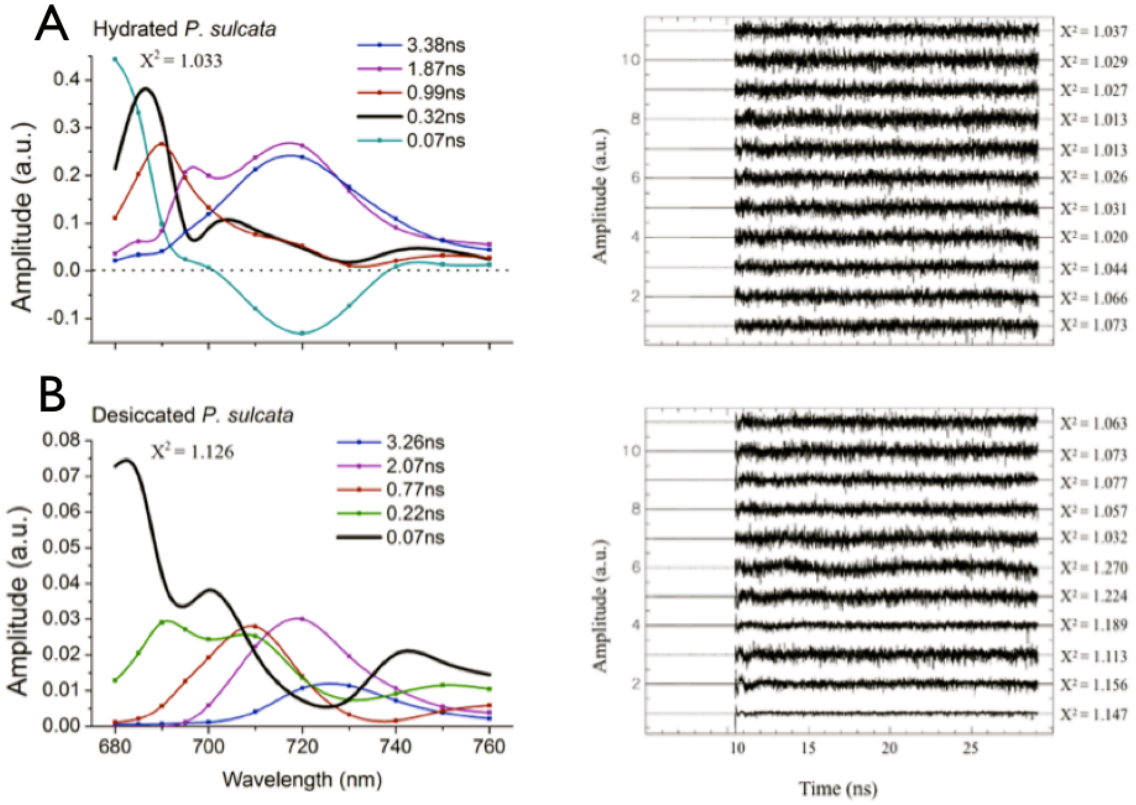

Figure 29: DAS and corresponding residuals of *P. sulcata* (A) hydrated and (B) desiccated. Upon desiccation, 0.32ns component becomes 4x faster, and loses short-wavelength associated peaks. Two distinct lifetime (0.22ns and 0.07ns) components dominate desiccated spectra in both PSII regions (680-700nm) and contain long-wavelength contributions (740-760nm). 0.07ns component displays spectral shape and lifetime consistent with quenching species discovered in *P. sulcata* previously and is associated with LHCII. 6 component residuals and fit Appendix XVI.

Hydrated

In all samples, hydrated spectra from all species tested showed consistent spectral shapes and signatures similar to those seen in unstacked thylakoids with both PSII and PSI associated components present (Van der weij-de *et al*, 2007) (Figure 29, appendixes XIV & XV). PSI associated peaks display a notable trend, as lifetimes increase PSI peak wavelengths become more red-shifted, representing the downhill energy transfer within light harvesting and the PSI reaction centre. A PSI peak wavelength of 720nm is most reminiscent of PSI peak seen in 77K fluorescence emission spectra, thus representing the bulk PSI pigment pool.

The fastest lifetime components in hydrated DAS is representative of energy transfer at a lifetime range of 0.03-0.07ns and 0.17-0.33ns, indicating the transfer of energy from short wavelengths, out into the long wavelengths. This energy transfer pattern is indicative of energy transfer from between LHCII and LHCI, and from LHCII to PSII reaction centre and LHCI to PSI reaction centre. The broad positive peak ranging from 700-720nm in the 0.32ns trace is hypothesized to be direct energy transfer from LHCII to PSI via an LCHII-LHCI-PSI super complex (Van der weij-de *et al*, 2007; Lin & Knox, 1991).

Desiccated

For desiccation tolerant species (*P. sulcata* Figure 29, *Chlorella sp.* BC4VF9 and *S. rotundus* appendix XIV), desiccation causes a lifetime decrease in the LHCII-LHCI energy transfer component (Figure 30), and exhibits a decrease in amplitude of the PSII peaks relative to PSI. This decrease in PSII fluorescence emission is also seen in 77K fluorescence emission spectra by the absence of 685nm and 695nm peaks in the desiccated state (Figures 25&26).

The quenching component in desiccated DAS is hypothesized to originate from LHCII in *P. sulcata, Chlorella sp.* BC4VF9 and *S. rotundus,* quenching excitation energy from wavelengths 680-700nm and 740-760nm, reminiscent of the quenching component previously identified in lichens (Veerman *et al*, 2007; Figure 30). Ultimately, *P. sulcata* has the most efficient energy quenching mechanism seen, as shown by a 4x decrease in lifetime, and also by its dominating amplitude when compared to the other components. BC4VF9 and *S. rotundus* appear to be using the LHCII quenching seen in *P. sulcata* (Figure 30). A blue-shift observed in peak wavelengths of this quenching component suggests red chlorophylls of LHCII are involved in quenching, as their fluorescence decay is no longer detected. Further work on isolated *Trebouxia sp.* from *P. sulcata* will determine if this increase in efficiency is due to symbiosis.

Intermediate desiccation-tolerant *Chlorella sp.* UTEX318 shows a quenching component with the same spectral shape as seen in desiccation tolerant species, but lacking a decrease in lifetime generally associated with quenching (Figure 30), despite the quenching observed from raw decay data (Figure 28).

Desiccation intolerant *S. costatus* (Figure 30) shows a LHCII associated component that is qualitatively different from the others and in essence a large energy transfer component from 685 to 720nm.

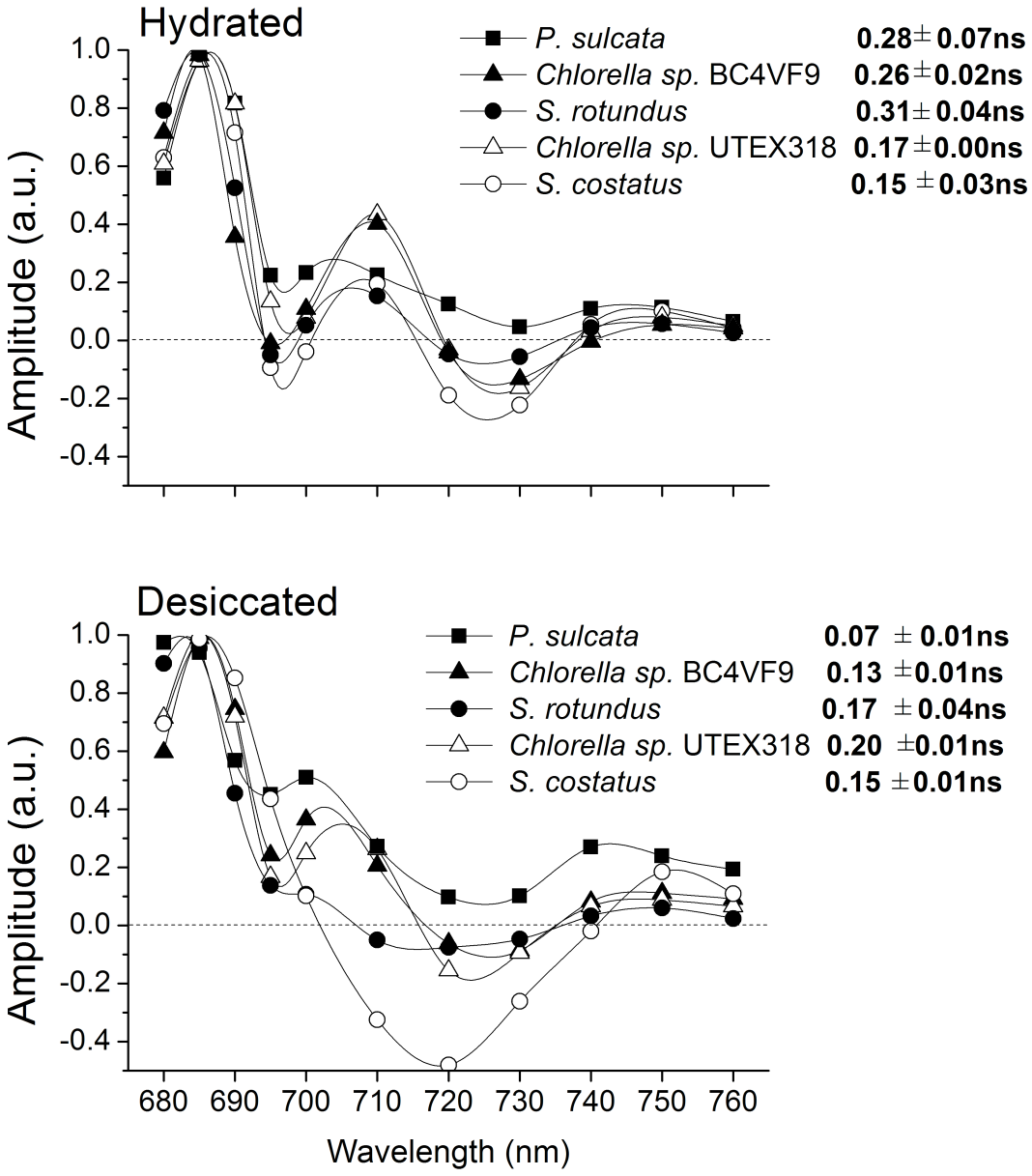

Figure 30: Quenching signature from *P. sulcata* and algae as seen in hydrated DAS (top) and upon desiccation (bottom). Hydrated component is assigned to LHCII and shows a high level of resemblance between species, regardless of desiccation tolerance (black shapes) or intolerance (white shapes). Lifetimes range between 0.15ns to 0.33ns and represents energy transfer from LHCII to PSII core, and to LHCI. Upon desiccation, lifetimes of desiccation tolerant species are shorter, corresponding to the formation of a quencher. *P. sulcata* shows the largest decrease in lifetime, 4x average, followed by desert dwelling algae, 2x average, all showing components with similar spectral shoulders. *Chlorella sp.* UTEX318 and *S. costatus* show no decrease in lifetime upon desiccation, and the spectral shape does not fully resemble desiccation tolerant species. In contrast *S. costatus* has a very different DAS and has a large energy transfer component.

Discussion

Symbiosis Enhances Natural Desiccation Tolerance

This present work expands on green algae desiccation tolerance research on the green algae containing lichen, *P. sulcata* (Veerman *et al*, 2007). By comparing green algae in situ in the lichen with free-living algae that have been isolated from the lichen, current knowledge has been broadened by examining how dNPQ responses vary between two distinct algae lifestyles. It is well noted in the literature that lichen symbiosis provides enhanced desiccation protection, supplied by the mycobiont, in the form of increased antioxidants, photoprotection and the production of secondary phenolic metabolites, all of which are absent or drastically reduced upon symbiont culturing (Kranner *et al*, 2005; Kranner & Birtic, 2005; Yamakawa & Itoh, 2013). This idea is supported in the data, where *P. sulcata* is able to recover a higher level of photosynthetic ability than the desert algae after being held desiccated up to 30 days (Figure 15).

After culturing isolated *Trebouxia sp*. in the lab for 3 months, it was shown that the isolated algae maintained fluorescent signatures identified in intact lichens that were associated with desiccation tolerance, specifically the 760nm spectral shoulder in their low temperature fluorescence emission spectra (Figure 24). This supports the conclusions of Veerman *et al*, 2007 who suggested that the fast-lifetime quencher identified in *P. sulcata* originates in the algal symbiont, and is not a feature of the fungal component. Previous work has shown that symbiosis induced changes in algae size and chloroplast structure start reversing approximately 10 days after isolation of algae from the lichen, and are complete by 30-40 days post isolation (Ahmadjian, 1992; Peksa & Skaloud, 2008). Cultured *Trebouxia sp.* were much more sensitive to photoinhibition than when still within the lichen and exhibited a greater similarity to other species of free living

algae in terms of photoprotection (Figure 19&20) than to lichens, further suggesting significant changes upon liberation from symbiosis.

This work suggests that lichen symbiosis enhances an intrinsic ability to survive desiccation within *Trebouxia sp.* Unlike other species of lichen symbionts, there is conflicting evidence about the occurrence of free-living *Trebouxia sp*., as these species are generally only found within symbiosis (Ahmadjian, 1988) with rare discoveries of small numbers of individual cells (Bubrick *et al*, 1984; Sanders, 2005). It is interesting despite the alga's natural survival ability that evolution as favoured a seemingly entirely symbiosis based existence for *Trebouxia sp*., but not for all terrestrial green algae. As cultured *Trebouxia sp.* was able to recover a high level of photosynthetic ability after desiccation for 24 hours, it is hypothesized that over longer time periods a difference in ability to recover would be seen. While both *Chlorella* and *Scenedesmus sps* can occur as lichen symbionts, they are also largely found free-living in desert crust ecosystems. As shown in this study and in Gray *et al*, 2007, these species are able to survive long periods of time in a desiccated state, and interestingly, survived for longer periods of time in this study than the lichen *P. sulcata* (Figure 15). For all species tested, a decline of desiccation tolerance occurs after 30 days of desiccation at <45% relative humidity. This decline in recovery may be due to these relatively extreme desiccation conditions, as compared to the natural environment these species would typically endure acclimated to St. Catharines weather. Green algae and lichens containing green algae symbionts are able to take up water from the air in the form of fog or morning dew, or perhaps as snow in the dry winter (Kappen *et al*, 1996) making it unlikely that in natural conditions they would be exposed to constant low RH for as long as 30-60 days. Still, the high level of

photosynthetic ability rapidly recovered after desiccation at all time points suggests that damage is minimal to the photosystems, suggesting desiccation induced quenching is far more efficient then hydrated photoprotection.

Algae species from aquatic habitats have limited desiccation tolerance

The designation as *S. rotundus* as the most desiccation resistant free-living algae in this study is consistent with what was seen previously (Gray *et al*, 2007). At 60 days both *S. rotundus* and *Chlorella sp.* BC4VF9 show rehydration recovery, perhaps reflecting the different selection pressures driving the evolution of desiccation tolerance in these green algae based on their respective habitat. *P. sulcata* is a lichen that may often be exposed to high illumination in full sunlight, while desert green algae live in lower light environments within structured communities in desert crust ecosystems, ranging from 1-5mm in thickness (Hu *et al*, 2003; Figure 6). These biological soil crusts (BSCs) are packed full of various photosynthesizing organisms all specialized for light harvesting in their local environment. BSCs have a strong exponential attenuation of light with depth where at a depth of 1mm the light penetration is approximately 1% what is measured at the surface (Evans & Johansen, 1999). The majority of this light available for photosynthesis reaches the algae via light scattering off of a high concentration of reflecting and refracting particles (Jorgensen & Des Marais, 1988; Kuhl *et al*, 1996). On the other hand, *Chlorella sp.* UTEX318 show short-term desiccation tolerance but not long-term, suggesting that the original habitat of this alga may be characterized by relatively short cycles hydration and desiccation, and therefore not fully aquatic. This same trend was seen in Gray *et al*, (2007). After a period of 24 hours rehydration in the darkness, UTEX318 was the only aquatic algae tested that showed a significant further recovery after protein synthesis was able to take place (Gray *et al*, 2007). *S. costatus*

represents a species that is most likely completely aquatic and was shown to be desiccation intolerant. Although the F_V/F_M of *S. costatus* after desiccation is reported to be above 0.1, this was only true for the first two SLPs that show a hint of recovery, but by the end of 10 mins there was no variable fluorescence or active photosynthesis in this organism. Although this is the first of these studies to utilize *S. costatus*, Gray *et al*, (2010) used another *Scenedesmus sp.* (*S. platydiscus*) from an aquatic habitat in their study and found a similar result, with no further recovery even after 24 hours of recovery in the dark.

Hydrated Photoprotective/Repair Mechanisms Are Species Specific.

Desiccation induced quenching in all species showed fast reversal kinetics associated with NPQ energy quenching. It was important to characterize the hydrated photoprotective mechanisms within these algae, as the involvement of these mechanisms in desiccation tolerance, specifically involvement of the xanthophyll cycle, is widely debated in the lichen literature. It was also interesting to note that the differences observed in hydrated photoprotection were greatest between the different classes of algae tested, and not between desert and aquatic dwelling algae. Originally in this thesis, it was hypothesized that desert dwelling algae and lichen would show greater photoprotection in both the hydrated and desiccated states than the aquatic algae.

All hydrated algae demonstrated the ability to build up photoprotective (NPQ) mechanisms upon exposure to highlight stress and also the ability to repair photodamage. The kinetics of NPQ development and recovery as well as the response to DTT treatment shows class-specificity. Results from all algae species suggest the xanthophyll cycle carotenoids are not the only NPQ response to high-light stress, and are used to different extents in *Scenedesmus sps*. compared to *Chlorella sps*. (Figure 19). Xanthophyll related

quenching relies on changes linked with the antenna complex, which accounts for the quenching of F_O seen in Figure 20 for *Chlorella sps*. With the application of DTT, this strong F_O quenching is absent, indicating the remaining NPQ signal is originating from effective reaction centre quenching. This lack of strong F_O quenching is absent in *Scenedesmus sps*, regardless of DTT treatment, suggesting that in *Scenedesmus sps.* NPQ relies more heavily on reaction centre quenching mechanisms (Ivanov *et al*, 2003; Koblizek *et al*, 1999).

Recovery from photodamage was tested to determine how these algae were affected by photoinhibitory light exposure and to determine their PSII repair capacity. All species tested showed damage after 1 hour of high light treatment, followed by a significant recovery of F_V/F_M after 1 hour of low light treatment (Figure 21). Recovery was assayed by a gradual increase in F_M during the 1 hour of low light recovery treatment (Appendix VII). Application of the protein synthesis inhibitor chloramphenicol, as expected, caused an increase in accumulated damage (low F_M), and a decrease in recovery slope. Chloramphenicol blocks chloroplast protein synthesis, and inhibited recovery as damaged D1 proteins could not be replaced. The accumulation of damage after chloramphenicol treatment was not as high as after cycloheximide treatment, however chloramphenicol treatment suppressed recovery more than cycloheximide treatment. Cycloheximide treatment is responsible for blocking cytosolic protein synthesis, which includes the nuclear encoded LHCII subunits (Dunsmuir *et al*, 1983). Under highlight conditions, the accumulation and binding of caroteinoids under highlight stress is inhibited with cycloheximide treatment (Schtifer *et al*, 1994). This interference of cycloheximide with photoprotective mechanisms is consistent with the higher

accumulation of damage and lower recovery from photodamage seen in this study (Figure 22). Cycloheximide has also been reported to inhibit the removal of damaged PSII RCs from thylakoid membranes, and these damaged RCs have also been shown to quench excitation energy (Raven, 2011).

Chloramphenicol in this study was most effective at suppressing recovery in all species tested, while cycloheximide was not as efficient, however recovery proceeded at a lower rate than untreated controls. This result is common in studies of this kind (Lindholm *et al*, 1987). Any residual recovery seen after application of chloramphenicol represents an incomplete inhibition of *de novo* D1 synthesis. Recovery after cycloheximide treatment represents the *de novo* D1 synthesis occurring within the chloroplast to repair damaged RCs, specifically noted in *S. rotundus*, *Chlorella sp.* UTEX318, and *Trebouxia sp*., where during photoinhibition *de novo* protein synthesis in the cytosol plays a small role in recovery. It must be noted the concentration used in this study for cycloheximide is large, and negative side effects of this high treatment can be seen in control data for *S. costatus* and *Chlorella sp.* BC4VF9. This result is problematic as protein turnover and *de novo* synthesis was hypothesized to be due to light induced PSII damage and repair in this experiment, however clearly there is high protein turnover of other essential proteins in the cells that must be considered.

Hydrated Photoprotective/Repair Mechanisms Are Not Responsible For Desiccation Tolerance.

Characterizing the hydrated NPQ response and PSII repair provided a platform to determine the necessity of these aspects in desiccation tolerance. Despite the closely matched NPQ relaxation kinetics between Xanthophyll cycle and desiccation induced quenching, desiccating algae in the presence of DTT did not inhibit the ability to recover

photosynthetic ability after rehydration (Figure 23). Desiccation in the presence of protein synthesis inhibitors also did not inhibit the ability to recover. Despite the need for xanthophyll cycle carotenoids and *de novo* protein synthesis in hydrated photoprotection mechanisms, this result indicates that even though these mechanisms may increase the extent of desiccation tolerance, they are not *necessary*.

Treatments with protein inhibitors on desiccation tolerant mosses and bryophytes have noted similar results, with initial fast F_V/F_M recovery after rehydration. The effect of these inhibitors was seen more so on long-term recovery (inability to reach pre-desiccation F_V/F_M values even after days) and importantly on CO_2 uptake and carbon fixation (Procter *et al* 2007; Proctor & Smirnoff, 2000). Treatment with cycloheximide showed significant negative effects on desiccation tolerance in all species, suggesting the synthesis of cytosol-encoded proteins play a role in desiccation tolerance. The build up of low weight molecular compounds has been shown in *Chlorella sps*., and some *Scenedesmus sps*. when exposed to water stress, such as high salinity environments (Flameling & Krompkamp, 1994; Gustavs *et al*, 2010). The negative effect on the recovery of *P. sulcata*, is higher than is seen in the isolated *Trebouxia sp.*, and therefore it is hypothesized to have been affecting secondary metabolite products produced by the fungal component of the lichen. For other species, the photosynthetic recovery after desiccation is greater than observed in hydrated photoinhibition experiment, suggesting photosystem damage accumulated under desiccation stress is less that that accumulated under photoinhibition.

The necessity of xanthophyll cycle carotenoids in desiccation tolerance in lichens has been debated in the literature and dark accumulation of zeaxanthan varies between

species. The same may be noted for desiccation tolerant green algae. DTT treatment in hydrated *Chlorella sp.* UTEX318 significantly lowered NPQ response under light stress, and DTT treatment was found to lower PSII recovery after desiccation. While the accumulation of xanthophyll carotenoids in NPQ response in hydrated *S. rotundus* was not the dominant NPQ response, DTT did significantly lower the NPQ signal. The decline in desiccation tolerance from both DTT and cycloheximide treatment suggests in both these algae, zeaxanthan may be a contributor to desiccation induced quenching. DTT treatment is a non-specific inhibitor of violaxanthin de-epoxidase, and treatment alone in plant studies has been shown to inhibit ΔpH formation by inhibiting electron transport, as well as negatively effecting dark reaction enzymes and even the ATP-ase (Schreiber & Neubauer, 1990). While these effects are usually seen after treatment with a higher concentration, they might also be present after a long-time exposure.

The light sensitivity shown by these algae during rehydration further suggests these mechanisms are not responsible for desiccation recovery, but may work in tandem to provide photoprotection. By desiccating in the dark, the build up of photoprotection unrelated to desiccation tolerance is inhibited. The lack of these light-induced photoprotective mechanisms leave these algae unprotected when desiccation induced quenching is reversed upon rehydration. When rehydrated under low light conditions, these algae showed a decrease of ΦPSII at light intensities of 40μE and below (Figures 16). Table 3 shows hydrated algae with high F_V/F_M values when exposed to 25μE, and thus suggests an increased light sensitivity in the desiccated state. A major flaw in this experiment was not taking dark recovery measurements after the light test to determine if this decrease in ΦPSII is related to photosystem damage or quenching. To make up for

this however, we can examine the photochemical quenching parameter qP which shows a shut down of photochemistry when rehydrated under increasing light (Figure 17). Typically, NPQ parameters would be associated with stability in qP, as light is being dissipated that would other wise lead to a closure of reaction centres. A decrease in qP under light stress can also be associated with NPQ parameters however, as closed RCs can act as non-radiative dissipation centres. When F_V/F_{Mmax} was examined to determine the efficiency of PSII at increasing light intensities, it was determined that at light intensities lowering ΦPSII, desert algae *Chlorella sp.* BC4VF9 and *S. rotundus* maintained a stable F_V/F_{Mmax} (Figure 18). Together with qP and ΦPSII values this suggests that there are indeed NPQ mechanisms working at these low light intensities.

To determine the photoprotective ability of the desiccated quencher, tests would have to be performed by exposing algae to light conditions while desiccating, and over the time held in the desiccated state. This was not done in this study, but was included in Gray *et al*, (2007) study. Results indicated that exposure to light treatments (130μE) had a lower recovery after rehydration than if rehydrated in the dark. Any further subsequent recovery was only achieved after 1-5 days of illumination and *de novo* protein synthesis. These results together suggest that the ability to build up photoprotective mechanisms during desiccation under light allows for the recovery of photosynthetic ability upon rehydration. The need for co-operation between desiccation-induced and light-induced fluorescence quenching mechanisms is important in desiccation tolerance in moss (*Rhytidiadelphus squarrosus* Heber *et al*, 2006).

Desiccation Induced Fluorescence Quenching Is Not Species Specific

Further evidence for desiccation induced quenching being a unique mechanism from NPQ in hydrated algae is the similarity of desiccation fluorescence parameters between all desiccation tolerant species. PAM fluorometer curves of desiccating *P. sulcata*, and *Chlorella sps.* BC4VF9 and UTEX318, all show similar trends despite (I) symbiosis or free living (II) desert vs. aquatic habitat and (III) short or long-term desiccation tolerance (Figure 13). Unique to the desiccation curves of green algae, F_O fluorescence quenching is indicative of a biphasic shut down of PSII complexes during the onset of desiccation (Figure 13). An increase in F_O fluorescence indicates a higher fluorescence yield coming from LHCII. This is typically associated with the shut down of the PSII RC, no longer receiving excitation energy from LHCII, and instead is dissipated as fluorescence (Yamane *et al*, 1997). This increase and the subsequent decrease to zero of F_O fluorescence has also been associated with the potential disassociation of LHCII or subunits of LHCII from the RC in heat treated chloroplasts (Schreiber & Armond, 1978), barley leaves and pea leaves (Briantais *et al*, 1996). This F_O fluorescence increase is concurrent with an increase in F_V from the reaction centre, representing the simultaneous shut down of PSII mediated electron transfer, and a decrease in F_V/F_M. By shutting down linear electron transport on the onset of desiccation, fluorescence from the RC (F_V) would increase, before PSII is completely inactive. In pea plants, the migration of LHCII during heat stress was shown to be towards stroma thylakoid regions, indicating the potential association with PSI (Mahanty *et al*, 2002). This association would successfully decrease the absorption cross-section of PSII during desiccation, and would increase absorbance for PSI to drive cyclic electron transfer, which can act as an efficient quencher (Iwai *et al*, 2010). This increase in cyclic electron transfer has been noted in desiccated lichens

previously (Komura *et al*, 2008), and similar effects on thylakoid membrane structure and organization during desiccation in lichen *Lobaria pulmonaria,* has lead to hypothesizes of LHCII-PSI associations as a similar mechanism of protection and fluorescence-quenching during desiccation stress (Chakir & Jensen, 1999). Shown in Figure 13, the observed increase of F_O fluorescence in free-living green algae is not seen in the lichen thallus in this thesis, and is suggested to be due to the desiccation-induced high-light scattering which would hinder the PAM from picking up the F_O signal. An overall decrease in F_O quenching during desiccation shows the formation of an effective quencher with a faster excitation and dissipation rate than reaction centre excitation (Heber, 2008).

Desiccation-induced PSII fluorescence quenching examined by steady-state fluorescence emission spectra at 77K for all species (Figures 26&27) shows the highest quenching exhibited is in the PSII range (680-700nm) with the highest quenching at 695nm (Veerman *et al*, 2007; Komura *et al*, 2010). This is the same regardless of presence/absence of a resolved 760nm spectral shoulder, and even the presence of a fast lifetime quencher in this region. This result suggests the origin of 695nm quenching is not LHCII quenching, but more reminiscent of reaction centre quenching (Schweitzer *et al*, 1998). Increased fluorescence quenching of PSII in a state where photochemistry is inactive decreases the probability of a charge separation event, also the higher the chances of formation of triplet chlorophyll and harmful reactive oxygen species.

In *P. sulcata* and *Chlorella sp.* BC4VF9, 760nm fluorescence emission is quenched as well, again indicating a coupling of the origin of this fluorescence to PSII (Veerman *et al*, 2007). While PSI fluorescence could not be measured using the PAM,

these fluorescence emission spectra show PSI fluorescence is quenched as well, hypothesized to be due to the removal of LHCII energy transfer to LHCI.

Time resolved fluorescence decay kinetics at 77K allow for a more detailed representation of fluorescence components than steady state. Kinetics collected of hydrated and desiccated algae show a decrease in average lifetime upon desiccation most notable in *P. sulcata*, but still seen in desert dwelling algae (Figure 27). *Chlorella sp.* UTEX318 and *S. costatus* shows decays dominated by slower lifetimes representing the slow fluorescence decay of chlorophyll when electron transfer is blocked. As this is not seen in algae that better survive desiccation, this slow decay is also associated with collective damage.

Individual lifetime components present within these decays and their associated spectral contribution can be visualized in decay-associated spectra. DAS of desiccated *P. sulcata* confirms the presence of an effective long-wavelength fast lifetime quencher identified previously by Veerman *et al* (2007) effectively causing the fluorescence quenching in PSII regions (Figure 29). While the relative amplitude of the long-wavelength contribution is lower than seen previously in the literature, the rest of the spectral components are strikingly similar. PSI kinetics remain largely unchanged upon desiccation as expected. DAS created in this study have included more points across the wavelength range, resulting in more detail than shown previously. With this detail, DAS for desiccated *P. sulcata* show a quenching signature consistent with quenching seen in the fluorescence emission spectra. While Veerman *et al*, 2007 did not include a hydrated DAS at 77K, I show that the lifetime changed from hydrated to desiccation is approximately 4x faster in desiccated form spanning across PSII associated wavelengths,

and with a long wavelength contribution. The presence of antenna energy transfer in this way is not surprising as green algae do not have photosystem separation in thylakoid membranes, thus suggesting that interactions between PSII and PSI maybe expected.

Algae Species Show Similar Fluorescence Signatures To *P. sulcata*

P. sulcata shows the highest level of desiccation induced quenching shown in Figure 25, and the associated desiccated DAS shows the highest amplitude and therefore clearest picture for the visualization of the quenching species (Figure 30). This DAS provides the specific spectral shape of the quenching species with the smallest amount of component overlap. This spectral shape is the template for the signature I hoped to identify within the algae.

In this study, *Chlorella sp*. BC4VF9 is the alga most closest related species to *P. sulcata*, and has the highest level of desiccation induced quenching of free-living algae showing the cleanest quenching signature (Figure 30) with a 2x faster lifetime change. This quenching signature is highly similar in desiccation tolerant species, however they are not the exact same. As the quenching signature becomes an increasingly smaller spectral contribution, it therefore becomes more difficult to de-convolute. This distortion arises from the overlap of many components with similar lifetimes, specifically fast-lifetime energy transfer components. This creates a problem when trying to determine if the quenching signature is the same between compared species. To use these DAS to determine more conclusive results, more hands-on spectral fitting would be required, as well as fitting with a physical kinetic model. A simplified method of comparison is presented in Figure 28 in the comparison of decay widths between hydrated and desiccated samples. These widths represent average lifetime at each wavelength measured and show the same desiccation induced quenching present in all terrestrial

species occurring in PSII regions (680-700nm) and also in far-red (740-760nm). The most far-red quenching is seen in *P. sulcata* and *Chlorella sp*. BC4VF9, the only two species tested to show steady-state spectral peaks in this region. Despite the lack of this feature in *Chlorella sp*. UTEX318, and *S. rotundus* in steady-state measurements, the presence of quenching in this area is hypothesized to be due to the narrowing of PSI fluorescence emission at these wavelengths. Clearly, within all desiccation-tolerant species tested, the same mechanism is being used for desiccation induced quenching. The amount of this quenching can be correlated to the desiccation-tolerance ability, *P. sulcata*, *Chlorella sp.* BC4VF9, and *S. rotundus*, followed by *Chlorella sp*. UTEX318, and *S. costatus*.

Support For LHCII-Aggregation Model for Energy Dissipation

LHCII complexes isolated from spinach thylakoids have shown that upon aggregation, fluorescence yield at 77K decreases by a factor of 10 or more (Horton *et al*, 1991; Ruban & Horton, 1992). This supports desiccation induced fluorescence quenching being high in PSII regions shown in this thesis by fluorescence emission spectra (Figure 25&27) and in DAS (Figure 30 and appendix XIV and XV). Aggregation of isolated trimeric LHCII has also shown a drastic decrease of lifetime compared to non-aggregates at 77K indicating the formation of an efficient high-energy quenching (Mullineaux *et al*, 1993), which is seen in this thesis to occur under desiccating conditions.

In hydrated algae DAS, energy transfer is occurring from LHCII to LHCI at 720nm via LHCII-LHCI-PSI supercomplex (Figure 30; Van der weij-de *et al*, 2007), indicating direct contact between PSII and PSI in green algae thylakoids. In pea plants with spatially separated PSII and PSI, this feature is absent. Absorbed energy in the PSII-LHCII is transferred via antenna energy transfer to the highly efficient quencher, oxidized

PSI ($P700^{+}$). This mechanism is hypothesized to be a very important quenching system in desiccation survival as seen by the decrease in F_O fluorescence during desiccation, showing PSII antenna is restricted in energy absorption. Upon desiccation, there is a blue-shift observed in this peak to 710nm. In higher plants, an increase in fluorescence emission at this wavelength is associated with LHCII aggregation and heat dissipation (Mullineaux *et al*, 1993). It is possible this shift is related to the blue shift of the PSI peak observed upon desiccation in steady state measurements (Figures 26&27). Isolation of the LHCII-LHCI-PSI supercomplex and further kinetic tests in both hydrated and desiccated state must be performed to know true origin.

It is hypothesized that this change in LHCII aggregation would drastically effect the conformation of the thylakoid membrane (Horton *et al*, 1991), which coincides with glutaraldehyde tests on desiccating lichens (Heber *et al*, 2011). This type of energy quenching has been shown to rapidly accumulate under dark conditions, which is in agreement with results of this study. The potential involvement of xanthophyll cycle carotenoids as well as the potential for enzymatic involvement in the allosteric movement of LHCII is still debated and unclear within the literature (Review see Ruban *et al*, 2012), however it is suggested in this thesis that the involvement of xanthophyll cycle pigments is minimal (Figure 13). Possible involvement of accumulation of low weight molecular compounds, or important proteins involved in carbon fixation cannot be ruled out (Proctor & Smirnoff, 2000). Biochemical studies need to be carried out on green algae derived LHCII complexes (as opposed to spinach) to match protein changes to those observed spectroscopically.

The inability of *Chlorella sp.* UTEX318 to withstand long periods of desiccation is the inability of LHCII to form an efficient quenching species, as seen in the maintenance of a lifetime matching that of the hydrated state (Figure 30). This suggests this LHCII reorganization may be the most important feature in terms of long-term desiccation survival.

Conclusions

In conclusion, it appears that all desiccation tolerant algae tested in this study are using the same desiccation induced fluorescence quenching mechanism hypothesized to be located in LHCII. This desiccation-induced fluorescence quenching mechanism is also different to what is seen in the hydrated algae NPQ response where there was clear genus related differences in high light dissipation. Desiccation induced quenching involves quenching in both the PSII spectral regions (680-700nm) and far-red (740-760nm), the extent of which can be correlated to the desiccation-tolerance of the green algae species tested. The main hypothesis is the involvement of aggregated LHCII to form a quenching species, caused by a desiccation induced reorganization of the thylakoid membrane occurring when chloroplasts become reduced in diameter, and thylakoid membranes become wrinkled and bent in appearance (Holzinger & Lutz, 2011). This reorganization allows for preferential energy transfer to PSI away from PSII, and organizational changes necessary with LHCII to form an effective quencher of PSII excitation energy. The presence of 760nm fluorescence quenching, despite the presence or absence of this spectral feature in steady-state measurements further supports LHCII aggregation model as far-red fluorescence is hypothesized to be a marker for chlorophyll-chlorophyll charge transfer states (Mullineaux *et al*, 1993).

Future Studies

This study provides a starting point for various branching projects in biophysics, fluorescence spectroscopy, evolutionary biology, and genetics. At this point, this study represents only a two species comparison between algae originating from desert and aquatic ecosystems relating to desiccation recovery, and is thus not able to generalize on the evolution of desiccation tolerance. With the number of cultures of green algae of all different genus and species available from both desert and aquatic habitats it is very possible to perform the studies presented in this thesis on them all. By combining time-resolved fluorescence measurements with genetics, it is possible to map the evolution from aquatic to terrestrial habitats for species lineages and thus the evolution of desiccation induced quenching mechanisms.

Further advances to the direct mechanism of desiccation-induced fluorescence quenching requires DAS further fit with physiology-derived kinetic models to determine exact assignment of components and confirm the presence of spill-over, or LHCII aggregation. The exploration of long-wavelength chlorophylls associated with PSII antenna complexes is on going in desiccation tolerant organisms. The next goal would be discover a way to isolate these complexes from thylakoid membranes with minimum disturbance to their configuration and arrangement. Isolation of these complexes would allow for deeper studies into their fluorescent nature and conformation, allowing for further understanding as to how the complex aids in desiccation induced quenching.

Desiccation induced fluorescence quenching is by no means controlled by only one mechanism. Reaction centre quenching (Heber *et al*, 2011), spill-over (Slavov *et al*, 2013) and LHCII quenching (Veerman *et al*, 2007; Miyake *et al*, 2011) work together to appropriately protect photosystems from desiccation-induced damage. The ability to

produce these quenching species are vital to the survival of an algal species, however it is not the first step in determining desiccation tolerance. It has been suggested in a recent study that the orders of magnitude stronger quenching observed in lichen thalli then in isolated algae is by the production of the sugar arabitol in the fungi (Kosugi *et al*, 2013) which has been shown to have high stabilizing capacities of thylakoid membranes during periods of desiccation. Incubation of isolated lichen algae with arabitol was shown to have an increase in dNPQ ability. The presence of arabitol in highly desiccation tolerant photosynthetic species should be quantified and if absent, should be tested if the presence of this disaccharide can increase desiccation tolerance (Kosugi *et al*, 2013).

An interesting long-term question is the ability of genetically modifying plant crops to include these mechanisms to potentially protect the highly delicate leaf tissue and thus have plant survival during sever drought. Of course the advantages and the benefits of this type of research would be obvious if this indeed could be the case. It should be noted that while the majority of desiccation tolerant plants are ferns or bryophytes, there are instances of desiccation tolerant vascular plants, they however represent only 0.2% of total flora (Oliver *et al*, 1998). If genetic variants could be discovered that underlie the unique quenching abilities noted in green algae, it would be interesting to see if transformation would increase the desiccation tolerance of vascular plants. As all terrestrial plants came about by a single evolutionary lineage of aquatic green algae, it would make sense to hypothesize it was much more beneficial to the plant to lose the trait than maintain it. It would also be interesting to see along the evolutionary lineage of terrestrial plants at which point and potentially why this trait was lost and what the energetic cost would be to maintain the trait.

References:

Ahmadjian, V. 1967. The Lichen Symbiosis. Copyright Blaisdell Publishing Company A Division of Ginn and Company. Printed in Massachusetts, USA.

Ahmadjian V. 1988. The lichen algae Trebouxia: does it occur Free-Living? Plant Systematics and Evolution 158:243-247

Ahmadjian V. 1992. Resynthesis of lichens In: Algae and Symbioses. Ed: Reisser W. Biopress Ltd. Bristol:325-338

Alpert P., & Oliver M.J. 2002. Drying without dying. In: Desiccation and survival in plants: drying without dying. CAB international.

Andrizhiyevskaya E.G., Chojnicka A., Bautista J.A., Diner B.A., van Grondelle R., & Dekker J.P. 2005. Origin of the F685 and F695 fluorescence in Photosystem II. Photosynthesis Research 84:173-180

Aro E-M., Suorsa M., Rokka A., Allahverdiyeva Y., Paakkarinen V., Saleem A., Battchikova N. & Rintamaki E. 2004. Dynamics of photosystem II: a proteomic approach to thylakoid protein complexes. Journal of Experimental Botany 56(411):347-356

Baena- Gonzalez E., Barbato R., & Aro E.M. 1999. Role of phosphorylation in the repair cycle and oligomeric structure of photosystem II. Planta 208:196-204

Baena- Gonzalez E. & Aro E.M. 2002. Biogenesis, assembly and turnover of photosystem II units. Philosophical Transactions of the Royal Society of Biological Sciences 357:1451-1460

Bartak M., Solhaug K.A., Vrablikova H., & Gauslaa Y. 2006. Curling during desiccation protects the foliose lichen Lobaria pulmonaria against photoinhibition. Oecologia 149:553-560

Bjorkman O., & Demmig B. 1987. Photon yield of O_2 evolution and chlorophyll fluorescence characteristics at 77K among vascular plants of diverse origins. Planta 170:489-504

Bold H.C. 1949. The morophology of *Clamydomonas chlamydogama* sp. Nov. Bulletin of the Torrey Botanical Club 76:101-108

Briantais J.M., Dacosta J., Goulas Y., Ducruet J.M., & Moya I. 1996. Heat stress induces in leaves an increase of the minimum level of chlorophyll fluorescence, Fo: A time-resolved analysis. Photosynthesis Research 48:189-196

Brock T.D. 1961. Chloramphenicol. Microbiology and Molecular Biology Reviews. 25(1):32-48

Brown D.H., Rapsch S., Beckett A., & Ascaso C. 1987. The Effect of Desiccation on Cell Shape in the Lichen Parmelia sulcata Taylor. New Phytologist 105:295-299

Bubrick P., Galun M., & Frensdorff A. 1984. Observations on free-living Trebouxia DePuymaly and Pseudotrebouxia Archibald and evidence that both symbionts from Xanthoria parietina (L.) Th.Fr. can be found free-living in Nature. New Phytologist 97:455-462

Calatayud A., Deltoro V.I., Barreno E., & del Valle- Tascon S.1997. Changes in in vivo chlorophyll fluorescence quenching in lichen thalli as a function of water content and suggestion of zeaxanthin-associated photoprotection. Physiologia Plantarum 101:93-102

Chakir S., & Jensen M. 1999. How does *Lobaria pulmonaria* regulate photosystem II during progressive desiccation and osmotic water stress? A chlorophyll fluorescence study at room temperature and at 77K. Physiologia Plantarum 105:257-265

Davey M.C. 1989. The Effect of Freezing and Desiccation on Photosynthesis and Survival of Terrestrial Antarctic Algae and Cyanobacteria. Polar Biology 10:29-36

de los Rios A., Ascaso C., Wierzchos J. 1999. Study of lichens with different state of hydration by the combination of low temperature scanning electron and confocal laser scanning microscopes. International Microbiology 2:251-257

Demmig- Adams B., & Adams W.W III. 1996. The role of xanthophyll cycle carotenoids in the protection of photosynthesis. Trends in plant Science Reviews. 1(1):21-26

DePriest P.T. 2004. Early molecular investigations of lichen-forming symbionts 1986-2001. Annual Reviews in Microbiology 58:273-301

Dunsmuir P., Smith S.M., & Bedbrook J. 1983. The Major Chlorophyll a/b Binding Protein of Petunia is Composed of Several Polypeptides Encoded by a Number of Distinct Nuclear Genes. Journal of Molecular and Applied Genetics. 2:285-300

Evans R.D. & Johansen J.R. 1999. Microbiotic crusts and Ecosystem Processes. Critical Reviews in Plant Sciences 18(2):183-225

Fernandez-Marin B., & Becerril J.M. 2010. Unravelling the roles of desiccation-induced xanthophyll cycle activity in darkness: a case study in *Lobaria pulmonaria*. Planta 231:1335-1342

Ferreira K.N., Iverson T.M., Maghlaoui K., Barber J. & Iwata S. 2004. Architecture of the Photosynthetic Oxygen-Evolving Center. Science 303:1831-1838

Flameling I.A. & Kromkamp J. 1994. Responses of respiration and photosynthesis of Scenedesmus protuberans Fritsch to gradual and steep salinity increases. Journal of Plankton Research 16(12):1781-1791

Flechtner V.R., Johansen J.R. & Clark W.H. 1998. Algal composition of microbiotic crusts from the central desert of Baja California, Mexico. Great Basin Naturalist 58(4):295-311

Fleischmann M.M., Ravanel S, Delosme R, Olive J, Zito F, Wollman F.A., Rochaix J.D. 1999. Isolation and characterization of photoautotrophic mutants of *Chlamydomonas reinhardtii* deficient in state transition. Journal of Biological Chemistry 274:30987–94

Ford J.H. & Leach B.E. 1948. Actidione, an Antibiotic from *Streptomyces griseus*. Journal of the American Chemical Society. 70(3):1223-1225

Gagne G., & Guertin M. 1992. The early genetic response to light in the green unicellular alga *Chlamydomonas eugametos* grown under light/dark cycles involves genes that represent direct responses to light and photosynthesis. Plant Molecular Biology 18:429-445

Green T.G.A., Schlensog M., Sancho L.G., Winkler J.B., Broom F.D. & Schroeter B. 2002. The photobiont determines the pattern of photosynthetic activity within a single lichen thallus containing cyanobacterial and green algae sectors (photosymbiodeme). Oecologia 130:191-198

Gibbs S.P. 1979. The route of entry of cytoplasmically synthesized proteins into chloroplasts of algae possessing chloroplast ER. Journal of Cell Science 35:253-266

Gray D.W., Cardon Z.G., & Lewis L.A. 2006. Simultaneous collection of rapid chlorophyll fluorescence induction kinetics, fluorescence quenching parameters, and environmental data using an automated PA<-2000/CR10X data logging system. Photosynthesis Research 87:295-301

Gray D.W., Lewis L.A., Cardon Z.G. 2007. Photosynthetic recovery following desiccation of desert green algae (Chlorophyta) and their aquatic relatives. Plant, Cell and Environment 30:1240-1255

Green T.G.A. & Smith D.C. 1974. Lichen Physiology XIV. Differences between lichen algae in symbiosis and in isolation. New Phytologist 73:753-766

Gunning B.E.S., & Schwartz O.M. 1999. Confocal microscopy of thylakoid autofluorescence in relation to origin of grana and phylogeny in the green algae. Australian Journal of Plant Physiology 26(7):695-708

Gustavs L., Eggert A., Michalik D., & Karsten U. 2010. Physiological and biochemical responses of green microalgae from different habitats to osmotic and matric stress. Protoplasma 243:3-14

Hader D.P., Leber M., Sinha R., Barbieri E.S., & Helbling E.W. 2002. Role of protective and repair mechanisms in the inhibition of photosynthesis in marine macroalgae. Photochemical and Photobiological Sciences 1:809-814

Heber U. 2008. Photoprotection of Green Plants: A Mechanism of Thermal Energy Dissipation in Desiccated Lichens. Planta 228:641-650

Heber U., Azarkovich M. & Shuvalov V. 2007. Activation of mechanisms of photoprotection by desiccation and by light: poikilohydric photoautotrophs. Journal of Experimental Botany 58(11):2745-2759

Heber U., Bilger W., Turk R., & Lange O.L. 2009. Photoprotection of reaction centres in photosynthetic organisms: mechanisms of thermal energy dissipation in desiccated thalli of the lichen *Lobaria pulmonaria*. New Phytologist. 185:459-470

Heber U., Bilger W., & Shuvalov V.A. 2006. Thermal energy dissipation in reaction centres and in the antenna of photosystem II protects desiccated poikilohydric mosses against photo-oxidation. Journal of Experimental Botany 57(12):2993-3006

Heber U., Bilger W., Turk R., & Lange O.L. 2010. Photoprotection of reaction centers in photosynthetic organisms: mechanisms of thermal energy dissipation in desiccated thalli of the lichen *Lobaria pulmonaria*. New Phytologist 185:459-470

Heber U., Lange O.L. & Shuvalov V.A. 2006. Conservation and dissipation of light energy as complementary processes: homiohydric and poikilohydric autotrophs. Journal of Experimental Botany 57(6):1211-1223

Heber U., & Luttge U. 2011. Lichens and Bryophytes: Light Stress and Photoinhibition in Desiccation/Rehydration Cycles- Mechanisms of Photoprotection. Plant Desiccation Tolerance, Ecological Studies. Eds. U. Luttge *et al* (C) Springer-Verlag Berlin Heidelberg

Heber U., & Shuvalov V.A. 2005. Photochemical reactions of chlorophyll in dehydrated photosystem II: two chlorophyll forms (680 and 700 nm). Photosynthesis Research 84:85-91

Heber U., Soni V., & Strasser R.J. 2011. Photoprotection of reaction centers: thermal dissipation of absorbed light energy vs. charge separation in lichens. Physiologia Plantarum 142:65-78

Holzinger A., Lutz C., & Karsten U. 2011. Desiccation Stress Causes Structural and Ultrastructural Alterations in the Aeroterrestrial Green Algae *Klebsormidium crenulatum* (Klebsormidiophyceae, Streptophyta) Isolated from an Alpine Soil Crust. Journal of Phycology 47(3):591-602

Holzwarth A.R. 1996. Data Analysis of Time- resolved measurements. Biophysical Techniques in Photosynthesis vol. 3. Eds Jan Amesz and Arnold J. Hoff. Kluwer Academic Publishers. Dordrecht: The Netherlands. pgs 75-91

Holzinger A., Tschaikner A., & Remias D. 2010. Crytoarchitecture of the desiccation-tolerant green alga *Zygogonium ericetorum*. Protoplasma 243:15-24

Holzwarth A.R., Muller M.G., Niklas J., & Lubitz W. 2006. Ultrafast transient absorption studies on photosystem I reaction centers from *Chlamydomonas reinhardtii.* 2:Mutations near the P700 reaction center chlorophylls provide new insight into the nature of the primary electron donor. Biophysical Journal 90:552-565

Horton P., Ruban A.V., Rees D., Pascal A.A., Noctor G., & Young A.J. 1991. Control of the Light-Harvesting Function of Chloroplast Aggregation of the LHCII Chlorophyll- Protein Complex. FEBS 292(1,2):1-4

Horton P., Wentworth M., & Ruban A. 2005. Control of the light harvesting function of chloroplast membranes: the LHCII- aggregation model for non-photochemical quenching. FEBS Letters 579:4201-4206

Hu C., Zhang D., Huang Z., Liu Y. 2003. The vertical microdistribution of cyanobacteria and green algae within desert crusts and the development of the algal crust. Plant and Soil 257:97-111

Ivanov A.G., Sane P., Hurry V., Krol M., Sveshnikov D., Huner N.P.A., & Oquist G. 2003. Low-temperature modulation of the redox properties of the acceptor side of photosystem II: photoprotection through reaction centre quenching of excess energy. Physiologia Plantarum 119:376-383

Jahns P., & Holzwarth A.R. 2012. The role of the xanthophyll cycle and of lutein in photoprotection of photosystem II. Biochimica et Biophysica Acta 1817:182-193

Johnson M.P. & Ruban A.V. 2009. Photoprotective Energy Dissipation in Higher Plants Involves Alteration of the Excited State Energy of the Emitting Chlorophyll(s) in the Light Harvesting Antenna II (LHCII). The Journal of Biological Chemistry 284(35):23592-23601

Joneson S., Armaleo D., & Lutzoni F. 2011. Fungal and algal gene expression in early developmental stages of lichen-symbiosis. Mycologia 103(2):291-306

Jorgensen B.B. & Des Marais D.J. 1988. Optical Properties of Benthic Photosynthetic Communities: Fiber-Optic Studies of Cyanobacterial Mats. Limnology and Oceanography 33(1):99-113

Kappen L., Schroeter B., Scheidegger C., Sommerkorn M., & Hestmark G. 1996. Cold Resistance and Metabolic Activity of Lichens Below 0ºC. Advances in Space Research 18(12):119-128

Karsen U., Schumann R., & Mostaert A.S. 2007. Aeroterrestrial Algae Growing on Man-Made Surfaces: What are the Secrets of their Ecological Success? In: J. Seckbach (ed.), Algae and Cyanobacteria in Extreme Environments 583-597 (C) Springer

Kato Y., Sun X., Zhang L. & Sakamoto W. 2012 Cooperative D1 Degradation in the Photosystem II Repair Mediated by Chloroplastic Proteases in Arabidopsis. Plant Physiology 159L1428-1439

Kim J.H., Nemson J.A., & Melis A. 1993. Photosystem II Reaction Center Damage and Repair in *Dunaliella salina* (Green Alga): Analysis under Physiological and Irradiance-Stress Conditions. Plant Physiology 103:181-189

Koblizek M., Ciscato M., Komenda J., Kopecky J., Siffel P. & Masojidek J. 1999. Photoadaption in the green alga *Spongiochloris sp*. A three-fluorometer study. Photosynthetica 37(2):307-323

Komura M., Iwasaki I., & Itoh S. 2008. Drought-Induced Ultra-Fast Fluorescence Quenching in Photosystem II in Lichens Revealed by Picosecond Time-Resolved Fluorescence Spectrophotometry. Photosynthesis. Energy from the Sun: 14th International Congress on Photosynthesis. Eds. J.F. Allen, E. Gantt, J.H. Golbeck and B. Osmond. 1023-1026 (c) Springer

Komura M., Yamagishi A., Shibata Y., Iwasaki I. & Itoh S. 2010. Mechanism of strong quenching of photosystem II chlorophyll fluorescence under drought stress in a lichen, *Physciella melanchla*, studied by subpicosecond fluorescence spectroscopy. Biochimica et Biophysica Acta 1797:331-338

Kopecky J., Azarkovich M., Pfundel E.E., Shuvalov V.A., & Heber U. 2005. Thermal Dissipation of Light Energy is Regulated Differently and by Different Mechanisms in Lichens and Higher Plants. Plant Biology 7:156-167

Kosugi M., Arita M., Shizuma R., Moriyama Y., Kashino Y., Koike H., & Satoh K. 2009. Responses to desiccation stress in lichens are different from those in their photobionts. Plant Cell Physiology 50:879-888

Kosugi M., Miyake H., Yamakawa H., Shibata Y., Miyazawa A., Sugimura T., Satoh K., Itoh S., &
Kashino Y. 2013. Arabitol Provided by Lichenous Fungi Enhances Ability to Dissipate Excess Light Energy in a Symbiotic Green Alga Under Desiccation. Plant and Cell Physiology 0(0):1-10

Kranner I., & Birtic S. 2005. A Modulating Role for Antioxidants in Desiccation Tolerance. Integrative and Comparative Biology 45:734-740

Kranner I., Cram W.J., Zorn M., Wornik S., Yoshimura I., Stabentheiner E., & Pfeifhofer H.W. 2005. Antioxidants and photoprotection in a lichen as compared with its isolated symbiotic partner. PNAS 102(8):3141-3146

Kruse O, Nixon P.J., Schmid G.H., Mullineaux C.W. 1999. Isolation of state transition mutants of *Chlamydomonas reinhardtii* by fluorescence video imaging. Photosynthesis Research 61:43–51

Krause G.H., & Weis E. 1991. Chlorophyll Fluorescence and Photosynthesis: The Basics. Annual Review of Plant Physiology and Plant Molecular Biology 42:313-49

Kuhl M., Glud R.N., Ploug H. & Ramsing N.B. 1996. Microenvironmental Control of Photosynthesis and Photosynthesis- Coupled Respiration in An Epilithic Cyanobacterial Biofilm. Journal of Phycology 32:799-812

Lakowicz, J.R. 2006. Principles of fluorescence spectroscopy. third edition. Springer science. Printed in Singapore

Lai H.T., Hou J.H., Su C.I., & Chen C.L. 2009. Effects of chloramphenicol, florfenicol and thiamphenicol on growth of algae *Chlorella pyrenoidosa*, *Isochrysis galbana*, and *Tetraselmis Chui*. Ecotoxicology and Environmental Safety 72:329-334

Lewis L.A. 2007. Chlorophyta on Land: Independent Lineages of Green Eukaryotes from Arid Lands IN: J. Seckbach (ed.) Algae and Cyanobacteria in Extreme Envionrments 569-582 (C) Springer

Lewis L.A., & Flechtner V.R. 2002. Green algae (Chlorophyta) of desert microbiotic crusts: Diversity of North American Taxa. Taxon 51:443-451

Lewis L.A., & Lewis P.O. 2005. Unearthing the Molecular Phylodiversity of Desert Soil Green Algae (Chlorophyta). Systems Biology 54(6):936-947

Li X.P., Bjorkman O., Shih C., Grossman A.R., Rosenquist M., Jansson S., & Niyogi K.K. 2000. A pigment-binding protein essential for regulation of photosynthetic light harvesting. Nature 403:391-395

Lidholm J., Gustafsson P., & Oquist G. 1987. Photoinhibition of Photosynthesis and its Recovery in the Green Alga *Chlamydomonas reinhardii.* Plant Cell Physiology 28(6):1133-1140

Lin S., & Knox R.S. 1991. Studies of Excitation Energy Transfer Within the Green Algae *Chlamydomonas reinhardtii* and its Mutants at 77K. Photosynthesis Research 27:157-168

Loll B., Kern J., Saenger W, Zouni A., & Biesiadka J. 2005. Towards complete cofactor arrangement in the 3.0 Angstrom resolution structure of photosystem II. Nature Letters

Lumbsch H.T., & Kothe H.W. 1988. Anatomical features of *Chondropsis semiviridis* in relation to its vagrant habit. Lichenologist 20:25-29

Luttge U., & Budel B. 2010. Resurrection kinetics of photosynthesis in desiccation-tolerant terrestrial green algae (Chlorophyta) on tree bark. Plant Biology 12:437-444

Mahanty P., Vani B., & Prakash J.S.S. 2002. Elevated Temperature Treatment Induced Alteration in Thylakoid Membrane Organization and Energy Distribution between the Two Photosystems in *Pisum sativum*. Zeitschrift fur Naturforschung 57:836-842

Maxwell K., & Johnson G.N. 1999. Chlorophyll-Fluorescence- a practical guide. Journal of Experimental Botany 51(345):659-668

Miloslavina Y., Wehner A., Lambrev P.H., Wientjes E., Reus M., Garab G., Croce R., & Holzwarth A.R. 2008. Far-red fluorescence: A direct spectroscopic marker for LHCII oligomer formation in non-photochemical quenching. FEBS Letters 582:3625-3631

Miyake H., Komura M., Itoh S., Kosugi M., Kashino Y., Satoh K., & Shibata Y. 2011. Multiple dissipation components of excess light energy in dry lichen revealed by ultrafast fluorescence study at 5K. Photosynthesis Research 110:39-48

Mou S., Zhang X., Ye N., Dong M., Liang C., Liang Q., Miao J., Xu D., & Zheng Z. 2012. Cloning and expression analysis of two different LhcSR genes involved in stress adaptation in an Antarctic microalga, *Chlamydomonas sp*. ICE-L. Extremophiles 16:193-203

Mullineaux C.W., Pascal A.A., Horton P. & Holzwarth A.R. 1993. Excitation-energy quenching in aggregates of the LHCII chlorophyll-protein complex: a time-resolved fluorescence study. Biochimica et Biophysica Acta 1141:23-28

Obrig T.G., Culp W.J., McKeehan W.L. & Hardesty B. 1971. The mechanism by which cycloheximide and related glutarimide antibiotics inhibit peptide synthesis on reticulocyte ribosomes. The Journal of Biological Chemistry. 246(1):174-181

Ohad I., Kyle D.J. & Arntzen C.J. 1984. Membrane protein damage and repair: Removal and replacement of inactivated 32-kilodalton polypeptides in chloroplast membranes. Journal of Cell Biology 99:481-485

Oliver M.J., Wood A.J., & O'Mahony P. 1998. "To dryness and beyond" - preparations for the dried state and rehydration in vegetative desiccation-tolerant plants. Plant Growth Regulation 24:193-201

Peksa O. & Skaloud P. 2008. Changes in chloroplast structure in lichenized algae. Symbiosis 46:153-160

Proctor M.C.F., Ligrone R., & Duckett J.G. 2007. Desiccation Tolerance in the Moss *Polytrichum formosum*: Physiological and Fine-Structural Changes during Desiccation and Recovery. Annuals of Botany 99:75-93

Proctor M.C.F., & Smirnoff N. 2000. Rapid recovery of photosystems on rewetting desiccation-tolerant mosses: chlorophyll fluorescence and inhibitor experiments. Journal of Experimental Botany 51(351):1695-1704

Prokhorenko V.I., & Holzwarth A.R. 2000. Primary processes and structure of the photosystem II reaction center: a photon echo study. Journal of Physical Chemistry B 104:11563-11578

Ramakrishnan S., & Subramanian S.S. 1966. Amino-acids of *Lobaria subisidosa, Umbilicaria pustulata*, *Parmelia nepalensis* and *Ramalina sinensis*. Current Science (India), 35:124-125

Raven J.A. 2011. The cost of photoinhibition. Physiologia Plantarum 142:87-104

Ruban A.B. & Horton P. 1992. Mechanism of Delta-pH dependent dissipation of absorbed excitation energy by Photosynthetic Membranes. I. Spectroscopy analysis of isolated Light-Harvesting Complexes. Biochimica et Biophysica Acta 1102:30-38

Ruban A.B., Johnson M.P., & Duffer C.D.P. 2012. The Photoprotective Molecular Switch in the Photosystem II Antenna. Biochimica et Biophysica Acta 1817:167-181

Sanders W.B. 2005. Observing Microscopic Phases of Lichen Life Cycles on Transparent Substrata Placed in Situ. Lichenologist 37:373-382

Scheidegger C., Schroeter B., & Frey B. 1995. Structural and functional processes during water vapour uptake and desiccation in selected lichens with green algal photobionts. Planta 197:399-409

Schreiber U. 2004. Pulse-Amplitude-Modulation (PAM) Fluorometry and Saturation Pulse Method: An Overview. IN Chlorophyll a Fluorescence: A Signature of Photosynthesis Editors Papageorgiou G.C., & Govindjee. Springer MA, USA:279-319

Schreiber U. & Armond P.A. 1978. Heat-induced changes of chlorophyll fluorescence in isolated chloroplasts and related heat-damage at the pigment level. Biochimica et Biophysica Acta. 502:138-151

Schreiber U. & Neubauer C. 1990. O2- dependent electron flow membrane energisation and the Mechanism of Non-Photochemical Quenching of Chlorophyll Fluorescence. Photosynthesis Research. 25:279-293

Schtifer C., Schmid V., & Roos M. 1994. Characterization of High-Light-Induced Increases in Xanthophyll Cycle Pigment and Lutein Contents in Photoautotrophic Cell Cultures. Journal of Photochemistry and Photobiology B: Biology 22:67-75

Schweitzer R.H., Melkozernov A.N., Blankenship R.E., & Brudvig G.W. 1998. Time-Resolved fluorescence measurements of Photosystem II: The effect of quenching by oxidized Chlorophyll Z. Journal of Physical Chemistry B 102:8320-8326

Scigelova M., Green P.S., Giannakopulos A.E., Rodger A., Crout D.H.G., & Derrick P.J. 2001. A practical protocol for the reduction of disulfide bonds in proteins prior to analysis by mass spectrometry. European Journal of Mass Spectrometry 7:29-34

Sigfridsson B. & Oquist G. 1980. Preferential distribution of excitation energy into photosystem I of desiccated samples of the lichen *Cladonia impexa* and the isolated lichen-alga *Trebouxia pyriformis*. Physiologia Plantarum 49:329-335

Sigma-Aldrich. 2013. Chloramphenicol Product information. www.sigmaaldrich.com
Sigma- Aldrich. 2013. Cycloheximide Product information. www.sigmaaldrich.com

Singh K.K., Shyam R., & Sane P.V. 1996. Reactivation of photosynthesis in the photoinhibited green alga *Chlamydomonas reinhardtii*: Role of dark respiration and of light. Photosynthesis Research 49:11-20

Slavov C., Reus M., & Holzwarth A.R. 2013. Two Different Mechanisms Cooperate In The Excited State Quenching in *Parmelia* Lichen. The Journal of Physical Chemistry B 117:11326-11336

Trebst A. & Soll-Bracht E. 1996. Cycloheximide retards high light driven D1 protein degradation in *Chlamydomonas reinhardtii*. Plant Science 115L191-197

Umena Y., Kawakami K., Shen J.R., & Kamiya N. 2011. Crystal structure of oxygen-evolving photosystem II at a resolution of 1.9A. Nature 473:55-61

van Stokkum I.H.M., Larsen D.S., & van Grondelle R. 2004. Global and target analysis of time-resolved spectra. Biochimica et Biophysica Acta 1657:82-104

Vasil'ev S., & Bruce D. 1998. Nonphotochemical quenching of excitation energy in photosystem II: a picosecond time-resolved study of the low yield of chlorophyll a fluorescence induced by single-turnover flash in isolated spinach thylakoids. Biochemistry 37:11046-11054

Vasil'ev S., Wiebe S., & Bruce D. 1998. Non-photochemical quenching of chlorophyll fluorescence in photosynthesis: 5-hydroxy-1,4-naphthoquinone in spinach thylakoids as a model for antenna based quenching mechanisms. Biochimica et Biophysica Acta 1363:147-156

Veerman J., Vasil'ev S., Paton G.D., Ramanauskas J., & Bruce D. 2007. Photoprotection in the Lichen *Parmelia sulcata*: The origins of Desiccation-Induced Fluorescence Quenching. Plant Physiology 145:997-1005

Wieners P.C., Mudimu O., & Bilger W. 2012. Desiccation-induced non-radiative dissipation in isolated green lichen algae. Photosynthesis Research 113:239-247

Yamakawa H., & Itoh S. 2013. Dissipation of Excess Excitation Energy by Drought- Induced Nonphotochemical Quenching in Two Species of Drought-Tolerance Moss: Desiccation-Induced Acceleration of Photosystem II Fluorescence Decay. Biochemistry 52:4451-4459

Yamamoto H.Y., & Kamite L. 1972. The Effects of Dithiothreitol on Violaxanthin De-Epoxidation and Absorbance Changes in the 500-nm Region. Biochimica et Biophysica Acta 267:538-543

Yamane Y., Kashino Y., Koike H. & Satoh K. 1997. Increases in the fluorescence F_o level and reversible inhibition of photosystem II reaction center by high-temperature treatments in higher plants. Photosynthesis Research 52:57-64

Appendix

Appendix I

Table 4: Exact average F_V/F_M and standard deviation for desiccation length test. Samples run in triplicate.

Desiccation Length	***P. sulcata*** (F_V/F_M±SD)	***Trebouxia sp.*** (F_V/F_M±SD)	***Chlorella sp.* BC4VF9** (F_V/F_M±SD)	***Chlorella sp.* UTEX318** (F_V/F_M±SD)	***S. rotundus*** (F_V/F_M±SD)	***S.costatus*** (F_V/F_M±SD)
Hydrated	0.665 ±0.110	0.656 ±0.011	0.641 ±0.013	0.642 ±0.016	0.599 ±0.013	0.627 ±0.017
24 hours	0.635 ±0.019	0.513 ±0.015	0.406 ±0.016	0.495 ±0.009	0.425 ±0.022	0.161 ±0.026
7 days	0.609 ±0.014		0.409 ±0.011	0.122 ±0.011	0.403 ±0.020	0.090 ±0.043
30 days	0.390 ±0.065		0.269 ±0.017	0.052 ±0.003	0.305 ±0.010	
60 days	0.202 ±0.046		0.239 ±0.006		0.316 ±0.004	

Appendix II

Table 5: Average photosynthetic yield and standard deviation for desiccation light rehydration test. Solid gray squares indicate light intensities for which data has not been collected. Samples run in triplicate.

Light Intensity (μE)	**P. *sulcata*** (ΦPSII±SD)	***Chlorella sp.* BC4VF9** (ΦPSII±SD)	***Chlorella sp.* UTEX318** (ΦPSII±SD)	***S.costatus*** (ΦPSII±SD)	***S.rotundus*** (ΦPSII±SD)
Hydrated	0.742 ±0.013	0.576 ±0.004	0.668 ±0.009	0.656 ±0.004	0.645 ±0.007
0.06	0.673 ±0.036	0.425 ±0.019	0.429 ±0.014	0.270 ±0.025	0.505 ±0.018
4*		0.305 ±0.023	0.314 ±0.040	0.168 ±0.029	
9*	0.565 ±0.049	0.207 ±0.001	0.227 ±0.025	0.127 ±0.009	0.224 ±0.009
20		0.133 ±0.005	0.180 ±0.005		0.169 ±0.008
25		0.115 ±0.009			
35	0.564 ±0.056	0.106 ±0.014	0.127 ±0.013		0.121 ±0.008
50	0.504 ±0.087				0.087 ±0.002
130	0.381 ±0.030				
310	0.166 ±0.024				

* indicates the application of blue light, where other light intensities are white light.

Appendix III

Table 6: Average photochemical quenching and standard deviation for desiccation light rehydration test. Solid gray squares indicate light intensities for which data has not been collected. Samples run in triplicate.

Light Intensity (μE)	**P. *sulcata*** (qP±SD)	***Chlorella sp.* BC4VF9** (qP±SD)	***Chlorella sp.* UTEX318** (qP±SD)	***S.costatus*** (qP±SD)	***S.rotundus*** (qP±SD)
Hydrated	1.035 ±0.009	1.049 ±0.030	1.026 ±0.016	1.053 ±0.013	1.091 ±0.010
0.06	1.069 ±0.048	1.222 ±0.013	1.170 ±0.019	1.433 ±0.059	1.072 ±0.006
4*		1.070 ±0.011	0.921 ±0.010	1.288 ±0.054	
9*	0.993 ±0.025	0.969 ±0.006	0.814 ±0.039	1.160 ±0.041	0.617 ±0.014
20		0.763 ±0.017	0.869 ±0.004		0.493 ±0.026
25		0.675 ±0.024			
35	0.873 ±0.009	0.619 ±0.068	0.650 ±0.027		0.348 ±0.029
50	0.844 ±0.037				0.244 ±0.030
130	0.634 ±0.041				
310	0.510 ±0.047				

* indicates the application of blue light, where other light intensities are white light.

Appendix IV

Table 7: Average F_V/F_{Mmax} and standard deviation (ΦPSII/qP) for desiccation light rehydration test. Solid gray squares indicate light intensities for which data has not been collected. Samples run in triplicate.

Light Intensity (μE)	**P. *sulcata*** (F_V/F_{Mmax}±SD)	***Chlorella sp.* BC4VF9** (F_V/F_{Mmax}±SD)	***Chlorella sp.* UTEX318** (F_V/F_{Mmax}±SD)	***S.costatus*** (F_V/F_{Mmax}±SD)	***S.rotundus*** (F_V/F_{Mmax}±SD)
Hydrated	0.718 ±0.011	0.549 ±0.006	0.652 ±0.014	0.623 ±0.002	0.591 ±0.007
0.06	0.629 ±0.006	0.348 ±0.019	0.367 ±0.011	0.189 ±0.024	0.472 ±0.016
4*		0.285 ±0.018	0.341 ±0.047	0.132 ±0.028	
9*	0.570 ±0.062	0.214 ±0.002	0.279 ±0.021	0.110 ±0.009	0.364 ±0.007
20		0.175 ±0.010	0.278 ±0.006		0.342 ±0.016
25		0.170 ±0.007			
35	0.647 ±0.070	0.171 ±0.004	0.195 ±0.012		0.350 ±0.049
50	0.601 ±0.126				0.360 ±0.054
130	0.604 ±0.065				
310	0.327 ±0.056				

* indicates the application of blue light, where other light intensities are white light.

Appendix V

Table 8: Calculated NPQ values and standard deviations for NPQ induction test. NPQ signal was inhibited within DTT treated samples. Samples run in triplicate.

Species	Treatment 1 min (NPQ±SD)		Treatment Max. (NPQ±SD)		Relaxation 15s (NPQ±SD)		Relaxation 10mins (NPQ±SD)	
	Control	DTT	Control	DTT	Control	DTT	Control	DTT
P. sulcata	0.041 ±0.012	0.105 ±0.040	1.795 ±0.389	0.335 ±0.039	2.067 ±0.278	0.541 ±0.059	0.462 ±0.150	0.202 ±0.020
Trebouxia sp.	0.654 ±0.090	0.328 ±0.062	1.600 ±0.089	0.420 ±0.011	0.891 ±0.046	0.131 ±0.027	0.248 ±0.027	0.084 ±0.031
Chlorella sp. BC4VF9	0.292 ±0.007	0.202 ±0.037	0.715 ±0.078	0.370 ±0.033	0.493 ±0.086	0.277 ±0.043	0.252 ±0.015	0.223 ±0.039
Chlorella sp. UTEX318	0.320 ±0.183	0.092 ±0.020	1.315 ±0.119	0.259 ±0.116	0.663 ±0.080	0.024 ±0.011	0.254 ±0.054	0.132 ±0.081
S. rotunudus	0.805 ±0.060	0.768 ±0.014	1.221 ±0.141	0.876 ±0.045	0.224 ±0.105	0.125 ±0.003	0.066 ±0.083	0.016 ±0.013
S. costatus	1.344 ±0.030	1.357 ±0.044	2.206 ±0.147	1.675 ±0.056	0.726 ±0.138	0.040 ±0.036	-0.097 ±0.031	-0.133 ±0.094

Appendix VI

Table 9: Average photosynthetic yield and standard deviation for NPQ induction test corresponding to PAM traces. In all cases, despite the presence of DTT and inhibition of high levels of calculated NPQ (except in *Scenedesmus sp.*) photosynthetic ability was consistent between DTT and control trials at every measured stage. Algae were in no way inhibited from regaining photosynthetic yields matching the control group after highlight treatment. Samples run in triplicate.

Species	Pre-NPQ treatment (ΦPSII±SD)		NPQ Treatment (ΦPSII±SD)		Relaxation (ΦPSII±SD)	
	Control	DTT	Control	DTT	Control	DTT
P. sulcata	0.658 ±0.018	0.708 ±0.009	0.092 ±0.037	0.172 ±0.047	0.554 ±0.066	0.630 ±0.006
Trebouxia sp.	0.612 ±0.007	0.623 ±0.005	0.098 ±0.010	0.067 ±0.003	0.543 ±0.006	0.520 ±0.016
Chlorella sp. BC4VF9	0.650 ±0.007	0.644 ±0.019	0.125 ±0.015	0.098 ±0.007	0.611 ±0.005	0.576 ±0.026
Chlorella sp. UTEX318	0.539 ±0.036	0.562 ±0.007	0.102 ±0.008	0.108 ±0.004	0.438 ±0.018	0.467 ±0.008
S. rotunudus	0.643 ±0.007	0.638 ±0.003	0.116 ±0.002	0.131 ±0.015	0.595 ±0.007	0.596 ±0.002
S. costatus	0.633 ±0.017	0.635 ±0.027	0.098 ±0.009	0.086 ±0.026	0.645 ±0.001	0.638 ±0.010

Appendix VII

Table 10: Exact average F_V/F_M and standard deviation for protein inhibition test. Cycloheximide treated samples were exposed to 1hr of photo-inhibitory light, followed by subsequent recovery. Samples run in triplicate.

Species	Dark Adapted (F_V/F_M±SD)	Post Treatment (1hr) 2200µE (F_V/F_M±SD)	Recovery (1hr) 25µE (F_V/F_M±SD)	Slope
P. sulcata[α]	0.534±0.005	0.084±0.016**	0.105±0.019*	1.38E-4
Trebouxia sp.	0.531±0.018	0.225±0.066*	0.229±0.122	9.90E-4
Chlorella sp. BC4VF9	0.545±0.014	0.150±0.027**	0.227±0.033**	7.47E-4
Chlorella sp. UTEX318	0.587±0.004	0.359±0.045	0.445±0.020	1.80E-3
S. rotunudus	0.594±0.015	0.278±0.091	0.351±0.089	1.36E-3
S. costatus	0.098±0.029	0.035±0.009**	0.013±0.011**	-1.81E-4

[α] Applicaion of 4200µE *P<0.05 vs. control value **P<0.005 vs. control value

Table 11: Exact average F_V/F_M and standard deviation for protein inhibition test. Chloramphenicol treated samples were exposed to 1hr of photo-inhibitory light, followed by subsequent recovery. Samples run in triplicate.

Species	Dark Adapted (F_V/F_M±SD)	Post Treatment (1hr) 2200µE (F_V/F_M±SD)	Recovery (1hr) 25µE (F_V/F_M±SD)	Slope
P. sulcata[α]	0.537±0.011	0.089±0.017**	0.110±0.023*	4.39E-4
Trebouxia sp.	0.564±0.010	0.304±0.021*	0.346±0.013**	6.16E-4
Chlorella sp. BC4VF9	0.641±0.004	0.292±0.034	0.327±0.028*	7.25E-4
Chlorella sp. UTEX318	0.595±0.003	0.302±0.055	0.290±0.056*	-1.76E-4
S. rotundus	0.390±0.005	0.147±0.013**	0.145±0.016**	-4.93E-5
S. costatus	0.548±0.001	0.285±0.009**	0.315±0.003**	2.94E-4

[α] Applicaion of 4200µE *P<0.05 vs. control value **P<0.005 vs. control value

Table 12: Exact average F_V/F_M and standard deviation for protein inhibition test. Non-treated controls were exposed to 1hr of photo-inhibitory light, followed by subsequent recovery. Samples run in triplicate.

Species	Dark Adapted (F_V/F_M±SD)	Post Treatment (1hr) 2200uE (F_V/F_M±SD)	Recovery (1hr) 25uE (F_V/F_M±SD)	Slope
P. sulcata[α]	0.599±0.008	0.268±0.012	0.385±0.054	1.93E-3
Trebouxia sp.	0.576±0.016	0.381±0.027	0.489±0.024	1.60E-3
Chlorella sp. BC4VF9	0.641±0.014	0.395±0.011	0.510±0.013	1.89E-3
Chlorella sp. UTEX318	0.557±0.010	0.317±0.011	0.461±0.005	2.35E-3
S. rotunudus	0.612±0.008	0.390±0.016	0.458±0.020	1.28E-3
S. costatus	0.617±0.001	0.436±0.008	0.489±0.002	6.07E-4

[α] Applicaion of 4200μE *P<0.05 vs. control value **P<0.005 vs. control value

Appendix VIII

Table 13: Exact average F_V/F_M and standard deviation for rehydrated protein inhibition test. Samples run in triplicate.

Treatment	*P. sulcata* (F_V/F_M±SD)	*Trebouxia sp.* (F_V/F_M±SD)	*Chlorella sp.* BC4VF9 (F_V/F_M±SD)	*Chlorella sp.* UTEX318 (F_V/F_M±SD)	*S. rotundus* (F_V/F_M±SD)
Hydrated	0.587 ±0.040	0.656 ±0.011	0.656 ±0.011	0.626 ±0.008	0.583 ±0.070
Desiccated	0.048 ±0.019	0.042 ±0.015	0.063 ±0.008	0.080 ±0.016	0.058 ±0.036
Control	0.530 ±0.007	0.468 ±0.002	0.539 ±0.010	0.577 ±0.014	0.416 ±0.011
DTT	0.535 ±0.029	0.456 ±0.007	0.551 ±0.001	0.408 ±0.035	0.305 ± 0.008
Chloramphenicol	0.519 ±0.052	0.458 ±0.017	0.546 ±0.004	0.481 ±0.009	0.418 ±0.020
Cycloheximide	0.202 ±0.010	0.393 ±0.022	0.500 ±0.005	0.487 ±0.008	0.235 ±0.005

Appendix IX

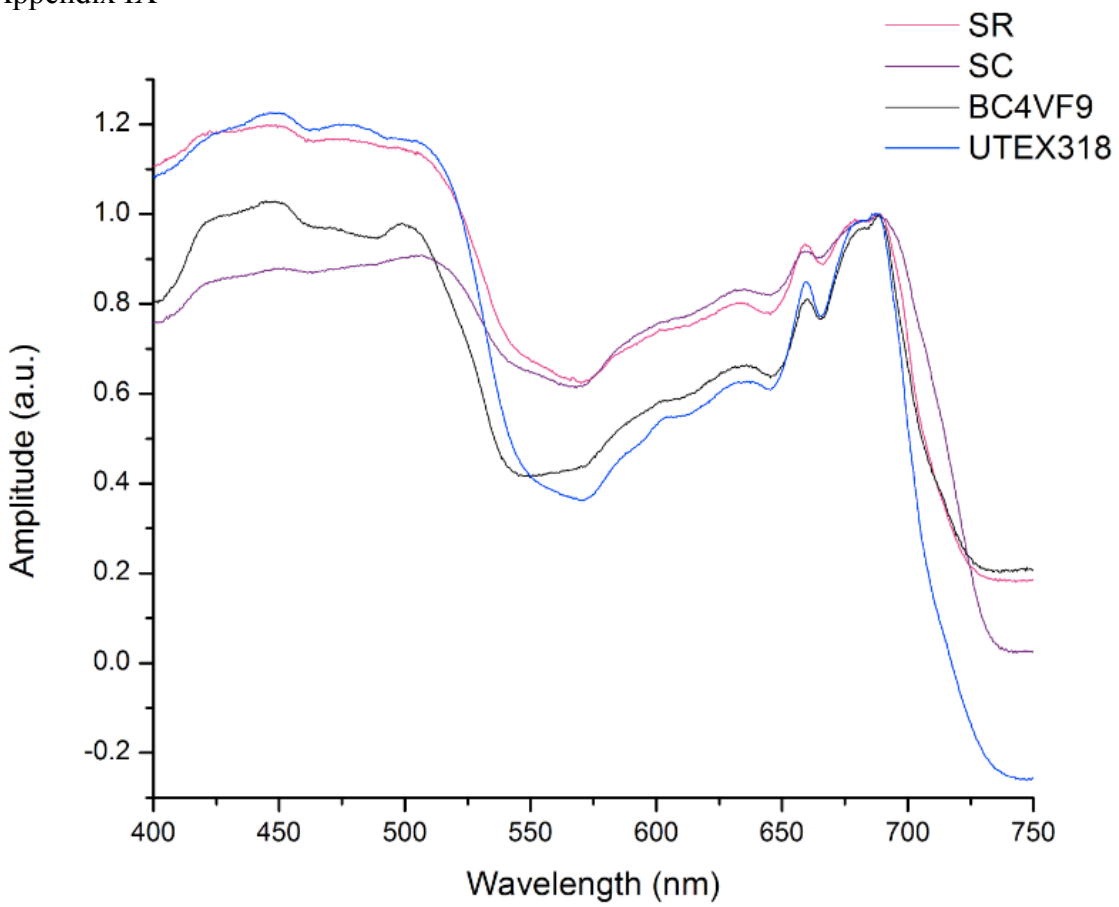

Figure 31: Low temperature (80K) absorbance spectra of free-living algae. Samples were used at 10μg/ml chlorophyll concentration. No major differences are seen towards the red edge of the spectra that may account for the presence of a 760nm spectral feature in the fluorescence emission spectra. Distortion in this area may be caused by self-absorption or low resolution in this wavelength area.

Appendix X

Table 14: Fluorescence emission spectra PSI peak differences and total fluorescence yield between hydrated and desiccated states.

Species	Hydrated (nm)	Desiccated (nm)	Fluorescence Ratio (hydrated/desiccated)
P. sulcata	717	720	11.475±1.379
Chlorella sp. BC4VF9	719	717	2.248±0.031
Chlorella sp. UTEX 318	724	721	1.195±0.035
S. rotundus	718	716	2.502±0.252
S. costatus	721	719	1.470±0.084

Appendix XI

Table 15: Differences in fluorescence yield of hydrated and desiccated decay kinetics. Desiccation tolerant species *P. sulcata*, *Chlorella sp.* BC4VF9, *S. rotundus* and *S. costatus*, show FH/FD ratios of quenched fluorescence upon desiccation, while *Chlorella sp.* UTEX318 seems to have higher fluorescence in the desiccated state. This data is consistent with Fo trace. In all cases, full width half maxima (FWHM) values become smaller upon desiccation, showing the switch to faster life times.

Species	FWHM Hydrated	FWHM Desiccated	Fluorescence Ratio F_H/F_D
P. sulcata	0.456±0.069	0.170±0.014	2.428±0.100
Chlorella sp. BC4VF9	0.596±0.062	0.192±0.020	3.413±0.270
Chlorella sp. UTEX318	0.459±0.026	0.378±0.045	1.312±0.541
S. costatus	0.500±0.023	0.201±0.012	1.722±0.140
S. rotundus	0.607±0.004	0.275±0.055	2.644±0.640

Appendix XII

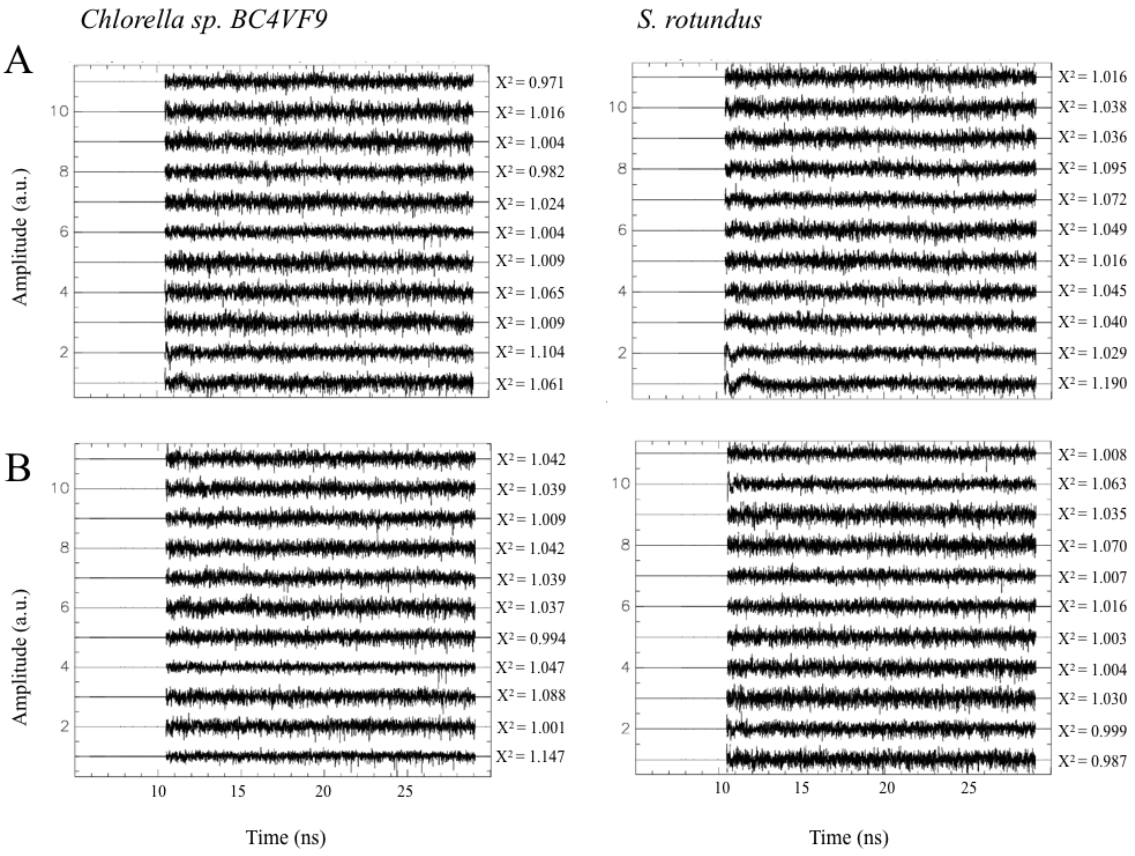

Figure 32: Weighted residuals of global analysis of desert dwelling (Left) *Chlorella sp.* BC4VF9 and (Right) *S. rotundus* in (A) hydrated and (B) desiccated state. Hydrated *Chlorella sp.* BC4VF9 has an over all χ^2 is 1.021 and desiccation χ^2 is 1.042. Hydrated *S. rotundus* has an over all χ^2 is 1.055 and desiccation χ^2 is 1.018.

Appendix XIII

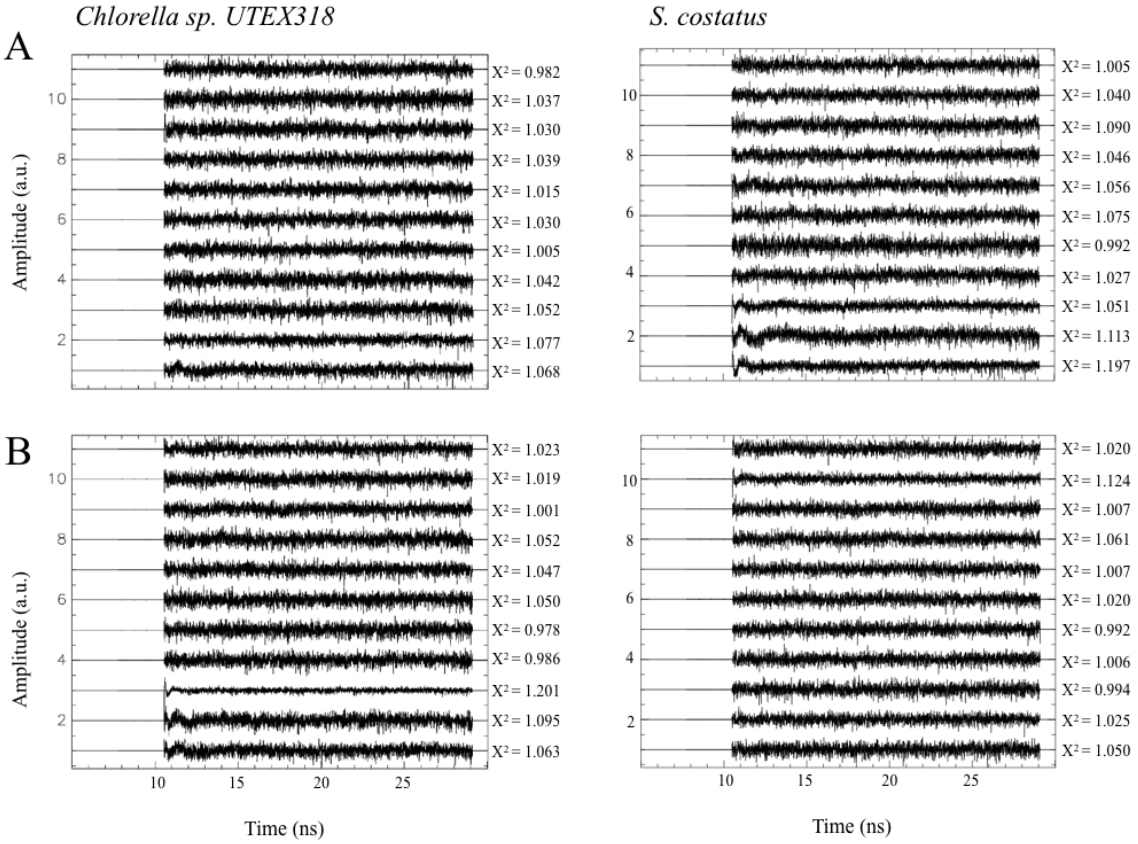

Figure 33: Weighted residuals of global analysis of aquatic algae (Left) *Chlorella sp.* UTEX318 and (Right) *S. costatus* in (A) hydrated and (B) desiccated state. Hydrated *Chlorella sp.* UTEX318 has an over all χ^2 is 1.048 and desiccation χ^2 is 1.045. Hydrated *S. costatus* has an over all χ^2 is 1.061 and desiccation χ^2 is 1.026.

Appendix XIV

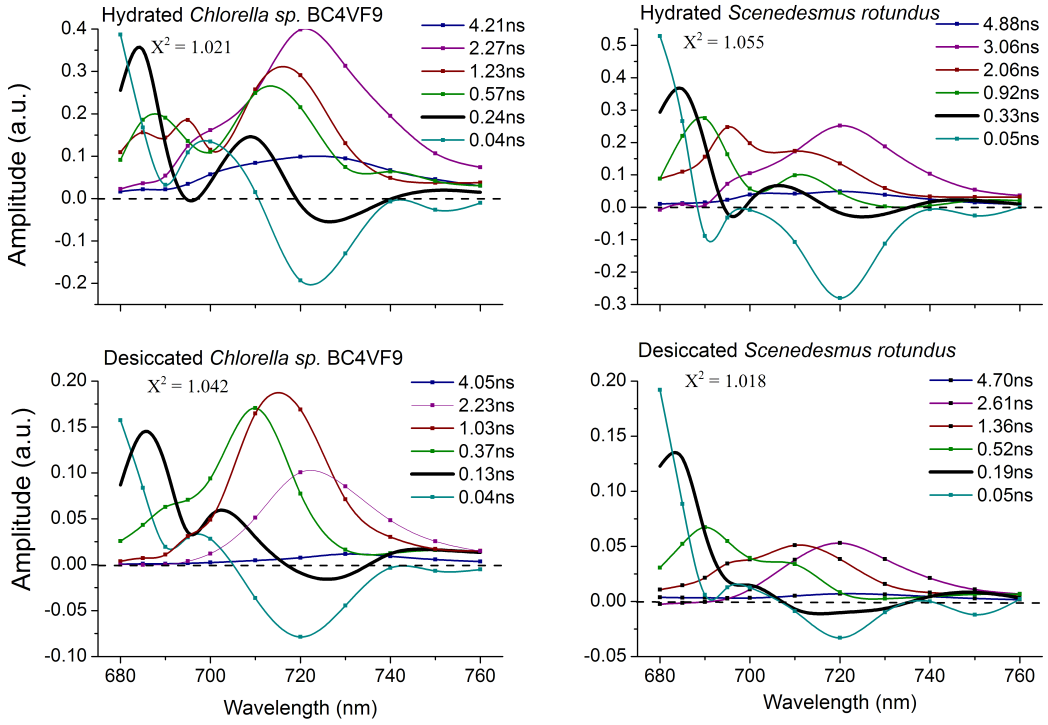

Figure 34: Decay associated spectra created with global analysis of desert dwelling (Left) *Chlorella sp.* BC4VF9 and (Right) *S. rotundus* in (Top) hydrated and (Bottom) desiccated state. Black spectral component in hydrated DAS represents LHCII which is seen to form a quenching species upon desiccation. Upon desiccation components become faster, and lose short-wavelength associated peaks. Energy transfer component stays the same between the two states. LHCII quenching signature identified in *P. sulcata* appears to be present within desiccated BC4VF9 (0.13ns) and *S. rotundus* (0.19ns), but not nearly as dominating in the spectra as seen in *P. sulcata*.

Appendix XV

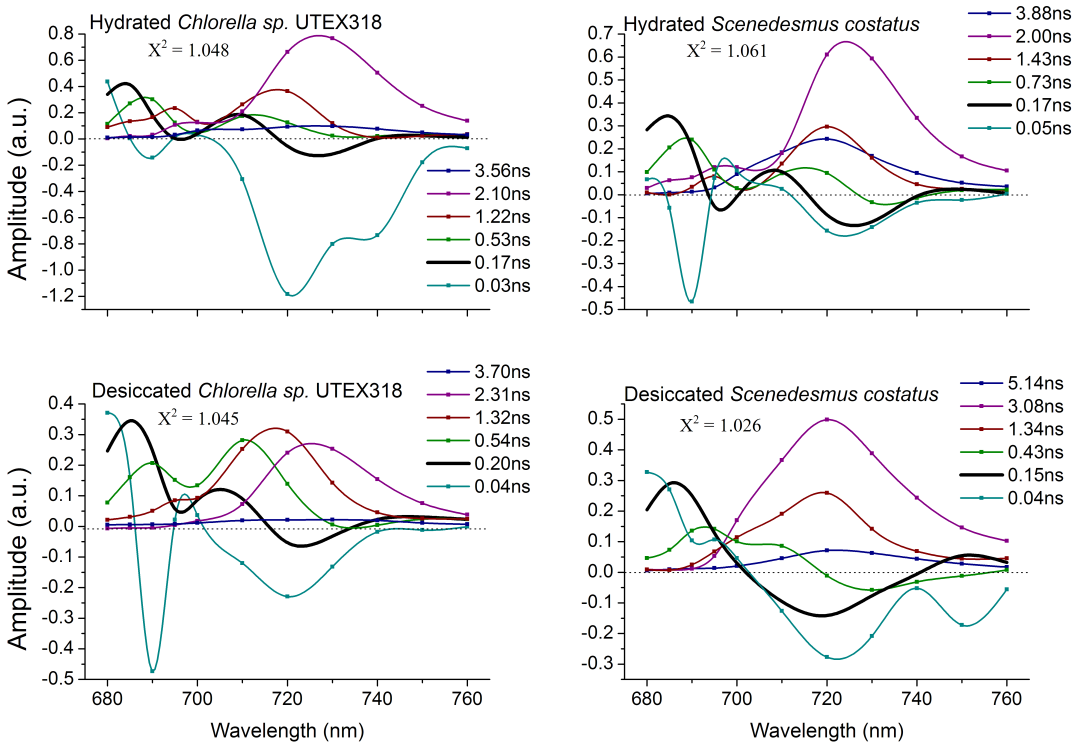

Figure 35: Decay associated spectra created with global analysis of aquatic algae (Left) *Chlorella sp.* UTEX318 and (Right) *S. costatus* in (Top) hydrated and (Bottom) desiccated state. Black spectral component in hydrated DAS represents LHCII which is seen to form a quenching species upon desiccation. Upon desiccation components do not exhibit the same dramatic decrease in lifetime as noted for desert dwelling species or *P. sulcata*. LHCII spectral signature identified in *P. sulcata* appears to be present within desiccated UTEX318 (0.20ns) but absent within *S. rotundus* (0.15ns).

Appendix XVI

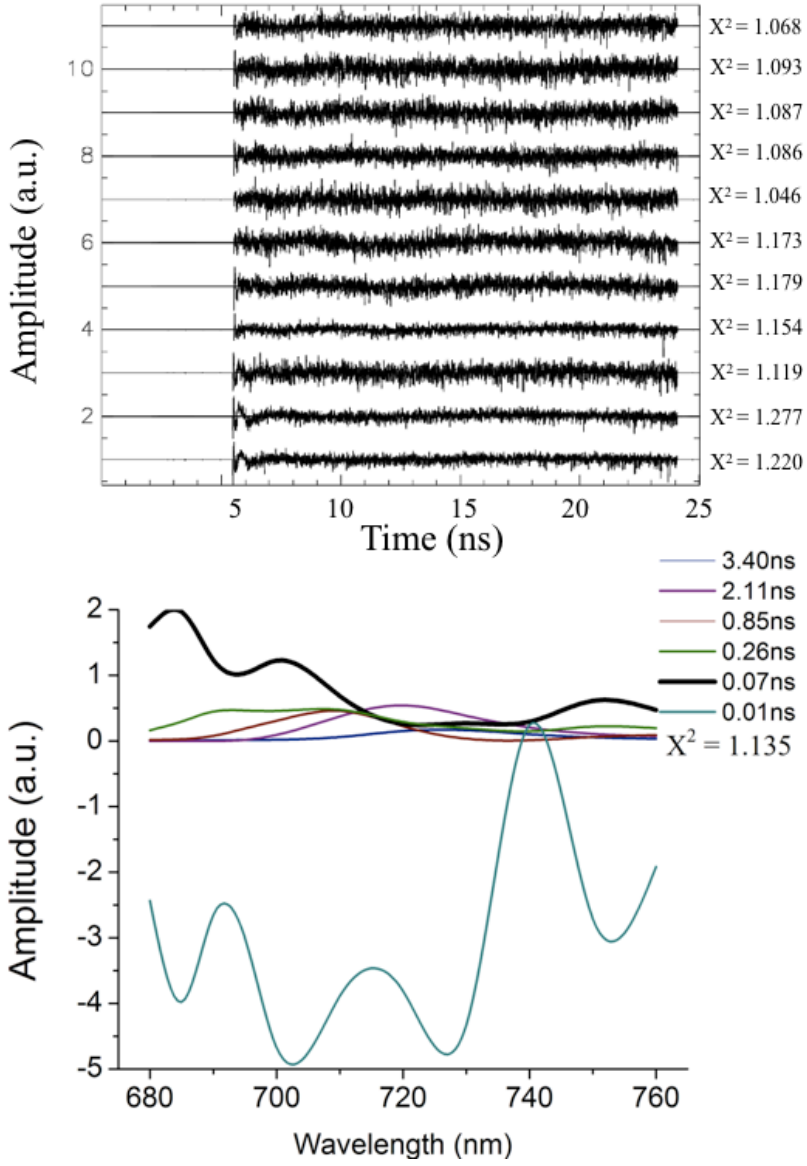

Figure 36: Desiccated *P. sulcata* fit with 6 components, and corresponding DAS. Residuals depicted for desiccated *P. sulcata* fit with 5 components (Figure 29 B) showed residuals from wavelengths 680-695nm with high X^2 values. When fit with 6 components, some X^2 values in this range became smaller, while some became higher. Corresponding DAS with 6-component fit showed the extraction of a fluorescence artifact from the DAS corresponding to a lower overall X^2, and representing a component that is physiologically not possible. By extracting this artifact however, long-wavelength contribution by "quenching" component becomes higher in amplitude that seen in 5 component fit, suggesting this may be one possible reason for the discrepancy between previously published DAS (Veerman *et al*, 2007).

Appendix XVII

Table 16: Fluorescence yield amplitudes from hydrated (H) and desiccated (D) DAS. DAS are normalized to 1. Wavelengths are representative of important photosynthetic components, PSII, PSI and 760nm fluorescent shoulder.

Species	685nm		695nm		720nm		760 nm	
	H	D	H	D	H	D	H	D
P. sulcata	0.51± 0.09	0.15± 0.02	1.27± 0.31	0.36± 0.05	2.29± 0.03	1.58± 0.16	1.79± 0.05	0.69± 0.06
Chlorella sp. BC4VF9	0.63± 0.02	0.17± 0.02	1.31± 0.09	0.42± 0.05	1.93± 0.20	1.19± 0.14	2.06± 0.17	0.93± 0.29
Chlorella sp. UTEX318	0.47± 0.03	0.41± 0.12	1.14± 0.13	0.88± 0.19	1.72± 0.10	1.65± 0.10	1.87± 0.12	1.37± 0.06
S. rotundus	0.70± 0.05	0.29± 0.04	1.98± 0.02	0.69± 0.15	2.78± 0.02	2.22± 0.12	2.21± 0.08	1.30± 0.17
S. costatus	0.57± 0.04	0.25± 0.01	1.22± 0.19	0.74± 0.07	2.16± 0.04	2.67± 0.06	2.01± 0.06	2.30± 0.01